FEDERAL UNIVERSITY OF SANTA CATARINA
GRADUATE PROGRAM IN CHEMICAL ENGINEERING

Lya Piaia

CHITOSAN/β-TCP/SILK FIBROIN COMPOSITES FOR TISSUE ENGINEERING APPLICATIONS

Florianópolis
2019

Lya Piaia

CHITOSAN/β-TCP/SILK FIBROIN COMPOSITES FOR TISSUE ENGINEERING APPLICATIONS

Thesis submitted to the Postgraduate Program in Chemical Engineering of the Federal University of Santa Catarina (UFSC) as part of the requirements to obtain a PhD in Chemical Engineering.

Advisors
Prof. Dr. Dachamir Hotza
Prof. Dr. Gean V. Salmoria

Supervisors/3B's
Prof. Dr. Rui Reis
Dra. Simone S. Silva

Florianópolis

2019

Ficha de identificação da obra elaborada pelo autor,
através do Programa de Geração Automática da Biblioteca Universitária da UFSC.

Piaia, Lya
CHITOSAN/b-TCP/SILK FIBROIN COMPOSITES FOR TISSUE ENGINEERING APPLICATIONS / Lya Piaia ; orientador, Dachamir Hotza , coorientador, Gean V. Salmoria, 2019.
119 p.

Tese (doutorado) - Universidade Federal de Santa Catarina, Centro Tecnológico, Programa de Pós-Graduação em Engenharia Química, Florianópolis, 2019.

Inclui referências.

1. Engenharia Química. 2. Tissue Engineering. 3. Chitosan. 4. b-TCP. 5. silk fibroin. I. Hotza , Dachamir . II. Salmoria, Gean V. . III. Universidade Federal de Santa Catarina. Programa de Pós-Graduação em Engenharia Química. IV. Título.

Lya Piaia

CHITOSAN/β-TCP/SILK FIBROIN COMPOSITES FOR TISSUE ENGINEERING APPLICATIONS

The present work at PhD level was evaluated and approved by an examining board composed of the following members:

Prof. Dra. Claudia Angela Maziero Volpato
Federal University of Santa Catarina

Prof. Dra. Mabel Cordeiro
Federal University of Santa Catarina

Prof. Dr. Marcio Fredel
Federal University of Santa Catarina

Prof. Dra. Samara Silva de Souza
Federal University of Technology Paraná

We certify that this is the **original and final version** of the final thesis, which was deemed appropriate to obtain the title of doctor in Program in Chemical Engineering.

Cintia Soares:02040162909
Digitally signed by Cintia Soares:02040162909
DN: cn=Cintia Soares:02040162909, o=ICPEdu, ou=UFSC - Universidade Federal de Santa Catarina
Date: 2019.09.23 17:02:57 -03'00'

Prof. Dra. Cíntia Soares
Program Coordinator

Dachamir Hotza:49523503987
Digitally signed by Dachamir Hotza:49523503987
Date: 2019.09.23 15:59:17 -03'00'

Prof. Dr. Dachamir Hotza
Advisor

Florianópolis, September 3, 2019

This work is dedicated for my mother Ilhete and for my aunt Inelve for the unconditional love throughout my life. I also dedicate for my grandparents in memory Santo and Mafalda for the teachings

ACKNOWLEDGMENT

I would like to thank God for life and blessings.

I would like to thank my advisors, Prof. Dachamir Hotza and Prof. Gean Salmoria, for their confidence in accepting me into their team, for their guidance, teachings, understanding and encouragement.

I would also like to thank Prof. Rui Reis for his acceptance, confidence, teachings and for joining his golden team at 3B's, as well as to Dr. Simone Silva for the confidence and experiences during the 10 month-stay in Portugal.

To my mother Ilhete and my aunt Inelve, for their dedication, courage and encouragement to never give up. I am the result of the good education they gave, along with Grandpa Santo and Grandma Mafalda. You are my pride and for you I will “move” mountains.

To my uncles, aunts, and cousins, who even at a distance, emanated good vibes and positive thoughts. The friends I made throughout the doctorate, in Brazil and Portugal, were essential for me to reach the end: my gratitude to the “malta”. To my friends from afar for the good vibes. By the words of comfort and sincerity, such as moments of relaxation.

To the teachers and staff of the Department of Chemical Engineering and Food Engineering (EQA/UFSC).

Thanks to NIMMA and 3B's laboratories for their assistance with materials, reagents and equipment.

To CNPq and CAPES for their financial support.

To all the people who have gone through my life in these years. I appreciate the affection and the teachings.

I am stronger because I have lived so intensely close to you.

"In nature nothing is created, nothing is lost, everything is transformed."

Antoine Lavoisier

RESUMO

Scaffolds são normalmente produzidos a partir de polímeros biocompatíveis com outros materiais que auxiliem na regeneração do tecido lesado. Para a regeneração do tecido ósseo pode ser adicionado aos polímeros um material cerâmico o qual favorecerá a produção de matriz osteocondutora, além de poder incorporar nestas estruturas fatores de crescimento celular para maior eficiência na recuperação do tecido. Para a região osteocondral é possível desenvolver um *scaffold* com duas camadas, bicamadas, o qual possibilitará um crescimento celular adequado para cada célula ali adicionada. Nesta tese, foram produzidos dois *scaffolds*, um que pode ser utilizado para a regeneração óssea e outro para a regeneração osteocondral. Foram utilizados dois polímeros naturais (quitosana e seda) e uma biocerâmica (fosfato tricálcico, TCP). Para a produção de *scaffold* para regeneração óssea foram empregadas duas concentrações de quitosana (2 e 3 vol.%) e 10 e 20 vol.% TCP, com revestimento de 1 vol% de seda. Para a produção de *scaffold* bicamada foi usado 3 vol.% quitosana ,10 e 20 vol.% TCP e genipin, agente de *crosslinking*, para estabilizar a estrutura. Os dados demonstraram o potencial na aplicação biomédica para lesões pequenas. Os scaffolds apresentam porosidade para cultivo celular, bem como comportamento de degradação, não interfere na viabilidade e proliferação celular.

Palavras-chave: Engenharia de Tecidos; andaime; quitosana; fosfato tricálcico; regeneração óssea; regeneração osteocondral; fibroína de seda; *scaffold* bicamada.

RESUMO EXPANDIDO

Introdução

A engenharia de tecidos (TE) tem como objetivo principal desenvolver andaimes capazes de regenerar o tecido lesionado, que serão utilizados na medicina regenerativa. Esses andaimes melhorarão, restaurarão ou substituirão os tecidos ou órgãos danificados, utilizando ferramentas de engenharia e ciências, incluindo células, materiais e fatores de crescimento (LANGER; VACANTI, 1993). Os andaimes também devem ser biocompatíveis, ter resistência mecânica, porosidade controlada e rede de poros interconectados, entre outras características que diferem de tecido para tecido (HUTMACHER, 2000).

Os enxertos são amplamente utilizados no cenário clínico, mas apresentam algumas desvantagens que podem limitar suas aplicações. Os autoenxertos podem apresentar reabsorção variável, risco de morbidade no local doador, altas taxas de falha em locais específicos e necessidade de cirurgia adicional. Aloenxertos, como matriz de ossos desmineralizados e xenoenxertos (de outras espécies) podem ser rejeitados pelo patógeno pelo organismo receptor (AGARWAL; GARCÍA, 2015; GRUSKIN et al., 2012). Como alternativa, podem ser empregadas próteses de materiais sintéticos ou naturais, como próteses, placas e parafusos de articulações e sistemas estruturais de suporte para articulações (ROSETI et al., 2017).

Idealmente, um enxerto sintético deve satisfazer uma série de propriedades, como biodegradabilidade, osteocondutividade, biocompatibilidade, porosidade interconectada e resistência mecânica adequada (BOSE; TARAFDER; BANDYOPADHYAY, 2017; PINA; OLIVEIRA; REIS, 2015), a fim de melhorar a vascularização, entrega de nutrientes, adesão celular, proliferação, diferenciação. Finalmente, o tecido nativo deve ser substituído pelo novo tecido ósseo (KHOJASTEH et al., 2016).

O desenvolvimento de andaimes emprega vários materiais, principalmente polímeros e cerâmicos, é uma forte tendência, pois as demandas (osso e tecido osteocondral) da substituição de tecidos têm aumentado em muitas aplicações clínicas para terapia traumática e implantes ortopédicos (FERNANDEZ-YAGUE et al. , 2015; KANG et al., 2014; MATASSI et al., 2011; SIONKOWSKA, 2011).

O desenvolvimento de uma estrutura semelhante ao tecido osteocondral é uma das principais dificuldades encontradas nesse processo. Uma interface entre a camada óssea e a camada de cartilagem pode ser formada e as células podem não penetrar na interface para formar uma cartilagem calcificada, resultando em uma interface instável de tecido ósseo / cartilagem (XIAO et al., 2019).

Objetivos

O objetivo geral deste trabalho é produzir e caracterizar compósitos de CH/β-TCP/fibroína de seda para aplicações em engenharia de tecidos.

Os objetivos específicos respectivos são, para regeneração óssea:

- Determinar a melhor proporção de CH e β-TCP para produzir a cultura de células adequada para biocompósitos.

- Caracterizar a fibroína de seda revestida e não revestida com microestrutura biocompósito.
- Analisar o comportamento das células quando em contato com a fibroína de seda revestida ou não revestida da superfície composta.
- Avaliar a liberação de BMP-2 nos andaimes em um período.

Por outro lado, para a regeneração osteocondral, espera-se:
- Desenvolver um andaime de duas camadas.
- Caracterizar a microestrutura da bicamada.
- Determinar características físico-químicas do andaime.
- Analisar o comportamento da célula quando em contato com a bicamada

Metodologia

Os scaffolds foram construídos utilizando quitosana de peso molecular médio (CH, 300-1000 cps, grau de desacetilação ≥ 90%, Glentham Life Sciences), fosfato de β-tricálcico (β-TCP), casulos de Bombyx mori gentilmente fornecidos pela associação APPACDM (Castelo Branco, Portugal) e proteínas morfogenéticas ósseas (BMP) (PeproTech, Portugal). Todos os outros produtos químicos tinham grau de reagente e foram usados como recebidos.

Os scaffolds para aplicação em regeneração de tecido ósseo foram produzidos utilizando 2 e 3% em peso de concentração de quitosana dissolvida em 3% vol de ácido acético, por 3 dias a 25 ° C, em agitação constante. Em seguida, foram adicionados 10 e 20% em peso de β-TCP (p / v) em cada concentração de quitosana, para obter quatro soluções diferentes. Os mesmos posteriormente receberam um *coating* de 1% de seda.

Os scaffolds bicamadas para aplicação em regeneração osteocondral foram fabricados utilizando soluções de 3% em peso de quitosana dissolvida em 3% em volume de ácido acético foram preparadas e deixadas por 3 dias a 25 °C, em agitação constante. Em seguida, 10 e 20% em peso de β-TCP foram adicionados à quitosana, produzindo três soluções diferentes.

Os scaffolds foram caracterizados utilizando as seguintes técnicas e análises para isso: FTIR, SEM, micro-CT, teste de bioatividade, degradação por enzima, taxa de inchamento, além da caracterização biológica: viabilidade celular, proliferação, atividade de ALP, SEM.

Resultados e Discussão

Os resultados obtidos da caracterização do scaffolds para regeneração óssea, sugerem que o fosfato β-TCP influencia a microestrutura dos andaimes desenvolvidos. A microestrutura dos andaimes mostrou porosidades de até 94% quando revestidas com seda, mantendo uma interconectividade de 99% e tamanhos de poros na faixa de 200-40 μm. As superfícies da estrutura foram capazes de formar cristais de apatita após 21 dias. Estudos de células in vitro demonstraram que os suportes foram capazes de suportar o crescimento e a proliferação celular até 14 dias de cultura. As propriedades físicas, químicas e biológicas obtidas indicaram que os andaimes desenvolvidos têm grande potencial para serem utilizados em aplicações de regeneração óssea.

No desenvolvimento de estruturas de duas camadas, foi necessário obter estabilidade entre os materiais envolvidos e garantir que essa estrutura não se dissolva em contato com o

fluido corporal. Os andaimes foram preparados usando quitosana / fosfato β-tricálcico para a parte óssea e fibroína da seda, para imitar a porção cartilaginosa. Além disso, as estruturas resultantes foram submetidas à reticulação usando genipin. As micrografias de MEV revelaram que as duas camadas dos andaimes estão bem definidas, enquanto os resultados da análise μ-CT indicaram que a porção de seda está infiltrada nos andaimes e que a camada de seda apresenta valores mais significativos de interconectividade e porosidade, 59% e 68 %, respectivamente. A concentração de Ca após o teste de bioatividade com amostras de CBSG10 atingiu 900 ppm e os testes de citotoxicidade realizados por contato direto com células MC3T3 e ATCD5 revelaram boa viabilidade e proliferação celular por até 14 dias. Os resultados sugerem que as estruturas podem ser utilizadas na regeneração osteocondral.

Considerações Finais

Podemos concluir que os andaimes desenvolvidos para regeneração óssea e ostecondral foram sintetizados com sucesso. Ambos apresentaram estabilidade na estrutura, microestrutura com porosidade diferenciada, permitindo um fluxo de células e fluido corporal. Assim, eles deveriam ser colonizados e produzir um novo tecido funcional. Por caracterização biológica, os andaimes mostraram viabilidade e proliferação celular quando em contato com células específicas para cada tecido. No entanto, testes adicionais para confirmar seu potencial de regeneração tecidual são sugeridos.

Palavras-chave: Engenharia de Tecidos; andaime; quitosana; fosfato tricálcico; regeneração óssea; regeneração osteocondral; fibroína de seda; *scaffold* bicamada.

ABSTRACT

Scaffolds are usually produced from biocompatible polymers with other materials, which aid in the regeneration of the injured tissue. For the regeneration of the osseous tissue a ceramic material may be added to the polymer to favor the production of matrix osteoconductive, and to incorporate factors of cellular growth for better recovering of the tissue. For the osteochondral region, it is possible to develop a scaffold with two layers, which will allow adequate cell growth for each cell added. In this thesis, two scaffolds were produced, one that can be used for bone regeneration and another for osteochondral regeneration. Two natural polymers (chitosan and silk fibroin) and one bioceramic (β-tricalcium phosphate, TCP) were used. For the production of scaffolds for bone regeneration different concentrations of chitosan (2 and 3 vol.%), TCP (10 and 20 vol%) were added to chitosan, with 1 vol.% coating of silk fibroin. For the production of bilayer scaffolds, a 3 vol.% chitosan and 10 and 20 vol% of TCP were used, with genipin, a crosslinking agent, to stabilize the structure. The results demonstrated the potential in biomedical application for small lesions. The scaffolds have adequate porosity for cell culture, as well as degradation behavior, while it does not interfere/influence on cell viability and proliferation.

Keywords: Tissue Engineering; scaffold; chitosan; β-tricalcium phosphate; bone regeneration; osteochondral regeneration; silk fibroin; bilayer scaffolds.

LIST OF FIGURES

LIST OF TABLES

LIST OF ACRONYMS

ATCD5 – Chondrocyte-line cells

BMP – Bone Morphogenetic Protein

CH – Chitosan

DMEM – Dulbecco's Modified Eagle Medium

DNA – Deoxyribonucleic acid

ECM – Extracellular Matrix

FBS – Fetal Bovine Serum

FTIR – Fourier transform infrared spectroscopy

HAp –Hydroxyapatite

ICP – Inductively coupled plasma

MC3T3 – Mouse osteogenic cell line

MTS – [3-(4,5-dimethylthiazol-2-yl)-5-(3-carboxymethoxyphenyl)-2-(4-sulfophenyl)-2H-tetrazolium]

PCL – Policapralactone

PGA – Poly(glycolic acid)

PLA – Poly(lactic acid)

rhBMP-2 – Recombinant human BMP-2

SBF – Simulated body fluid

SEM – Scanning Electron Microscope

SF – Silk fibroin

TCP – Tricalcium Phosphate

TE – Tissue Engineering

XDR – X-ray diffraction

SUMMARY

Chapter 1 – INTRODUCTION AND OBJECTIVES

1.1.INTRODUCTION

Tissue engineering (TE) has as main objective to develop scaffolds capable of regenerating the injured tissue, which will be used in regenerative medicine. This scaffolds will be improve, restore or replace damaged tissues or organs, using engineering and science tools, including cells, materials and growth factors (LANGER; VACANTI, 1993). Scaffolds must also be biocompatible, have mechanical strength, controlled porosity, and interconnected pore network, among other characteristics that differ from tissue to tissue (HUTMACHER, 2000).

Tissue regeneration is a complex biological system. Some tissues/organs have the ability to self-regenerate, such as skin, bone, or liver. However, most of the tissues does not have this potential, and thus they require a permanent or temporary replacement of damaged tissue. In the case of bone, human tissues that have biocompatibility with the receptor are used, in addition to using tissues from other animal species that have regeneration compatibility in the human biological system.

Tissue engineering uses concepts from different branches of science to produce 2D and 3D structures for temporary and permanent substitutes in injured tissues. The development of these structures requires some characteristics and materials for each type of tissue.

Grafts are widely used in the clinical setting, but have some disadvantages that may limit their applications. Autografts may present variable resorption, risk of donor site morbidity, high failure rates at specific sites, and a need for further surgery. Allografts, such as matrix of demineralized bones, and xenografts (of other species) may be rejected by the pathogen by recipient body (AGARWAL; GARCÍA, 2015; GRUSKIN et al., 2012). Alternatively, prosthetics of synthetic or natural materials can be employed, such as joint prostheses, plates and screws, and structural joint support systems (ROSETI et al., 2017).

In this context, tissue engineering seeks to construct scaffolds that mimic the natural tissue in morphology, composition, and mechanical strength (RAZAVI et al., 2015). Some researchers recommend that the manufacture of scaffolds with interconnected pore sizes greater than 300 μm may facilitate cell attachment, migration and tissue growth (FAHIMIPOUR et al., 2017; KHOJASTEH et al., 2017).

Ideally, a synthetic graft should satisfy a number of properties, such as biodegradability, osteoconductivity, biocompatibility, interconnected porosity and adequate mechanical strength (BOSE; TARAFDER; BANDYOPADHYAY, 2017; PINA; OLIVEIRA; REIS, 2015), in order to enhance vascularization, nutrient delivery, cell adhesion, proliferation,

differentiation. Finally, the native tissue should be replaced by the new bone tissue (KHOJASTEH et al., 2016).

The development of scaffolds employs various materials, mainly polymeric and ceramic, is a strong trend, as the demands (bone and osteochondral tissue) of tissue substitution have been increasing in many clinical applications for traumatic therapy and orthopedic implants (FERNANDEZ-YAGUE et al., 2015; KANG et al., 2014; MATASSI et al., 2011; SIONKOWSKA, 2011).

The development of a structure similar to the osteochondral tissue is one of the main difficulties found in this process. An interface between the bone layer and the cartilage layer may be formed, and the cells may not penetrate the interface to form a calcified cartilage, resulting in an unstable interface of bone/cartilage tissue (XIAO et al., 2019).

1.2. OBJECTIVES

The general objective of this work is to produce and characterize CH/β-TCP/silk fibroin composites for applications in tissue engineering.

The respective specific objectives are, for bone regeneration:

- To determine the best proportion of CH and β-TCP to produce the biocomposite suitable cell culture.
- To characterize the biocomposite microstructure coated and non-coated silk fibroin.
- To analyze the cell behavior when in contact with the composite surface coated or non-coated silk fibroin.
- To evaluate the release of BMP-2 in the scaffolds in a period.

On the other hand, for osteochondral regeneration, it is expected:

- To develop a bilayer scaffold.
- To characterize the microstructure of the bilayer.
- To determine physicochemical characteristics of the scaffold.

- To analyze the cell behavior when in contact with the bilayer.

1.3.ORGANIZATION OF THE THESIS

This thesis has been arranged in the following chapters.

- **Chapter 1** corresponds to the introduction and objective of the study
- **Chapter 2** is the literature review on the scaffolds production in addition to the biological, structural and compositional requirements for new scaffolds; it also includes a brief overview of bone osteochondral regeneration and its applications.
- **Chapter 3** describes the materials and detailed methodology used in the thesis, including preparation of the scaffolds for bone osteochondral regeneration and characterization techniques.
- **Chapter 4** presents the process of scaffolds manufacturing, and the respective results and discussion, regarding silk protein coated CH/β-TCP composites for bone tissue engineering applications.
- **Chapter 5** deals with genipin-crosslinked CH/β-TCP/silk for osteochondral regeneration, and presents the respective results and discussion
- **Chapter 6** finally lists the general conclusions and some ideas for future work.
- **References** are given in the end of this manuscript.

Chapter 2– LITERATURE REVIEW

2.1. ANATOMY AND BIOLOGICAL SYSTEMS OF BONE AND OSTEOCHONDRAL TISSUE

Bones have important roles in the body: locomotion, soft tissue support and protection, calcium and phosphate storage and bone marrow harboring. The mechanical properties of each bone type depend on the region of the body (FLORENCIO-SILVA et al., 2015).

Bone tissue consists of nanocrystalline hydroxyapatite (HAp), organic components (mainly collagens) and water. The present proteins will assemble to form a nanostructured extracellular matrix (ECM) that will stimulate adhesion, proliferation, and differentiation of various cell types: osteoblasts, bone-clad cells, osteocytes and osteoclasts (BIANCO et al., 2001; BLAIR; SUN; KOHANSKI, 2007; ZHANG et al., 2016a), as showed in Figure 1.

Figure 1 - Bone tissue cross section.

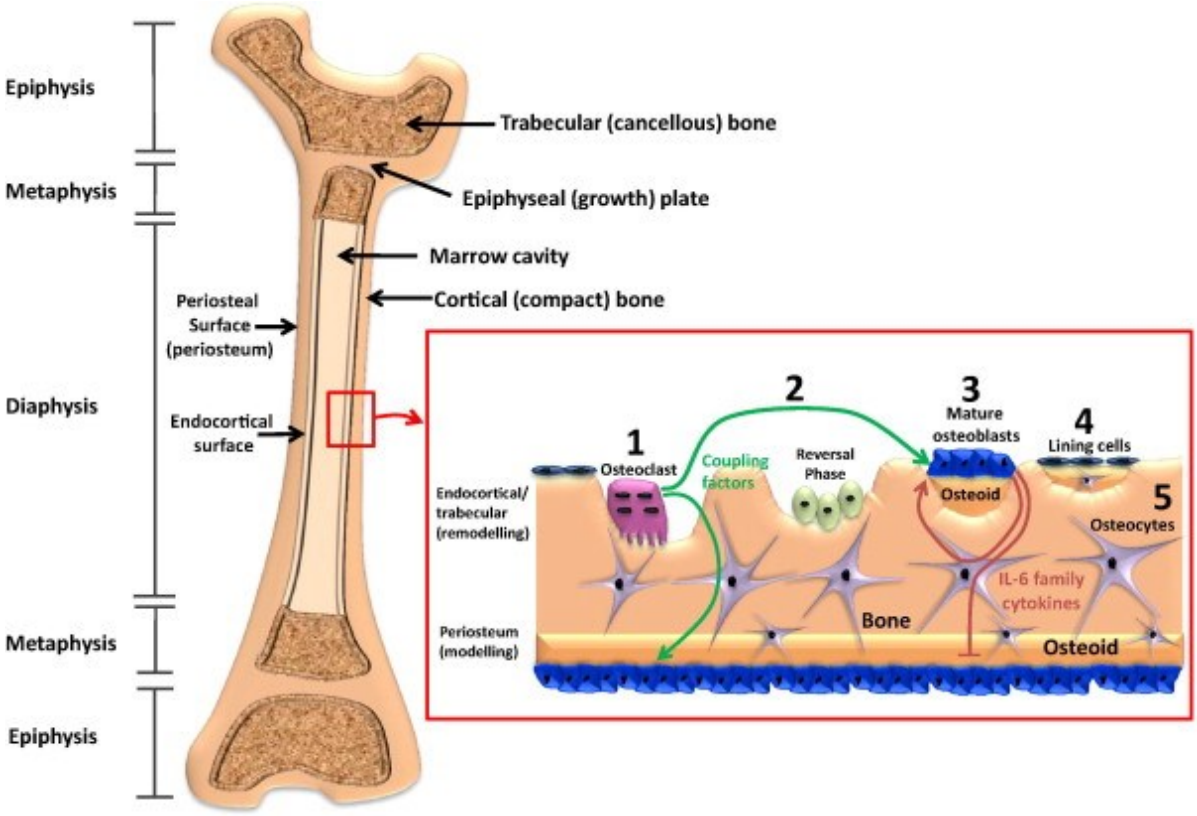

Fonte: Sims, N. A. & Vrahnas, C.(SIMS; VRAHNAS, 2014)

The development of a scaffold requires the use of some characteristics to make it similar to native tissue. Bones present different compositions along the human body. For example, the proximal tibial trabecular bone has typically 1 mm in diameter, 50-90% porosity, 0.30±0.10 g/cm^3 apparent density, 5.3 MPa maximum strength and 445 MPa elastic modulus.

In contrast, cortical femoral bone is compact with limited voids, and presents 3-12% porosity, 1.85±0.06 g/cm^3 apparent density, 193 MPa maximum strength and 17 GPa modulus of elasticity (KARAGEORGIOU; KAPLAN, 2005).

The articular cartilage and the bone represent the anatomy of the osteochondral tissue (Fig.2). The cartilage is a translucent tissue appearance (NOOEAID et al., 2012). The main components of cartilage are contains chondrocytes and extracellular matrix (ECM); it consists of water, proteoglycan and a collagen fiber network. Below the articular cartilage is the subchondral bone. In this zone, the bone maintains the shape of the contour of the articular bone and creates a biomechanical environment appropriate for the differentiation and development of cartilage (YANG; TEMENOFF, 2009). This is different from cartilage in which the major subchondral bone components include hydroxyapatite (Hap) and glycoproteins (type I and V collagen, fibronectin and laminin) (NOOEAID et al., 2012). The considerable amount of collagen fibers type I and Hap provides resistance to compression and strong stiffness for the subchondral bone movements (ARVIDSON et al., 2011). In comparison to the cartilage, subchondral bone has a higher compression modulus and a lower elastic modulus. Because its complexity, the presents a multicomponent structure (KEENEY; PANDIT, 2009; LOPA; MADRY, 2014).

Figure 2 - Osteochondral tissue structure and cross section of the long bone and its zonal cartilage.

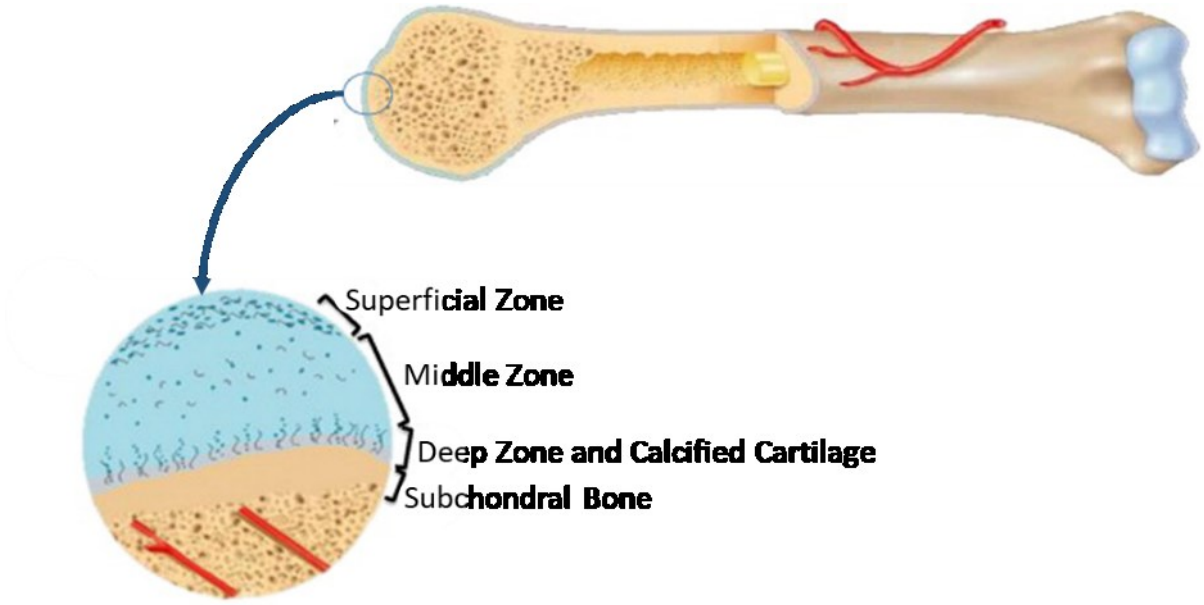

Fonte: Adapted of Nukavarapu and Dorcemus (NUKAVARAPU; DORCEMUS, 2013).

The thickness of the cartilage in the region of the subchondral bone is about 2.3 mm. The distance between the surface of the cartilage and the subchondral plate is about ~2.3 mm. The two levels of porosity distribution of the subchondral bone were as follows: approximately 20% porosity at 2.3 mm, corresponding to the subchondral bone plate and about 60% porosity, above 2.3 mm, corresponding to the spongy bone. The elastic modulus in the direction parallel to the cartilage is 42.2, 13 and 2.6 MPa for surface regions, while the elastic modulus in a perpendicular direction for the cartilage is 15.6, 4.7 and 1.1 MPa (ANSARI; KHORSHIDI; KARKHANEH, 2019; BIAN et al., 2016).

2.2. BONE AND OSTEOCHONDRAL REGENERATION AND USE OF BIOMATERIALS

Bone tissue has biological systems that have the ability to stimulate the regeneration of the fracture naturally. However, when these fractures are large and/or complex, they have some limitations to regenerate the bone properly. To widen the applicability of biomaterials, they are made of different materials, distinct compositions, to reproduce properly the native tissue that will be regenerated or replaced (AGARWAL; GARCÍA, 2015).

Usually the process of bone regeneration is composed of four steps. The first stage is the inflammatory response, which leads to differentiation in chondrocytes signaling stem cells,

and will produce cartilage and osteoblasts, forming a new bone. Later, the cartilaginous matrix will be mineralized, and then it will be "resorbed" forming the bone. This formation generates the primary bone, which undergoes a remodeling of the preformed bone callus; a second resorption occurs, which restores the anatomical structure (GERSTENFELD et al., 2003).

Throughout the injury repair process, bone morphogenetic proteins (BMPs) are produced, which with function independently or in collaboration with other proteins. BMPs stimulate a cascade of events that will promote the formation of cartilage and bone (DESCHASEAUX; SENSÉBÉ; HEYMANN, 2009).

Potential solutions for these problems equivalent to bone regeneration, would be the development of engineering structures by combining scaffolding, cells and/or soluble/mechanical factors (ROSETI et al., 2017). Thus, biomaterials are developed and studied to aid in the regeneration of bone and other tissues mainly of the human body. The composition of these biomaterials for bone regeneration usually aggregates an osteoinductive ceramic material, together with a biodegradable bioactive polymer. Some of these biomaterials are being tested using on their surfaces proteins that stimulate the differentiation of cells capable of creating new bone (FAROKHI et al., 2018; FERNANDEZ-YAGUE et al., 2015; GRIFFITH, 2002; HO-SHUI-LING et al., 2018; JUDAS et al., 2012; LEGEROS, 2002, 2008; MATASSI et al., 2011; SAI NIEVETHITHA et al., 2017).

A scaffold is an artificial structure used in the support for new tissue formation (BOUET et al., 2015). The scaffolds are commonly used in acellular systems or as a vehicle for cells and/or drugs, thus allowing the injured site to be colonized by host cells for regeneration purposes. Scaffolds can receive different types of cells before they are implanted, thus increasing the ability to promote bone formation in vivo, or to differentiate into an osteogenic lineage or release of specific soluble molecules. Another possibility is the use of scaffolds prepared with soluble molecules, such as antibiotics, chemotherapeutic agents or growth factors, i.e., bone morphogenetic proteins and vascular growth factor of the endothelium (ROSETI et al., 2017).

The development of scaffolds that support osteochondral regeneration should follow the principles of an "optimal" construction of this structure, since it should have a 3D environment as bioactive, biodegradable components that are compatible with the tissue to be implanted, for regeneration should effective.

The osteochondral tissue requires a complex structure that covers different layers with different environments so that the cells can naturally colonize this new environment. The choice of materials and growth factors should take into account the mechanical and biological requirements and thus develop an ideal structure.

The cartilage contains chondrocytes and ECM, which consists of water, proteoglycan and collagen, as well as fiber network. The cartilage can be divided in four different zones: surface, medium, deep and calcified cartilage (MADRY; VAN DIJK; MUELLER-GERBL, 2010). Each zone has a unique composition and cell organization as well as ECM proteins (GOLDRING, 2012). Below the calcified zone of the articular cartilage is the subchondral bone. The underlying subchondral bone is responsible for to maintaining the contour shape of the joint bone and creating an appropriate biomechanical environment for differentiation and development of cartilage (YANG; TEMENOFF, 2009).

Different materials are used for subchondral bone reconstruction. Subchondral bone can withstand the main compressive force at the joint and has a lower modulus of elasticity. In this way, it allows the use of materials for subchondral bone regeneration that have mechanical resistance. This bone presents vascularization, which allows the circulation of nutrients to itself and to the articular cartilage. Thus, materials that facilitate bone growth and promote the integration of bone and cartilage are preferred, such as bioglass and bioceramics (CHEN et al., 2011; ZHANG et al., 2013). Some works mention synthetic polymers such as PLA (WAYNE et al., 2005) and PCL (DU et al., 2017), which allow adequate mechanical properties for the scaffolds, and hydroxyapatite to promote the construction of the bony part, thus developing bilayer structures very close to the native osteochondral tissue.

2.3. SCAFFOLD FEATURES, COMPOSITION AND PROCESSING

The scaffold needs to be biocompatible and not toxic to the implanted organisms. Cells in contact with this structure need to adhere, proliferate, differentiate and thus produce the extracellular matrix at the site (BOUET et al., 2015; HENKEL et al., 2013). Structure must be biodegradable and/or bioabsorbable so that throughout the regenerative process this structure is degraded giving rise to a new tissue. In addition, the degradation products should be capable of being excreted by the body. Mechanical properties, resistance during degradation is critical in load bearing implants, because the load must be gradually transferred to the regenerating tissue (CHAN; LEONG, 2008; O'BRIEN, 2011). The bioactivity of the scaffolds is intended to promote the cell an adequate migration or differentiation of the tissue and integration into the

host tissue, avoiding undesirable processes, such as scars (INZANA et al., 2014; OVERMAN et al., 2013b; ZHANG et al., 2015).

A critical factor of the scaffolds when in initial contact with the native tissue is the surface of the scaffold because it will be a foreign body installing itself in a complex biological system, so that different biological processes activate the immunity of this system. Thus, this limitation must be mitigated by treating the scaffold surface with some cell growth stimulating expression protein as well as some material that will stimulate colonization avoiding rejection (AMINI; LAURENCIN; NUKAVARAPU, 2012).

Each tissue to regenerate has some physical and chemical characteristics that can be obtained by the method of production of the scaffolds and by the materials used. Considering that the bone tissue presents a heterogeneous, non-continuous structure, the development of scaffolds can be varied (ATESOK et al., 2016).

The osteochondral tissue consists of two fractions: hyaline cartilage and subchondral bone (BECK; DETAMORE, 2013; DI LUCA; VAN BLITTERSWIJK; MORONI, 2015). The osteochondral region exhibits cellular and molecular structures transitions from the cartilage to the bone layer. Cartilage can be divided into three zones of the surface: superficial, transitional, and radial zone. A composition of cells and molecules of ECM (YANG; TEMENOFF, 2009) recognize each zone. Chondrocytes are the only type of cell present in cartilage that represent 2% (wt) of the components in this tissue. There are different sizes and orientations along the different segments of the cartilage joint (ANSARI; KHORSHIDI; KARKHANEH, 2019).

Scaffolds can be produced using different manufacturing techniques. It is important to take into account porosity and interconnectivity between pores, in addition to pore size, as this will influence the colonization of cells. An average size for growth, proliferation and cell adhesion is in the range of 100-500 μm, and vascularization may occur in addition to the regeneration of bone tissue (THAVORNYUTIKARN et al., 2014).

Various materials are being used to produce scaffolds (Table 1), such as polymers, ceramics, hybrids, components, either natural or synthetic. These materials are defined according to the application, as well as the purpose of regeneration (MATASSI et al., 2011).

Natural polymers such as chitosan, chitin, collagen, glycosaminoglycans, gelatin, elastin, and bacterial cellulose have been used in various applications in tissue engineering (DI MARTINO; SITTINGER; RISBUD, 2005; FARRELL et al., 2006; KEOGH; O'BRIEN; DALY, 2010; PIAIA; PAES; PORTO, 2014; YAO et al., 2015). Some of these polymers are

present in the ECM of many native tissues, which enhance the adhesion and the functionality of the cells (FERNANDEZ-YAGUE et al., 2015). In this way, these polymers will support the cellular growth as well as the formation of new tissue.

In the search to develop structures with characteristics more similar as possible to the recovering tissues, other materials are used together with the polymers. Bioactive inorganic materials with properties such as biocompatible and osteoconductive, such as hydroxyapatite (HAp) and tricalcium phosphate (TCP) have been used in bone tissue engineering (ISHACK et al., 2015; LOCA et al., 2015). The respective properties are due to the chemical composition of these materials, which are close to the inorganic mineral phase found in the bone tissue (LEGEROS, 2002, 2008).

Table 1 - A brief list of materials for bone and osteochondral regeneration.

Materials	Tissue regenerated	Type	Year	Reference
calcium phosphate/ chitosan	Bone	membranes	2019	(CHEN et al., 2019)
chitosan/silk fibroin	bone	hidrogels	2019	(WU et al., 2019)
silk fibroin/chitosan/nano-hydroxyapatite	bone	scaffold	2017	(YE et al., 2017)
chitosan/hydroxyapatite/b-TCP	bone	scaffold	2015	(SHAVANDI et al., 2015)
gellan-gum/ hydroxyapatite	osteochondral	hidrogel	2018	(PEREIRA et al., 2018)
silk fibroin, chitosan, and nano-hydroxyapatite	osteochondral	scaffold	2019	(XIAO et al., 2019)
Silk/silk-nanoCaP	osteochondral	scaffold	2015	(YAN et al., 2015)

Bone regeneration can be accomplished by membranes, hydrogels, or scaffolds applied in the injured tissue. Histological and histomorphometric analyses revealed that the calcium phosphate/chitosan membrane had the most effective bone regeneration compared to the other two hybrid membranes. At three-week post-surgery, the calcium phosphate/chitosan membrane

could enhance new bone generation up to 57% of the original bone defect area (CHEN et al., 2019).

The resulting chitosan/silk fibroin/bioactive gels were found to exhibit well defined inject ability and to undergo rapid gelation at physiological temperature and pH. They were highly porous and showed the ability to administer Si, Ca and Cu ions at their respective safe doses in a sustained and controlled manner. In vitro studies revealed that the gels supported the growth of seeded MC3T3-E1 and human umbilical vein endothelial cells, and effectively induced them toward osteogenesis and angiogenesis, respectively(WU et al., 2019).

In the same way, the osteochondral regeneration can be carried out with the help of the supports, produced by chitosan, silk, and ceramic material. The scaffold (silk/chitosan/hydroxyapatite) strongly absorbs water, and has a suitable degradation rate, sufficient space for cell growth and proliferation, and good resistance to compression. Thus, the scaffold can provide sufficient nutrients and space for cell growth, proliferation, and migration. Further, bone marrow mesenchymal stem cells seeded onto the scaffold closely attach to the scaffold and stably grow and proliferate, indicating that the scaffold has good biocompatibility with no cytotoxicity (XIAO et al., 2019).

Natural polymers such as silk fibroin are also being used to evaluate osteochondral regeneration. Yan and his collaborators have identified that silk and nanoCaP promote osteogenesis differentiation, since the structure studied presented support for cell growth and cell viability because it presents an adequate porosity (20-100 μm) and when this structure was implanted there was no rejection by the body of the material (YAN et al., 2015).

Liu and colleagues used chitosan (CH), silk fibroin (SF) and HAp as CH/SF/HAp compounds, which were electroformed in nanofibrous membrane units with gradual composition and growth characteristics(LIU et al., 2018a). A developed structure was intended for osteochondral repair. The lower layer was constructed based on the CH/HAp components and served as the subchondral layer, while the nanofibrous membrane functioned as a middle layer to mimic a calcified layer and an upper layer was constructed using chondral CH/SF composites layer. The nanofibrous showed to be permeable to some molecules with limited molecular weight and was able to prevent the cells migrating along the wall, pressing like a calcified layer in the osteochondral matrix. At times, they were more subtle to promote the growth of both chondrocytes and osteoblasts were shown in their chondrocyte layer and in the bone layer, respectively. They were able to preserve of the chondrocyte medium and

mineralization of neotissues in the bone layer. The results of this type of scaffolds were analogous to the osteochondral matrix so that they have potential without osteochondral tissue repair (LIU et al., 2018b).

2.3.1. New scaffolds: gap in knowledge

New processing technologies and materials with different parameters have been employed in the production of new structures for use in tissue engineering, all following important features in structure maintenance and material compatibility with native tissue (BIAN et al., 2016; CASTRO; PATEL; ZHANG, 2015; DI LUCA; VAN BLITTERSWIJK; MORONI, 2015; DU et al., 2017; SIVASHANKARI; PRABAHARAN, 2016).

Polymers such as chitosan allow the structure to be able to withstand different stresses in the structure (LI et al., 2017a; MARTINS et al., 2014; PALLELA et al., 2012; ZHANG et al., 2016b). Depending on the fabric, it is necessary to add other polymers to better structure the scaffold. For bone and osteochondral substitutes, where bone tissue is present, it is important to have osteoinductive materials to restore the fractured bone (KUCHARSKA et al., 2012; SIQUEIRA et al., 2015).

Like this, bioactive ceramic scaffolds represent competitive options for clinical bone reconstruction, but their widespread use is restricted by inherent brittleness and poor mechanical performance under load. A strong, bioactive ceramic scaffold (strontium-hardstononite-gahnite) has been combined with single and multiple layers of silk fibroin to increase its toughness, producing composite scaffolds that combine with the mechanical properties of spongy bone and have increased capacity to promote osteogenesis in vitro. The results show that silk coating on a single ceramic scaffold can lead to a simple and effective enhancement of its mechanical and biological properties. In this way, the scaffolds can serve a wide range of applications in clinical bone reconstruction and the influence of ceramic microstructure on the effectiveness of silk coating as a reinforcing method when applied to different types of bone graft ceramic replacements (LI et al., 2017b).

Besides that, macroporous b-tricalcium phosphate (β-TCP) scaffolds were evaluated as potential carriers and delivery systems for bone morphogenetic protein-2 (BMP-2). Chemical etching was performed to increase the available surface and thus the protein loading. Scanning electron microscopy revealed interconnected porosity (64%) and a microporous surface after chemical etching. Histological observations confirmed the activity of the BMP-2 released from the scaffolds. The incorporation of BMP-2 resulted in an amount of newly formed bone that

was 1.3 times higher than with unloaded scaffolds. These results indicate the suitability of chemically etched β-TCP scaffolds as BMP-2 carriers, in the context of bone regeneration (SOHIER et al., 2010).

Silk fibroin is a biocompatible protein and has a dissolving capacity in water that allows it to adapt to specific structures and morphology. It can be employed for structure construction as well as for regulating the release kinetics of the incorporated compounds (WANG et al., 2007).

In recent years, research has been conducted using different proportions of chitosan, β-TCP and silk for the construction of scaffolds with application in bone and osteochondral regeneration. Their results identified that with the mixing of the components and the different processing, the scaffolds produced had a distinct environment, with pore sizes and porosity suitable for applications in lesions of different sizes.

The contribution of the work was the construction of a structure to be applied for bone regeneration, a mixture of chitosan and β-TCP with coated of silk fibroin. Chitosan and β-TCP were the fraction of support and the osteoinductive, while the silk completed with the surface coated, increasing the biocompatibility and nutrient flow through the structure. Throughout the work, the production of a second structure was evaluated, which produced two layers for osteochondral regeneration. The scaffold was produced one layer contains only silk and the other the mixture chitosan and β-TCP, and the structure was stabilized by genipin as a crosslinking agent.

Chapter 3– MATERIALS AND METHODS

3.1.MATERIALS

The materials used to develop this thesis, as detailed in next sections, were medium-molecular weight chitosan (CH, 300-1000 cps, degree of desacetylation ≥ 90%, Glentham Life Sciences), β-tricalcium phosphate (β-TCP), cocoons of *Bombyx mori* kindly supplied by the association APPACDM (Castelo Branco, Portugal), and bone morphogenetic proteins (BMP) (PeproTech, Portugal). All other chemicals were reagent grade and were used as received.

3.1.1. Chitosan

Chitosan is a natural polysaccharide, isolated from chitin by hydrolyzing acetyl groups ($COCH_3$), composed of N-acetyl-D-glucosamine and D-glucosamine, linked by β-1,4, forming a long linear chain, composed of three reactive functional groups, one amino group and two primary and the positions of the carbons C-2, C-3 and C-6 respectively. Chitosan has been used as a natural polymer in engineering applications of bone tissue in various forms (MINA et al., 2015; SIVASHANKARI; PRABAHARAN, 2016; TEIMOURI et al., 2015; ZANIN et al., 2015) because of its non-toxic properties, biocompatibility and biodegradation. Chitosan cytocompatibility is due to its chemical structure being similar to glycosaminoglycan, the main component of the extracellular bone matrix (LOW et al., 2015; SHAVANDI et al., 2015).

Chitosan can be used as a membrane for skin repair or as a scaffold for regeneration of a more complex tissue such as osteochondral. Depending on the purpose different aggregate materials may be added to chitosan (AZEVEDO et al., 2014; HARRIS et al., 2011; YIN et al., 2003).

To purify 10 g of chitosan (300-1000cps), 1 L solution of acetic acid (2 vol.%) was prepared. The mixture components were added slowly under stirring at room temperature for 12 h. A nylon filter and a Milipore membrane (5 μm) were used to remove undissolved residues. Thereafter, it was washed with distilled water several times. After the filtration steps, the solution remained at room temperature, the pH was corrected to 8, with 2 M NaOH to promote polymer precipitation. Afterwards, a solution was again filtered, to obtain the precipitated chitosan. Finally, when the pH reached 7, 300mL of an ethanol solution were precipitated to the chitosan, and it was filtered with nylon filter in each washing process. This procedure was repeated using ethanol-water solutions (80/20 and 50/50 and 90/10 in volume). Thereafter, the

suspension was filtered, removing the ethanol solution solvent from the purified chitosan. The material was transferred to Petri dishes to be frozen at -80 °C. Then, the frozen material was put into a lyophilize for at least 4 days to completely remove the water. After was done RMN analysis (SIGNINI; SÉRGIO, 2001).

3.1.2. β-tricalcium phosphate

Tricalcium phosphate (TCP, $Ca_3(PO_4)_2$) is a bioceramic, which presents polymorphism with three phases: β, α and α', ordered by the order of thermal stability. The β phase crystallizes in the hexagonal, the α phase in the orthorhombic and the α' phase in the monoclinic system. The phase transition α → α' occurs at 1475 ± 5 ° C; the phase transition β → α at 115 ± 10 ° C. Below this temperature, the reverse transition must occur, α → β. However, if the cooling rate is too high, the metastable α phase is preserved at room temperature (CARUTA, 2006; SCHWARTZ, 2010).

The use of tricalcium phosphate (β-TCP) is increasing due to its biocompatibility and bioactivity (FABBRI; CELOTTI; RAVAGLIOLI, 1994; WANG; JAIN, 2010). Bioabsorption and bioresorption occur through osteoclastic activity (ROOHANI-ESFAHANI et al., 2013). The main characteristic of this material is that it can build a direct chemical bond with the bone tissue (ARPORNMAEKLONG; PRESSLER, 2018) and this interaction is governed by the physical and chemical properties of the material (JAHAN; TABRIZIAN, 2015). However, low fracture toughness and wear resistance are considered as the main deficiencies of ceramics (IVIGLIA et al., 2016) and thus they must be used in association with other materials to compensate this characteristic.

Different polymeric materials (chitosan, silk, and gelatin) have been used to increase the mechanical behavior of the ceramic material, so the structures produced are more likely to be used in bone regeneration. The precise regeneration in addition to bioactive and biodegradable materials requires that these materials have mechanical properties and 3D structures so that an effective and most similar regeneration of the injured tissue occurs (KUCHARSKA et al., 2012; MAJI et al., 2018; PINA et al., 2017).

The synthesis of β-TCP was performed using following solid state reaction from two reagents in the form of powders, calcium hydrogen phosphate ($CaHPO_4$), also known as monetite, and calcium carbonate ($CaCO_3$):

$$CaCO_3 + 2CaHPO_4 \rightarrow \beta\text{-}Ca_3(PO_4)_2 + CO_2 + H_2O$$

The mixture of the two powders was carried out in mortar, with addition of acetone to facilitate the homogenization. Then, the mixture was place into crucibles and heated to 1050 °C, at a rate of 5 °C/min until reaching the desired maximum temperature. After 6 h, the mixture was slowly cooled down to room temperature.

After completion of the synthesis, powder samples were taken for characterization by X-ray diffraction (XRD), to verify the present phase(s), and their particle size distribution was also determined.

Figure 3 - Flowchart of the synthesis of ß-TCP.

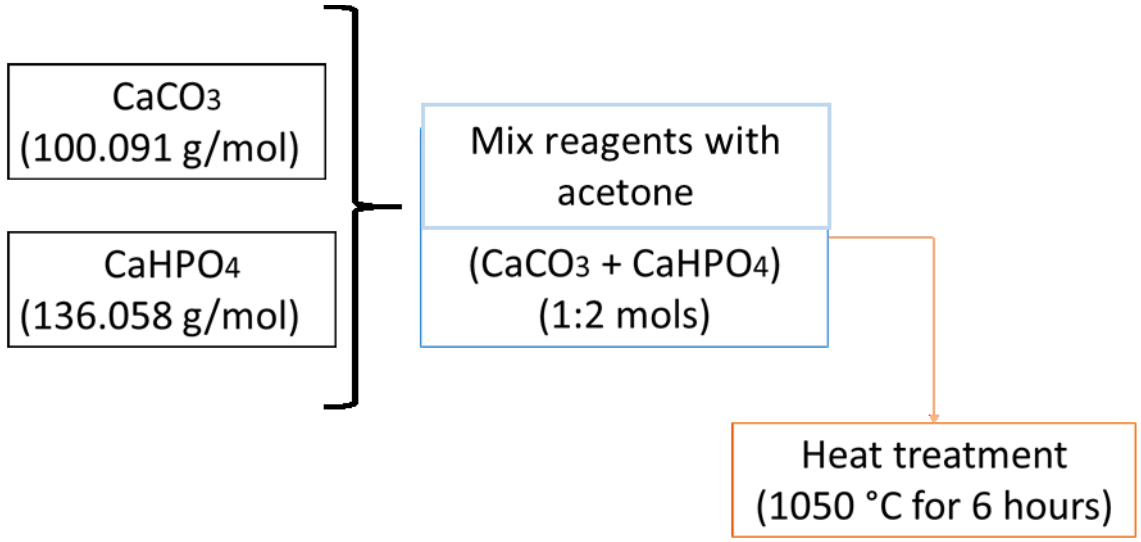

3.1.3. Silk fibroin

Silk comes from the *Bombyx mori* cocoon; it is a natural polymer, a kind of protein fiber. It is naturally composed of a filament nucleus protein, silk fibroin (SF), and a glue coating consisting of a serine protein family. SF consists of heavy (H) and light (L) polypeptides of ~ 390 kDa and ~ 26 kDa, respectively. It is bound by a disulfide bond at the C-terminus of the two subunits, which is associated with the H-L complex, thus having hydrophobic interactions (RIBEIRO et al., 2018; TANAKA et al., 1999; ZHANG; YAN; LI, 2009).

SF can be used in the manufacture of three-dimensional biodegradable scaffolds because of its non-inflammatory responses, low antigenicity, good biocompatibility,

controllable biodegradability and excellent mechanical strength (LEE et al., 2017; MAUNEY et al., 2007; MORI; TSUKADA, 2000). SF scaffolds are used in different tissues, such as: skeletal tissue (cartilage, bone) and conjunctive in the skin (FAROKHI et al., 2018; GOBIN; FROUDE; MATHUR, 2005; LI et al., 2017; RIBEIRO et al., 2018; WU et al., 2016).

SF cocoons were submitted to degumming process. Cocoons were boiled in sodium carbonate solution (0.02 M) for 1 h and then rinsed with distilled water. The degummed fibers were dried at room temperature. (KIM et al., 2005) and dissolved using 9.3 M lithium bromide solution for 4 h at 70 ºC. The resulting solution was dialyzed in distilled water for four days using benzoylated dialysis tubing. The obtained aqueous solution was centrifuged at 7 ºC, in 5000 rpm for 20 min, according to Figure 4.

Figure 4 – Representation of the production of silk fibroin.

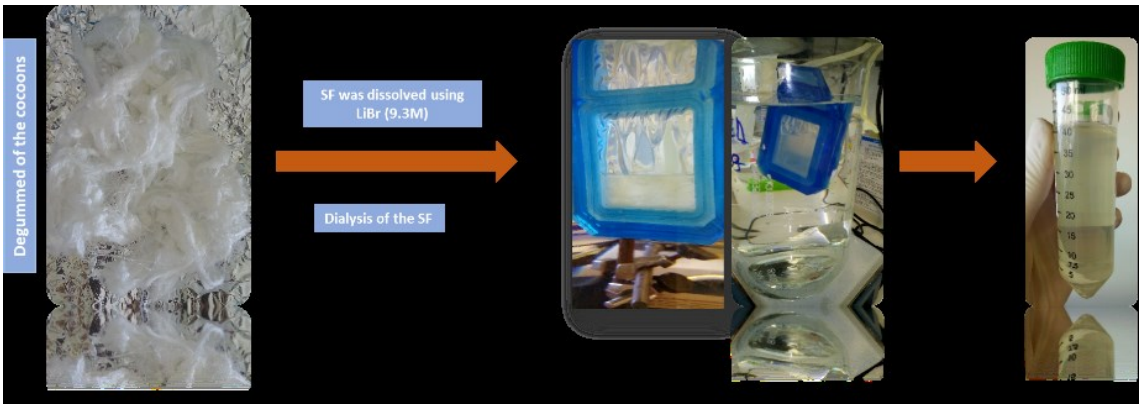

Finally, the tubing was carefully rinsed in distilled water, and the concentrated solution was collected, and kept at 4 °C before use.

3.1.4. Additives

Genipin is a natural compound extracted from the gardenia fruit (*Garnedia jasminoides*). It is an aglycone derived from a glycoside, called geniposide. Genipin has been used as a crosslinking agent for the synthesis of elastic gels in wound healing (HUH et al., 2018; QIU et al., 2013; SILVA et al., 2008a). It reacts with amino groups in amino acids or proteins to form dark blue pigments (CHIONO et al., 2008).

Bone morphological proteins (BMPs) are produced during bone repair. These proteins work independently or in collaboration with other proteins. The BMPs stimulate a series of

events to promote the formation of cartilage and bone (DESCHASEAUX; SENSÉBÉ; HEYMANN, 2009).

3.2. SCAFFOLDS PRODUCTION AND CHARACTERIZATION

The scaffolds were prepared to construct a 3D environment, in which a flow of nutrients and cells may occur (FENG; HE; YE, 2018; LEVINGSTONE et al., 2014; OLIVEIRA et al., 2006).

The freeze-drying process enables the production of scaffolds with a controlled pore range throughout the process. Freezing and sublimation need to be well defined to control the formation of the crystals that subsequently form the pores (HAUGH; MURPHY; O'BRIEN, 2009).

Scaffolds were produced for two purposes: bone regeneration; and osteochondral regeneration. In Figure 5, the steps of constructing and characterizing each structure can be identified and subsequently the respective methods are described.

Figure 5 - Scheme of production and characterization of structures for bone (top) and osteochondral regeneration (bottom).

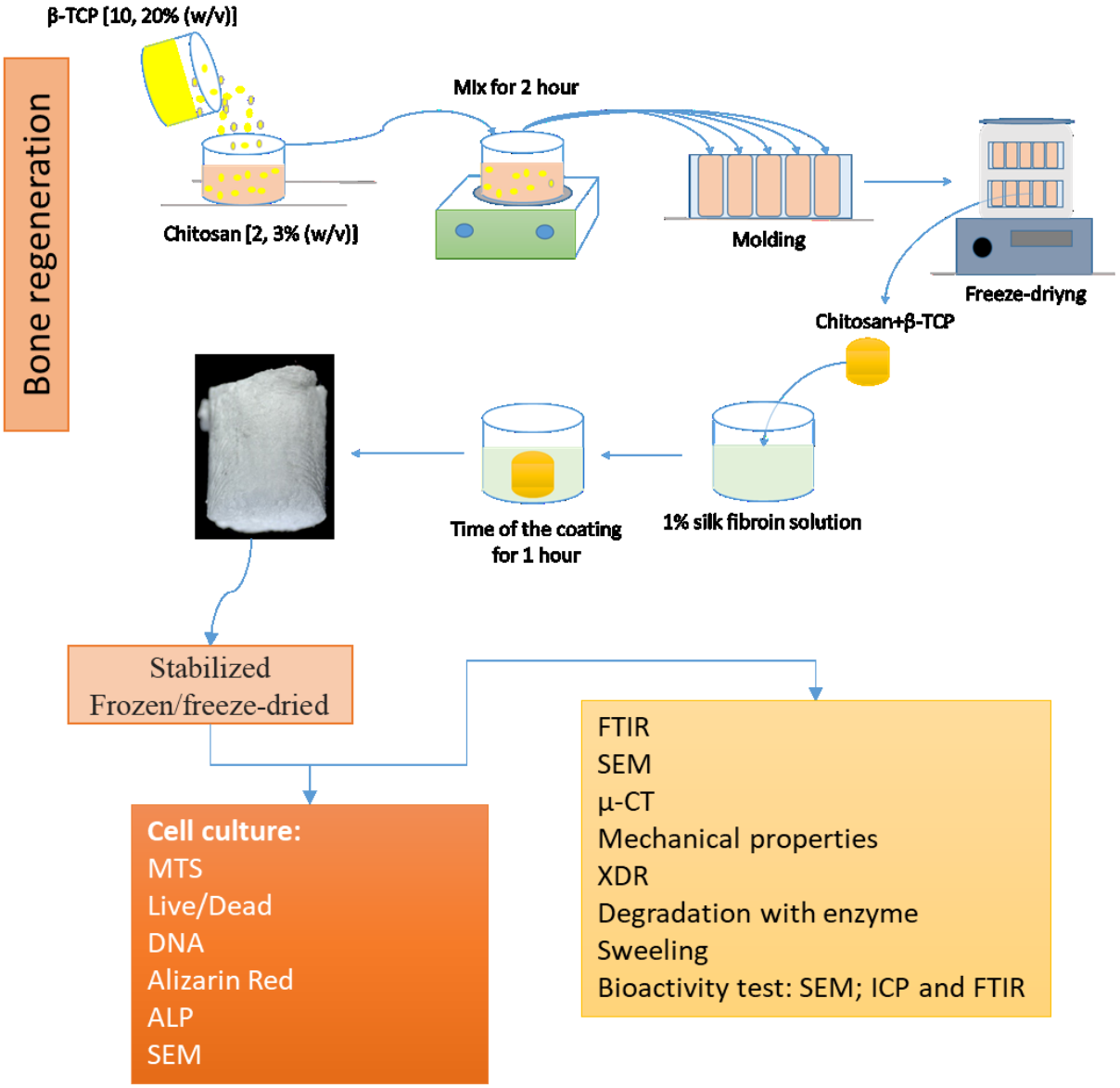

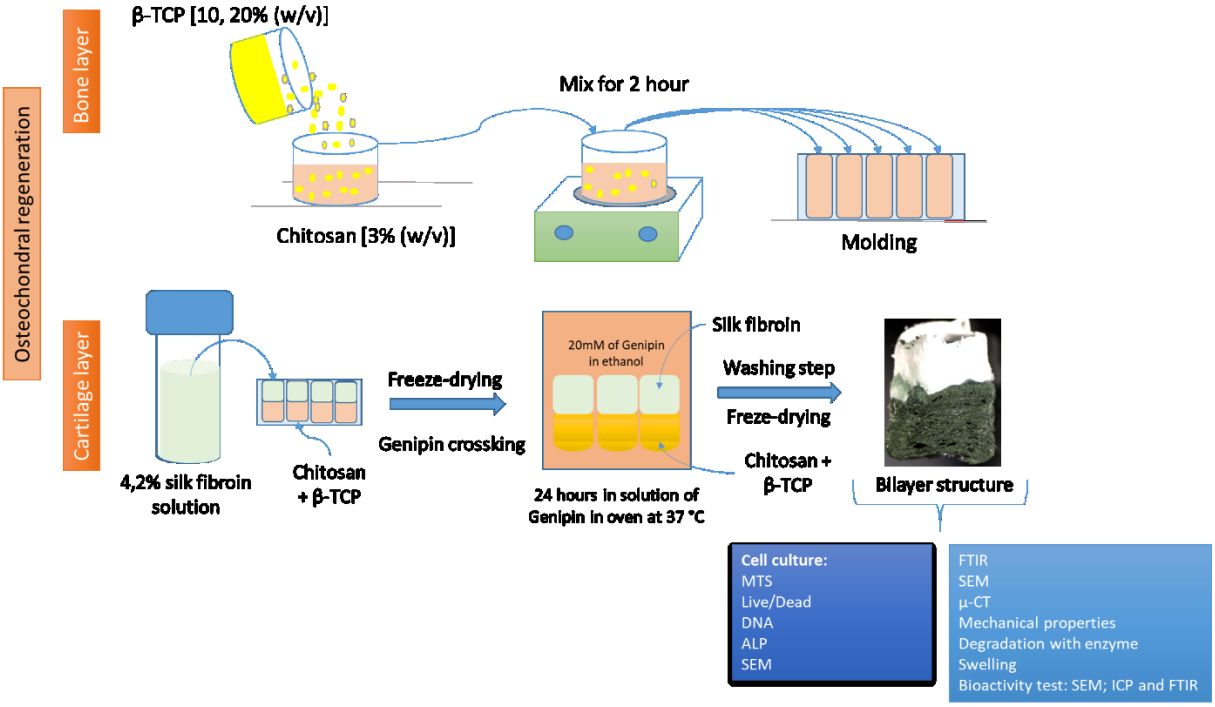

3.2.1.Production of scaffolds for bone regeneration

In the production of the scaffolds 2 and 3 wt.% chitosan concentration were used dissolved in 3 vol% acetic acid, for 3 days at 25 °C, in constant agitation. Then, it was added 10 and 20 wt.% β-TCP (w/v) in each concentration of chitosan, to obtain four different solutions, as shown in Table 2.

Table 2 - Mixtures of chitosan and β-TCP.

Sample	wt.% chitosan	wt.% β-TCP
β-TCP powder	-	100
CH2	2	-
CH3	3	-
CH2BT10	2	10
CH2BT20	2	20
CH3BT10	3	10
CH3BT20	3	20

Mixtures of chitosan and β-TCP were agitated for 2 h and then set into a mold at -80 °C for freeze-drying. The samples were neutralized with a 4% NaOH solution for 30 min. The pH of the samples was then adjusted to 7 and then they were lyophilized again. Later, the samples were coated with a 1% silk fibroin, Figure 6.

Figure 6 – Scheme of coating scaffolds of chitosan/β-TCP with silk fibroins.

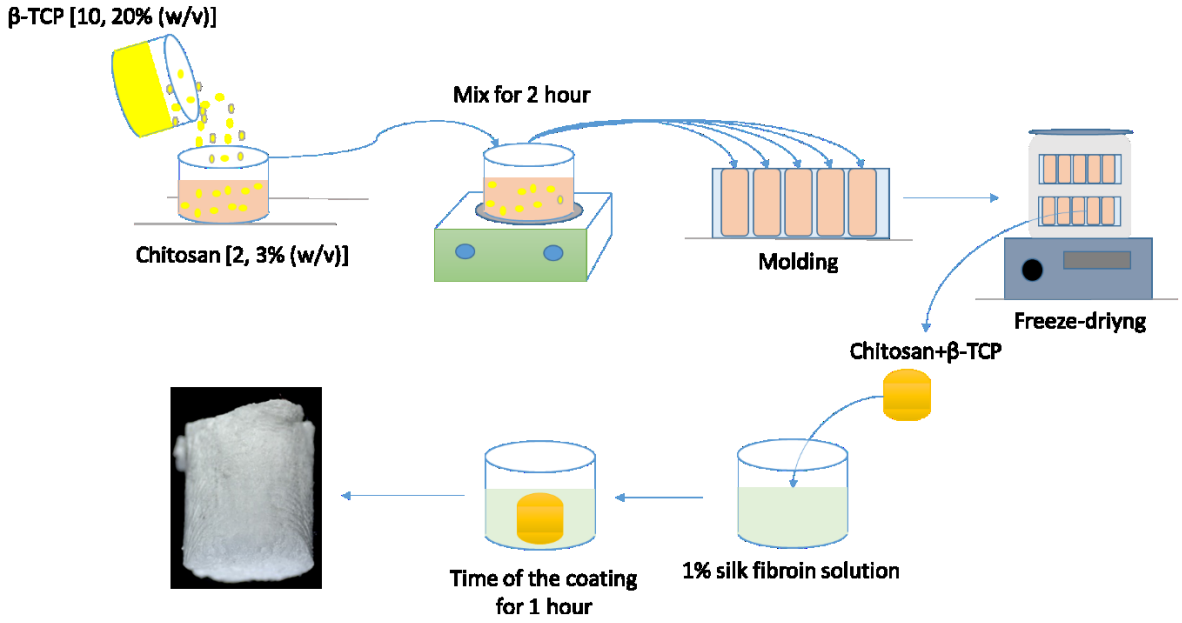

The samples were frozen and lyophilized. Then they were stabilized with a solution of methanol and water (80:20 in volume). Finally, the samples were lyophilized to permit the characterization tests of the samples, as in Table 3.

Table 3 - Mixtures of chitosan and β-TCP with 1 vol.% silk fibroin coating.

Sample	wt.% chitosan	wt.% β-TCP
β-TCP powder	-	100
CH2SF	2	-
CH3SF	3	-
CH2BT10SF	2	10
CH2BT20SF	2	20
CH3BT10SF	3	10
CH3BT20SF	3	20

3.2.2.Production of scaffolds for osteochondral regeneration

Three different scaffolds were fabricated for optimization of the base scaffolds for the cartilage-bone regions. Solutions of 3 wt.% chitosan dissolved in 3 vol.% of acetic acid were prepared, and left for 3 days at 25 °C, in constant agitation. Then, 10 and 20 wt.% β-TCP were added to chitosan, producing three different solutions. CSG is a bilayer scaffold of silk and chitosan; CSG10 is a bilayer with silk and chitosan/ β-TCP (10%wt); CSG20 is a bilayer with silk and chitosan/ β-TCP (20%wt), as shown in Table 4.

Table 4 - Mixtures of chitosan and β-TCP.

Sample	wt.% Chitosan	Wt.% β-TCP
CSG	3	-
CBSG10	3	10
CBSG20	3	20

The samples were used in the next stage of production of a bilayer structure, without neutralization in NaOH solution.

Silk solution was obtained from degummed cocoons of *B. mori,* which were dissolved in LiBr (9.3 M) for 4 h at 70 ºC. The solution was put in cassettes for dialysis for 4 days. The yield was calculated by the dry weight of silk and a concentration of 4.2 vol.% SF was added to the structure.

A bilayer structure was constructed by the junction of CH/β-TCP and SF, and left to freeze for 12 h. Subsequently, the samples were removed from the molds and placed in a solution of 20 mM genipin for 24 h, at 37 ºC in an oven for the crosslinking reaction. Further, the samples were washed and lyophilized. The production scheme is represented in Figure 7.

Figure 7 – Scheme of crosslinking of the samples with genipin.

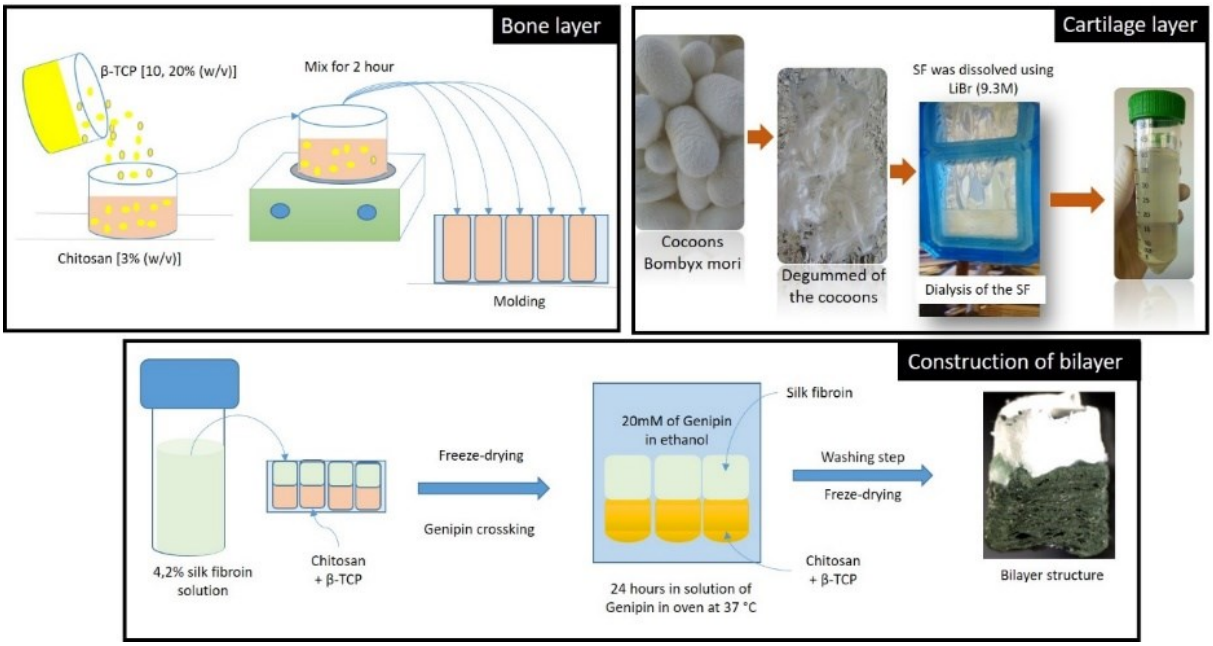

After 12 h, the samples were immersed in 20 mM solution of genipin dissolved in absolute ethanol absolute, for crosslinking, and placed in an oven at 37 °C for 24 h. The samples were then washed to remove genipin, and freeze-dried to allow the characterization tests.

3.2.3. Physical and chemical characterization

3.2.3.1. Morphological and microstructural characterization

The morphologies of the lyophilized samples were examined using scanning electron microscopy (SEM, JSM-6010 LV, JEOL, Japan). Samples were cut using a sheet after being frozen in nitrogen, and previously sputtered with gold. SEM was operated at low vacuum operation, 15 kV, at magnifications of 20 to 3000×.

The microstructure of the scaffolds was evaluated using a high-resolution micro-computed tomography (μ-CT, SkyScan 1272 scanner v1.1.3, Bruker, Boston, USA), with a resolution of pixel size of 8 μm. The X-ray source was set at 71 keV and 140 μA and 300 projections were acquired over a rotation range of 360°. Data sets were reconstructed using standardized cone-beam reconstruction software (NRecon 1.7.1.0, Bruker) and the output format for each sample was bitmap images. A representative data set of 300 slices of a region of interest was used for the analysis of the scaffolds architecture (including both polymeric and ceramic components). For the analysis of the ceramic component in the scaffolds, a threshold

of 120–255 was used. The same representative volume of interest (VOI) was analyzed for all the samples. These data sets were used for morphometric analysis (CT Analyser, v1.17.0.0, Skyscan) and to build the three-dimensional (3D) models (CT vox, v3.3.0 r1412, Skyscan).

3.2.3.2. Fourier Transform Infrared Spectroscopy (FTIR)

Samples were analyzed by Fourier transform infrared spectroscopy (FTIR, IR Prestige 21, Shimadzu, Japan), in the spectral range of 4000-400 cm^{-1}, with measurements in transmittance (%), apodization in Happ-Genzel, with 32 scans resolution of 4 cm^{-1}.

3.2.3.3. Bioactivity test

To evaluate the degradation, the scaffolds was immersed in a simulated body fluid solution (SBF) at 37 °C (KOKUBO et al., 1990) for up to 21 days. The rate of dissolution was measured as the amount of soluble ions (Ca e P) as a function of time. In addition, the deposition rate of the conversion was investigated by FTIR, and SEM. Samples immersed in SBF solution were evaluated by ICP. The SBF composition is similar to that of human blood plasma. It was prepared by dissolving NaCl, $NaHCO_3$, KCl, $K_2HPO_3 \times 3H_2O$, $MgCl_2 \times 6H_2O$ and $CaCl_2$ in distilled water and buffered with $(CH_2OH)_3CNH_2$ and HCl (6N) to adjust the pH value at 7.4.

3.2.3.4. Inductively coupled plasma optical emission spectroscopy (ICP)

Elemental concentrations, phosphor and calcium, in the SBF solution, before and after culturing with scaffolds, were measured using inductively coupled plasma optical emission spectroscopy (ICP-OES; JY2000-2, Jobin Yvon, Horiba, Japan). The solutions were filtered with a 0.22 μm filter, diluted (1:10) in 5% nitric acid (HNO_3) and kept at -20ºC until use. A minimum of 3 samples were used per condition and time point. (RODRIGUES et al., 2015)

3.2.3.5. X-ray diffraction (XRD)

X-ray diffraction (XRD, Bruker D8 Advance, US) was used for analysis of the structure of the green samples. Powder samples with different binder composition were

analyzed, as well as scaffolds after surface treatment. The angle of diffraction was measured at a scanning rate of 2°, with a range of either 4–70° (phase identification) or 25–38° (phase content quantification), with 0.02° steps and 10 s counts per step.

3.2.3.6. In vitro enzymatic degradation

Samples were also evaluated by enzymatic degradation test. Lysozyme (13, 0 mg/l) was prepared by dissolving the enzyme in PBS. The enzyme solution was changed every 48 h. The specimens were removed from the degradation solution at the end of 1, 3, 7, 14 and 21 days. The dry weight of the degraded specimen was measured after drying the sample at 37 °C for 12 h. The weight loss ratio was obtained using the following equation:

$$Weight\ loss\ ratio = \frac{mi - md}{md} * 100\% \qquad \text{Eq. (1)}$$

where *mi* is the initial dry weight of the sample, and *md* is the dry weight of the degraded sample at each time point. Three specimens per group were used for each time point.

3.2.3.7. Evaluation of the swelling behavior

The water-absorbing capacity was determined by gravimetric methods. Samples were immersed in 3 different pH solutions (5.4, 7.4 and 8.2) at 37 ºC. The samples were immersed for periods beginning every 15 min until the completion of 1 h of analysis; the weight of the samples was measured after 24 and 48 h of immersion in the solutions. To measure the weight of samples after swelling, samples were dried in an oven at 37 ºC for 24 h. The swelling ratio was measured by comparing the change in the weight of samples before and after incubating. The percentage of swelling ratio was calculated by the following formula:

$$Swelling\ ratio\ (\%) = (Ww - Wi) \times 100\% \qquad \text{Eq. (2)}$$

where Ww is the weight of the swollen samples and Wi is the initial weight of the samples.

3.2.4. In vitro release of BMP-2 from the functionalized scaffolds

Solutions were prepared using concentrations of 2.5 and 5 μg/ml of rhBMP-2 (PeproTech, Portugal) dissolved in PBS. The solutions were added in bottles with scaffolds (CH3BT10SF and CH3SF), which were immersed for 18 h at 4 °C. Scaffolds in PBS without rhBMP-2 were used as a negative control. After the loading period (18 h) the scaffolds were placed in new bottles with culture medium (DMEM without SBF) to enhance the rhBMP-2 release test in this medium for 72 h. After each incubation period (1; 2; 3; 6; 24 and 72 h), the supernatants were collected and stored at -80 °C. The human BMP-2 ELISA development kit (PeproTech, Portugal) was used to measure the cumulative concentration of BMP-2 released up to 72 h, using the protocol of the kit to quantify BMP-2.

3.2.5. Determination of crosslinking degree

The crosslinking of the scaffolds were evaluated by the modified trypan blue method (SHEN; YANG; RYSER, 1984; SILVA et al., 2016). For the construction of the standard curve, CH was used purified with an acetylation degree of 10%. To quantify the amount of crosslinked and non-crosslinked amines, the samples were immersed in a known trypan solution and the supernatant removed and read at 630 nm after 12 h. The crosslinking degree was calculated as followed:

$$CL\ \% = \frac{(NH3{+}non\ Xlinked\ solution){-}(NH3{+}\ Xlinked\ solution)}{(NH3{+}non - Xlinked\ solution\ )} \qquad \text{Eq. (3)}$$

where NH3+ non-Xlinked and NH3+ Xlinked solution are the free charge amines in non-cross-linked and cross-linked tubes, respectively.

3.3. BIOLOGICAL CHARACTERIZATION

The biological characterization in vitro was performed to preliminarily evaluate the effects of the biocomposites in contact with cell lines, before in vivo tests. All experiments were carried out in four experimental times: 1, 3, 7 and 14 days, in triplicates.

The samples biologically characterized were CH3BT10 and CH3; CH3BT10SF and CH3SF with 1 mm diameter and 3 mm thickness (samples for bone regeneration). The samples for osteochondral regeneration were biologically characterized: CSG, CBSG10 and CBSG20. All samples were previously sterilized with ethylene oxide. Afterwards, the samples were stored in a cool place and with controlled humidity until the test are performed.

The *in vitro* tests with samples for bone regeneration used the MC3T3 cell line (ATCC CRL-2593). From bilayer samples for osteochondral regeneration, two cell lines were used: MC3T3 and ATCD5 chondrocyte-line cells (mouse 129 teratacarcinoma AT805 derived, ECACC, UK), thus forming a co-culture.

MCT3T3 cells, mouse osteogenic cell line were used in vitro tests. The cells were subcultured in flasks using Minimum Essential Medium (α-MEM, Sigma) supplemented with 10 vol.% fetal bovine serum (FBS, Sigma) and 1% penicillin–streptomycin (Gibco). The cells, maintained at 37 °C in a humidified 5% CO_2 atmosphere, were dissociated with 0.25% trypsin-ethylenediaminetetraacetic acid (Sigma), centrifuged, and re-suspended in medium prior to cell seeding, cells passage P25-28.

ATCD5 chondrocyte-line cells were used with bilayer samples . The cells were subcultured, in the passage P30, in flasks using Dulbecco's Modified Eagle Medium- Low glucose (DMEM, Sigma) supplemented with 10 vol.% FBS (Sigma) and 1% penicillin–streptomycin (Gibco). The cells, maintained at 37 °C in a humidified 5%) CO_2 atmosphere, were dissociated with 0.25% trypsin-ethylenediaminetetraacetic acid (Sigma), centrifuged, and re-suspended in medium prior to cell seeding, cells passage P11-15.

On the surface of the samples 80 μL of MC3T3/α-MEM were added, with a cell density of 1×10^5 cell/cm^3 for each study used 24 well-plate. The samples were kept for 2 h in the proper atmosphere, and then 1 ml of culture medium was added to maintain culture for future tests. The medium was replenished every 2 days.

MC3T3 and ATCD5 were the cells used in the structures; a seeding of 100,000 cell/cm^3 was performed from each cell. Initially, the MC3T3 line was added to the chitosan part, and β-TCP after 24 h of cultivation was added to the ATCD5 line on the silk part, thereby forming a co-culture, Figure 8. A double medium was used for culturing cells α-MEM and DMEM. The cells were maintained at 37 °C in a humidified CO_2 (5%) atmosphere.

Figure 8 – Seeded cells in scaffolds for osteochondral regeneration.

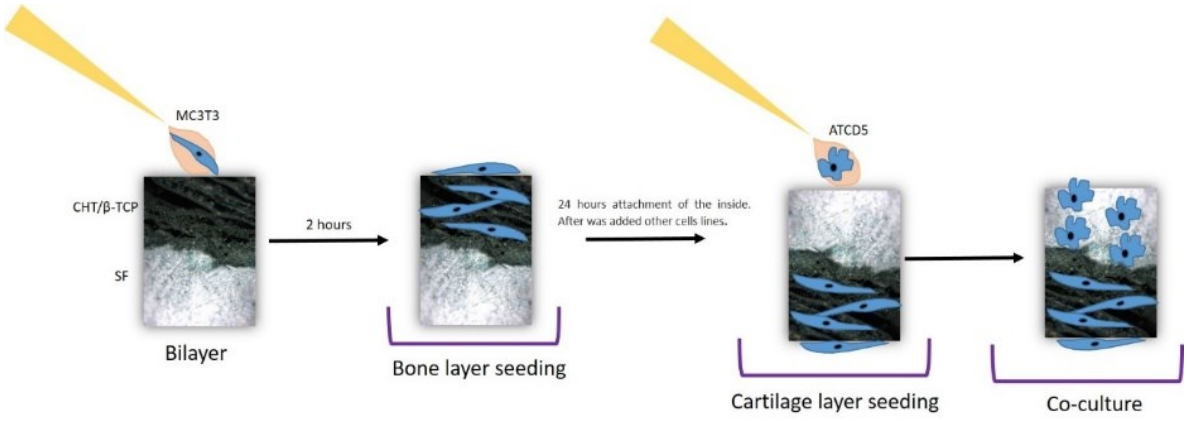

3.3.1. Cytotoxicity test and cell viability (MTS)

Initially, MC3T3 cells were cultured with a cell density of 10,000 cell/cm^3, from a 24-well plate. After 24 h of cell culture on the plate, 300 mL of extract (culture medium that was emerged the material that the structures were produced) was added. Extracts of all scaffolds were prepared as previously described by Gomes et al. (2001). After 24, 48 and 72 h, the cells in culture were analyzed regarding confluence (optical microscopic); cell lysis (trypsin solution); morphology (optical microscopic) and inhibition to cell growth, besides verifying cell viability using MTS [3-(4,5-dimethylthiazol-2-yl)-5- (3-caebozymethoxyphenyl)-2-(4-sulfophenyl)-2H-tetrazolium] with CellTiter 96® AQueous One Solution Cell Proliferation Assay Kit (Promega, Fitchburg, WI, USA), after 1, 3, 7 and 14 days. Alfa-MEM (Sigma) was used without supplemented fetal bovine serum (FBS, Sigma) and without phenol red, only with 1% penicillin–streptomycin. At each point of analysis 5:1 of medium to MTS was left in contact with the samples for 3 h. The solution was then homogenized and a volume of 100 µl was transferred into a 96-well cell culture plate for quantification. Colorimetric measurement of the samples was performed on a microplate reader (Synergy HT; Bio-Tek, VT, USA) at 490 nm.

3.3.2. Cell proliferation

The DNA content of MC3T3-samples constructs was measured using a Quant-iT^{TM} PicoGreen assay kit (Molecular Probes), according to the manufacturer's instructions. The normal procedure described in the kit protocol and the accompanying DNA standards (up to

1,000 ng/ml) were used. Cells (2×10^5 /ml in 1000 µl of α-MEM supplemented with 10% FBS) were seeded in wells containing the scaffolds and incubated for 1, 3, 7 and 14 days, in 24 weel-plate. At the end of each period, the medium was aspirated from the wells and the scaffolds were washed for two times with 500 µl of PBS. Subsequently, 1000 µl of ultra pure water was added to each sample, and frozen at –80 °C for 12 h. The samples were sonicated for 5 min each and then aliquots were taken in duplicate (100 µl) into a 96-well flat bottomed plate. PicoGreen reagent (100 µl) was added to the wells containing standard or sample and the plates were then read at excitation/emission wavelengths of 485/538 nm in a fluorometer (Perking Elmer).

3.3.3. Alkaline phosphatase (ALP) activity

The MC3T3 cells were cultured for 1, 3, 7 and 14 days as described before. In brief, the cell samples were reacted with the ALP mixtures containing 0.1M 2-amino-2-methyl-1-propanol (Sigma), 1mM $MgCl_2$, and 8mM p-nitrophenyl phosphate disodium. After 10 min incubation at 37 °C, the reaction was stopped with 0.1 N NaOH, and the absorbance of the resulting solution was measured photometrically at 405 nm.

3.3.4. Morphology (SEM)

The cells in culture, after 3 days were fixed in the samples and observed in SEM. Prior to observation, the samples were washed with PBS and exchanged plate, followed by immersion in 2.5% solution of glutaraldehyde left for 1 h at 4 °C for attachment of the cells to the material. Fixed constructs were dehydrated by immersion in a series of aqueous solutions of ethanol, with a gradually increasing concentration of ethanol (from 20% to 100%). The surface of the constructions was gold-plated and observed by SEM.

3.3.5. Live/dead cell viability assay

Calcein acetocymethylester (Calcein AM) was used to stain live cells and Propidium Iodide (PI) (Molecular Probes®; Life Technologies, Carlsbad, CA, USA) was used to stain dead cells. Calcein AM/PI stain (1:2) was added to 1 ml of DMEM; samples were immersed in 100 µl/ml of this solution for 20 min in the incubator. The samples were observed in a transmitted and reflected light microscope with apotome 2 (Axio Imager Z1 m; Zeiss, Jena, Germany),

showing viable cells green (Calcein AM) and non-viable cells red (PI). Laser setting was 488 nm and 543 nm for Calcein AM and PI respectively. With the aid of a dedicated software (Zen), a Z-stack function was used to combine images at different depths into one final image.

3.3.6. Calcium assay

Calcium deposition was analyzed with the Alizarin Red staining method (OZKAN et al., 2009). Cell scaffolds were fixed by 4% paraformaldehyde at 4 °C for 12 h and subsequently stained with 2% Alizarin Red (SigmaAldrich, USA) solution for 10 min.

3.3.7. Statistical analysis

All data were expressed as mean standard deviations of a representative of 3 similar experiments carried out in triplicate. Statistical analysis was performed with data of cell culture, using a one-way analysis of variance (ANOVA) by the Bonferroni test, with a P value <0.05 considered statistically significant by a dedicated software (Graph-Pad, San Diego, CA, US).

Chapter 4 – SILK PROTEIN COATED CHITOSAN/β-TCP COMPOSITES FOR BONE TISSUE ENGINEERING APPLICATIONS

In this chapter, the biomedical potential of scaffolds produced using chitosan, β-tricalcium phosphate at different ratios, and silk fibroin as coating was evaluated. The findings suggest that β-tricalcium phosphate influences the microstructure of the developed scaffolds. The microstructure of scaffolds showed porosities of up to 94% when coated with silk, while having an interconnectivity of 99% and pore sizes in the range of 200-40 μm. The surfaces of the structure were able to form apatite crystals after 21 days. *In vitro* cell studies proved that the scaffolds were able to support cell growth and proliferation up to 14 days of culture. Physical, chemical and biological properties obtained indicated that the developed scaffolds have great potential to be used in bone regeneration applications.

4.1.INTRODUCTION

The lesions of the bone tissue can be treated using different substitutes enabling its efficient regeneration (LEE; KIM, 2016; PATI et al., 2015; YIN et al., 2003). For a few decades, these treatments were done only by autograft and/or allograft substitutes, which have limitations (rejection, infection, discontinuous growth) and a tendency to be rapidly reabsorbed by the body (BURCHARDT, 2006).

The production of structures similar to native tissue gains strength and tissue engineering emerges, which focuses on the development of structures that served as guides for the regeneration of specific and functional human tissues or organs. Scaffolds are a platform for cells to develop and organize into new tissues. They should facilitate cell colonization and have properties and characteristics that enhance cell binding, proliferation, migration and expression. (FAROKHI et al., 2018; THEIN-HAN; MISRA, 2009; WAGNER-ECKER et al., 2013). Some scaffolds characteristics are fundamental, such as porosity, pore size, pore interconnectivity, structural strength and biocompatibility. (DE OBALDIA et al., 2015; DUPIN et al., 2012; FURUSAWA et al., 2017; GOBIN; FROUDE; MATHUR, 2005).

Scaffolds may be produced from natural, biodegradable, and non-toxic materials, such as chitosan (CH) and silk fibroin (SF) (BAE et al., 2013; COSTA-PINTO; REIS; NEVES, 2011; KIM et al., 2008; MAO et al., 2018; TORRES et al., 2011; WAGNER-ECKER et al., 2013). The addition of other materials to the constructs, such as β-tricalcium phosphate (β-TCP) and biological cues may provide the scaffolds with a more inductive character for the production of new osseous tissue (DADSETAN et al., 2015; RIBEIRO et al., 2017; YANG et al., 2011). In order to improve regeneration and to promote a better growth of the new bone tissue, some growth factors have been added to scaffolds (KHOJASTEH et al., 2016; LAFLAMME; ROUABHIA, 2008; MONTJOVENT et al., 2010; OVERMAN et al., 2013a). The delivery of bone morphogenetic protein (BMP) at the site of the lesion proved to be an effective strategy for the differentiation of osteoblasts, which are the promoters of osseous tissue growth (JI et al., 2012). Structure development should always aggregate tissue-specific characteristics as well as factors responsible for effective cell growth.

The present work aims to develop a composite of CH/β-TCP with a SF coating, which will efficiently promote the cellular growth and delivery of growth factors (BMP) when implemented in the injured tissue.

4.2. MATERIALS AND METHODS

The materials and methods used were described in Chapter 3.

4.3. RESULTS AND DISCUSSION

Initially, the TCP synthesized samples were analyzed by XRD to identify the crystalline phases. The only phase present was β-TCP, as observed in Figure 9.

Figure 9 – XRD spectra of TCP samples. The only phase identified was β-TCP.

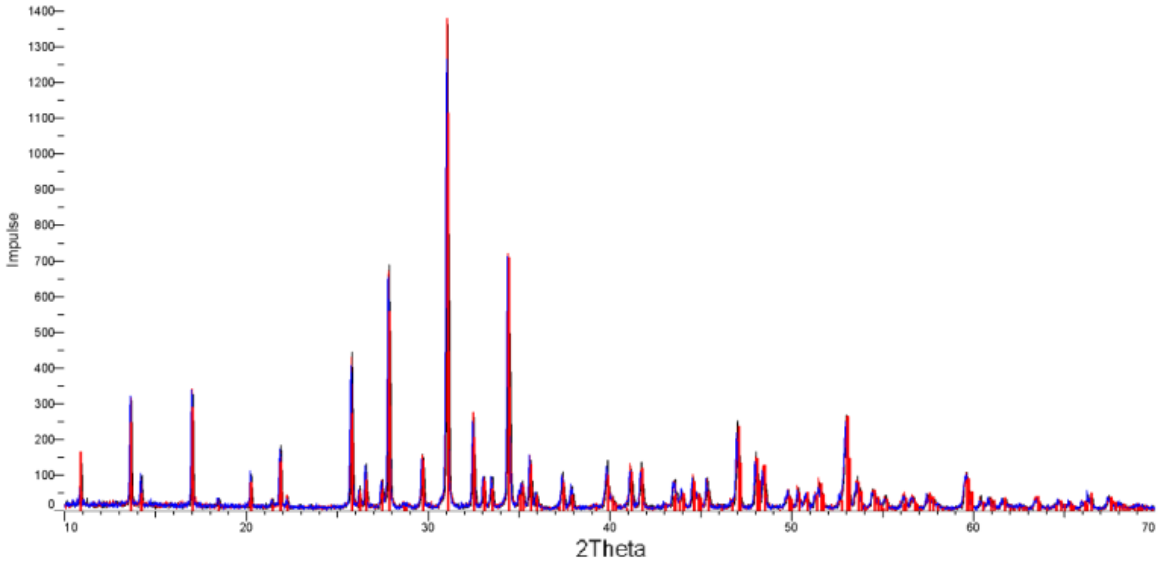

The particle size distribution of TCP powder is presented in Figure 10. The results showed that the particles had an average size (D50) of 13.71 μm, with a 97% below 40 μm. Particles have these sizes because of the solid-state reaction, where the reagents used were fine powders and the reaction temperature did not allow for a large particle size growth.

Figure 10 - Distribution of β-TCP particle size.

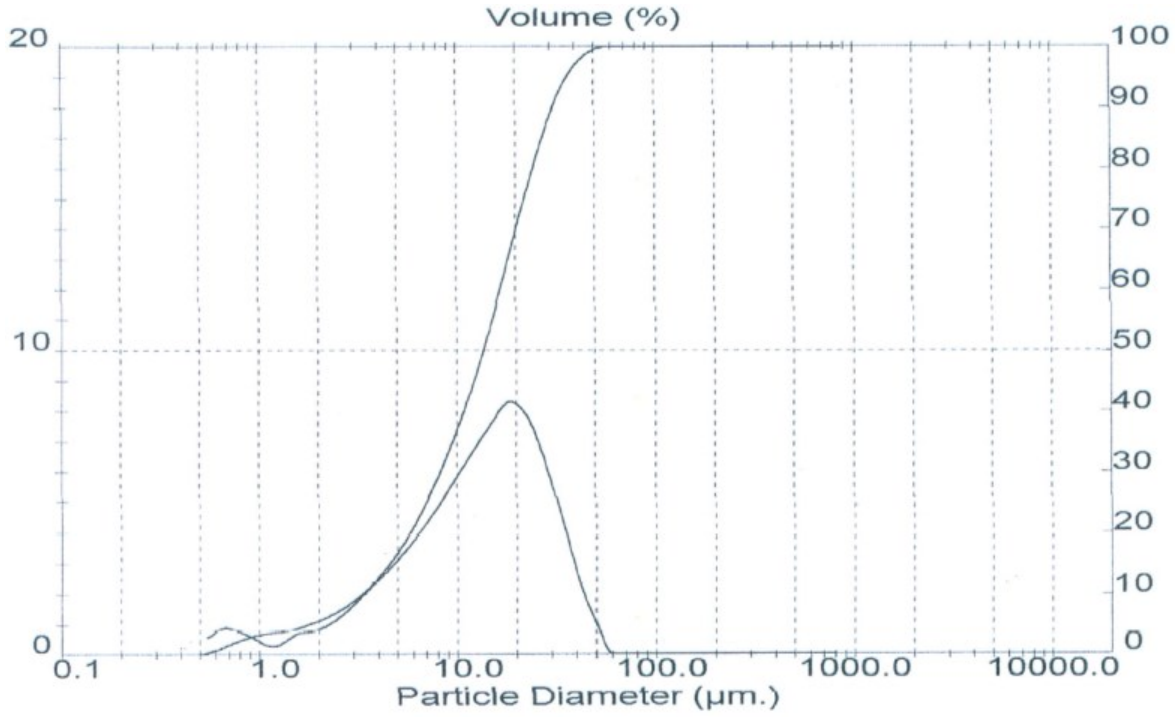

However, when the powder was subjected to a separation process using sieves, the vast majority of the powder was retained between size ranges of 25 to 45 µm, due to the agglomeration of the small particles.

The final product of CH purification was analyzed by RMN for detecting acetylation, according to Figure 11. The degree of acetylation was calculated using H (2 and 3.5 ppm) concentration and quantified as 89.15%.

Figure 11 - RMN spectrum of purified chitosan (unit in ppm).

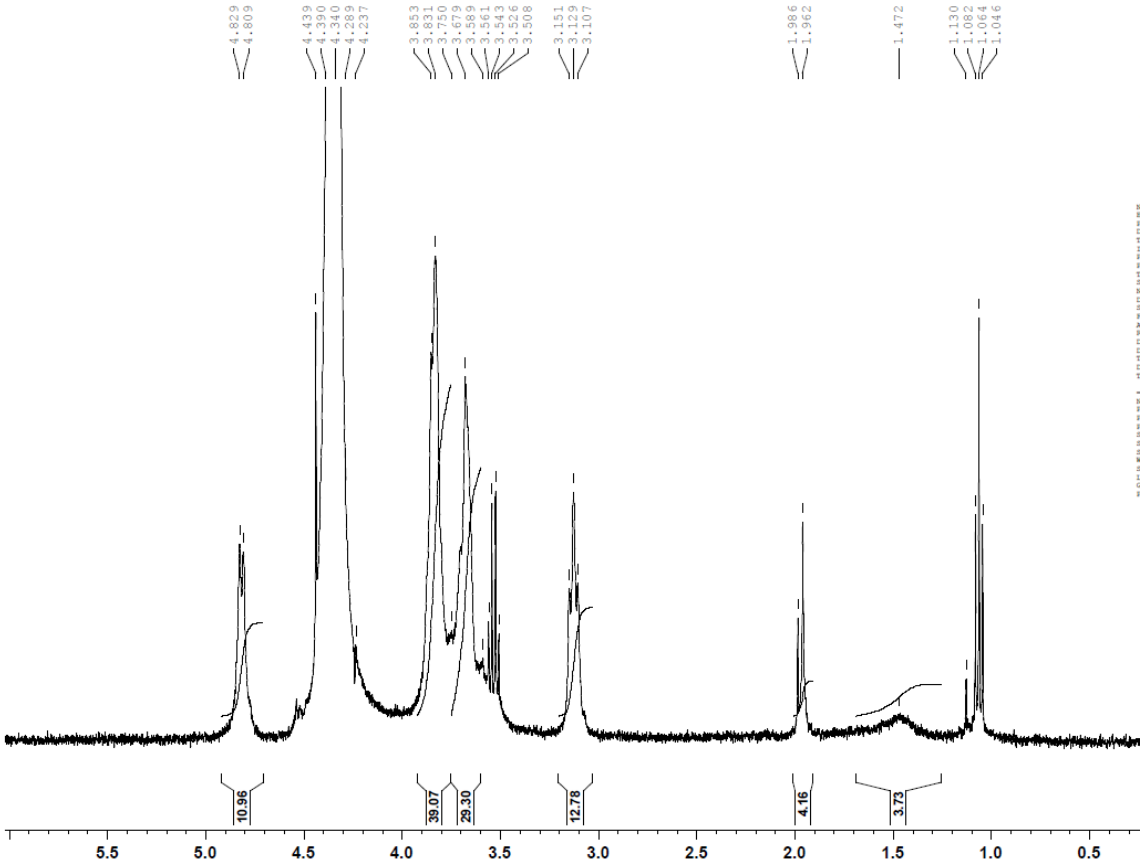

In Figure 12-A, the images of chitosan (CH2 and CH) and the four different CH/β-TCP scaffolds are showed. The differences in the structures during several stages of production are clearly noted. There are common layers formed when using CH, as observed in the literature (KEAN; THANOU, 2010; SILVA et al., 2008a). The SEM images (Figure 12-B and C) show the irregular shape of the developed scaffolds. In CH3 few pores are noticed at the, and in the scaffolds with β-TCP (CH3BT10 and CH3BT20), the structure is more layered with the presence of ceramic material.

Figure 12 – Non-coated scaffolds microstructures: (A) Optical microscopic (40 x). (B-C) Surface and (D-E) Cross section 50× and 200× magnification by SEM.

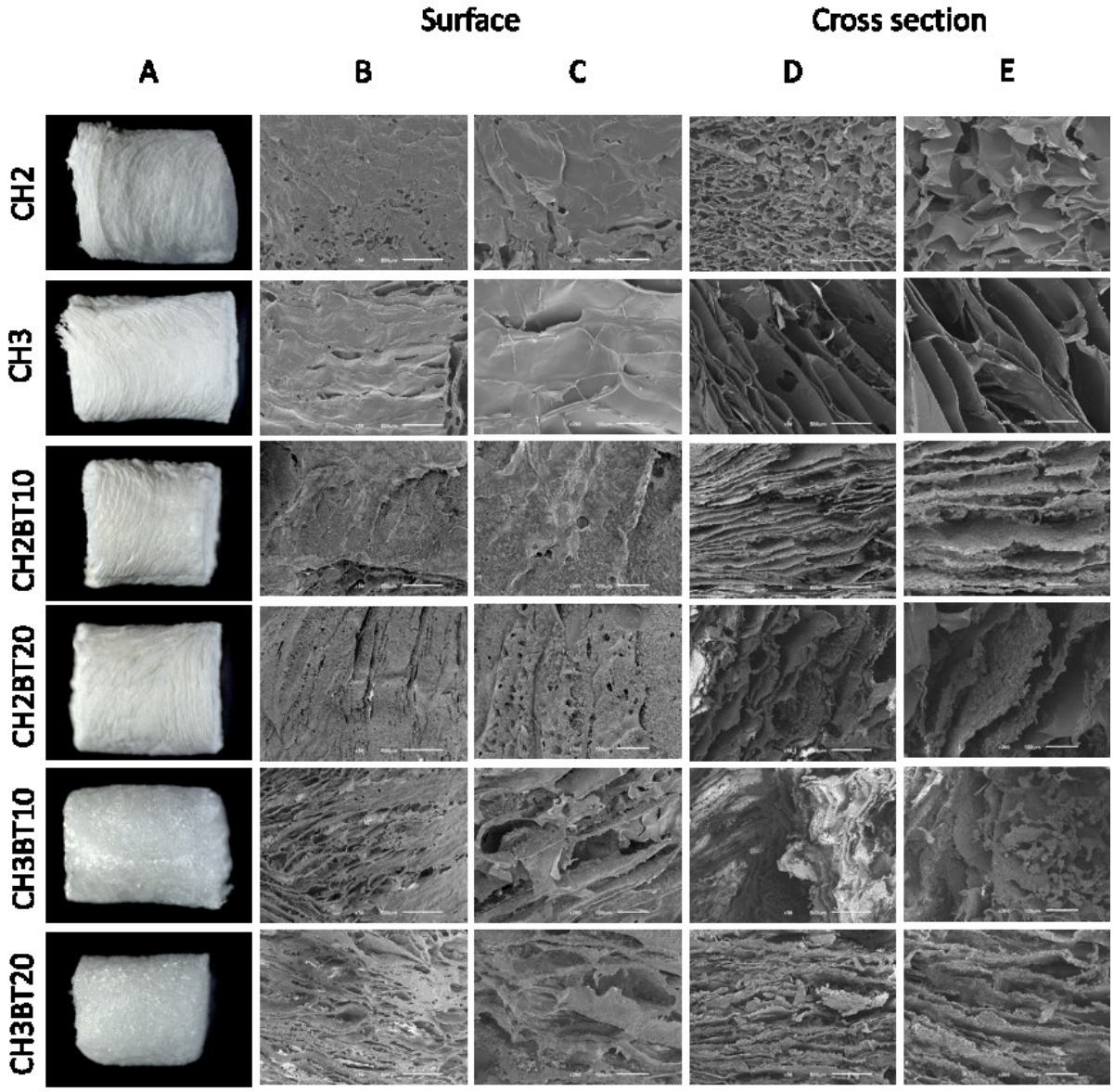

The microstructure of the CH/β-TCP scaffolds coated with silk coating are shown. Fig. 13-A shows the structures by optical microscopy and in the figures 13-B-E the coating layers in the scaffolds are shown both on the surface and at the cross section.

Figure 13 – Silk-coated scaffolds microstructures. (A) Optical microscopic (500 μm). (B-C) Surface and (D-E) Cross section 50× and 200× magnification by SEM.

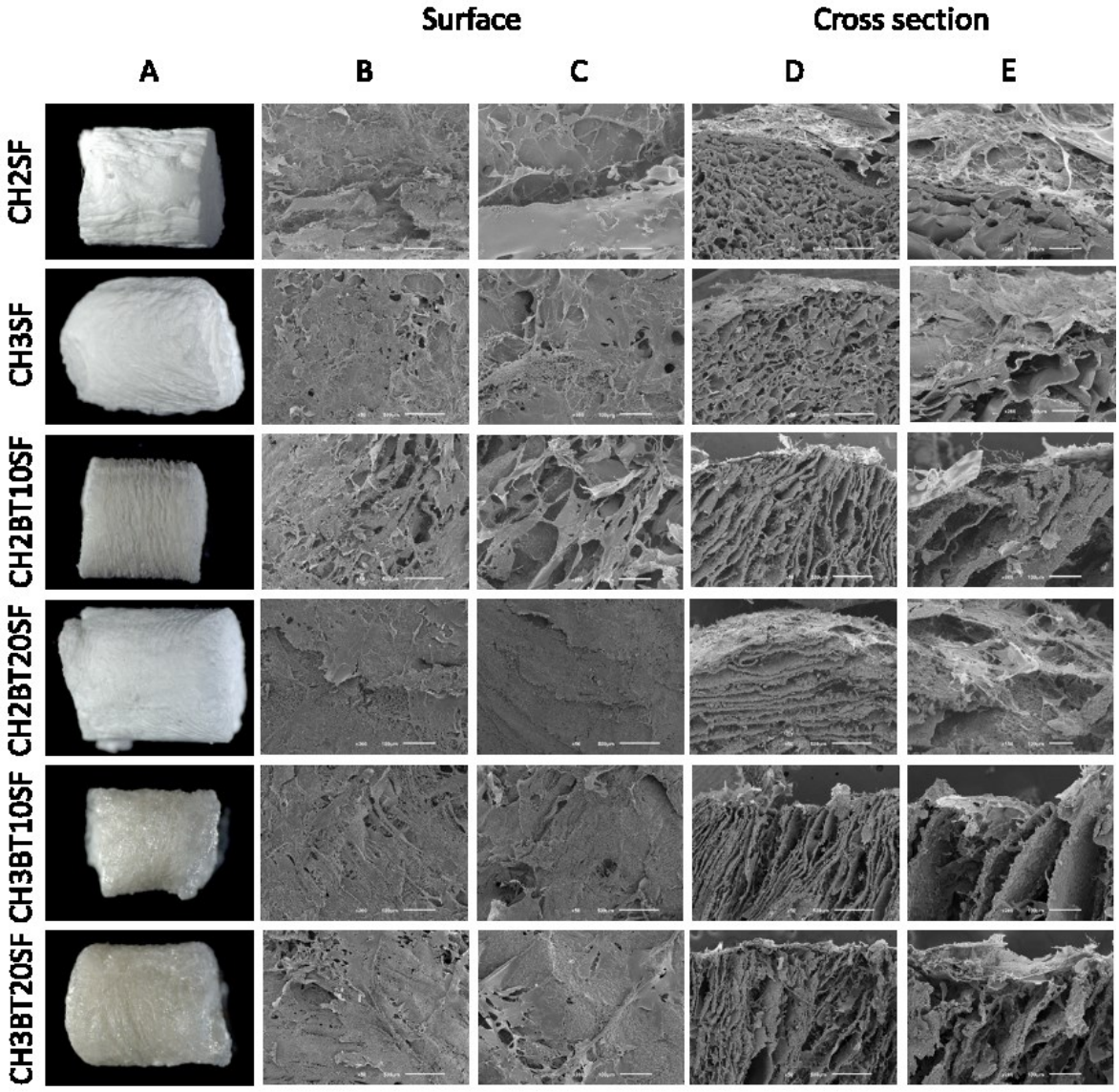

In Figure 12 and 13 (D and E) the cross sections of the structures are depicted, where it is possible to observe in more detail the layers formed typically by CH, as well as the presence of ceramic particles. The cross-section of the scaffolds shows that the internal layers of the scaffolds are homogeneous, confirming the interaction between polymer and ceramic, as well as their uniform distribution through the scaffolds. Moreover, the silk coating was also noticeable in the microstructure of the scaffolds (Figure 13-E).

The distribution of the components (organic and inorganic), porosity and interconnectivity of the scaffolds was analyzed by μ-CT (Figures 14 and 15). 3D images of the scaffolds were identified as CH (blue), β-TCP (red) and silk (green). All the components are

distributed equally by the structure, with varied porosity along the scaffolds (Figure 14-B and 15-B).

Figure 14 – Microcomputer tomography 3D non-coated scaffold structures (a).The blue color represents chitosan and red, β-TCP.

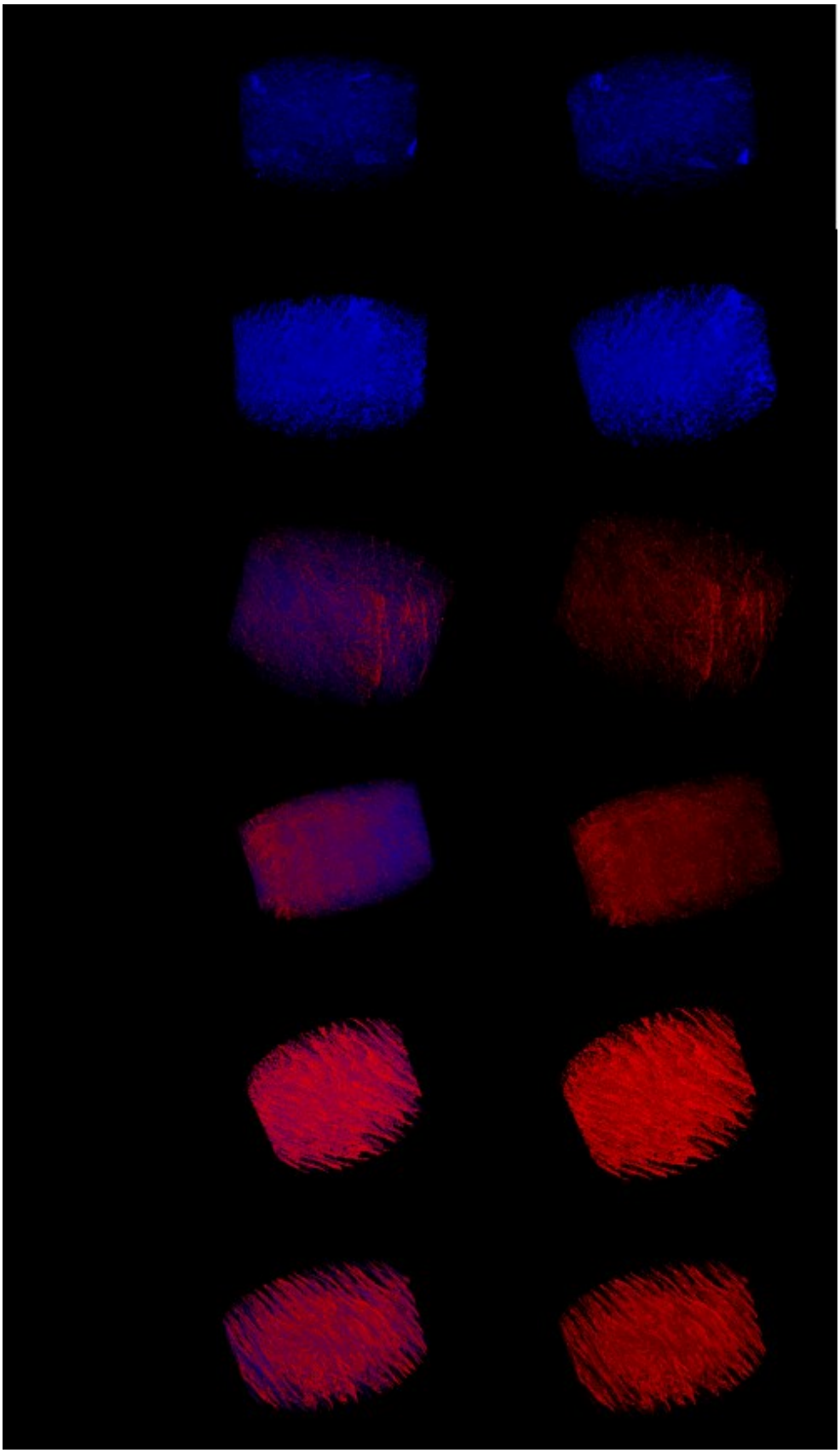

Figure 15 - Microcomputer tomography 3D of silk-coated scaffold structures. The green color represents silk; blue, chitosan, and red, β-TCP.

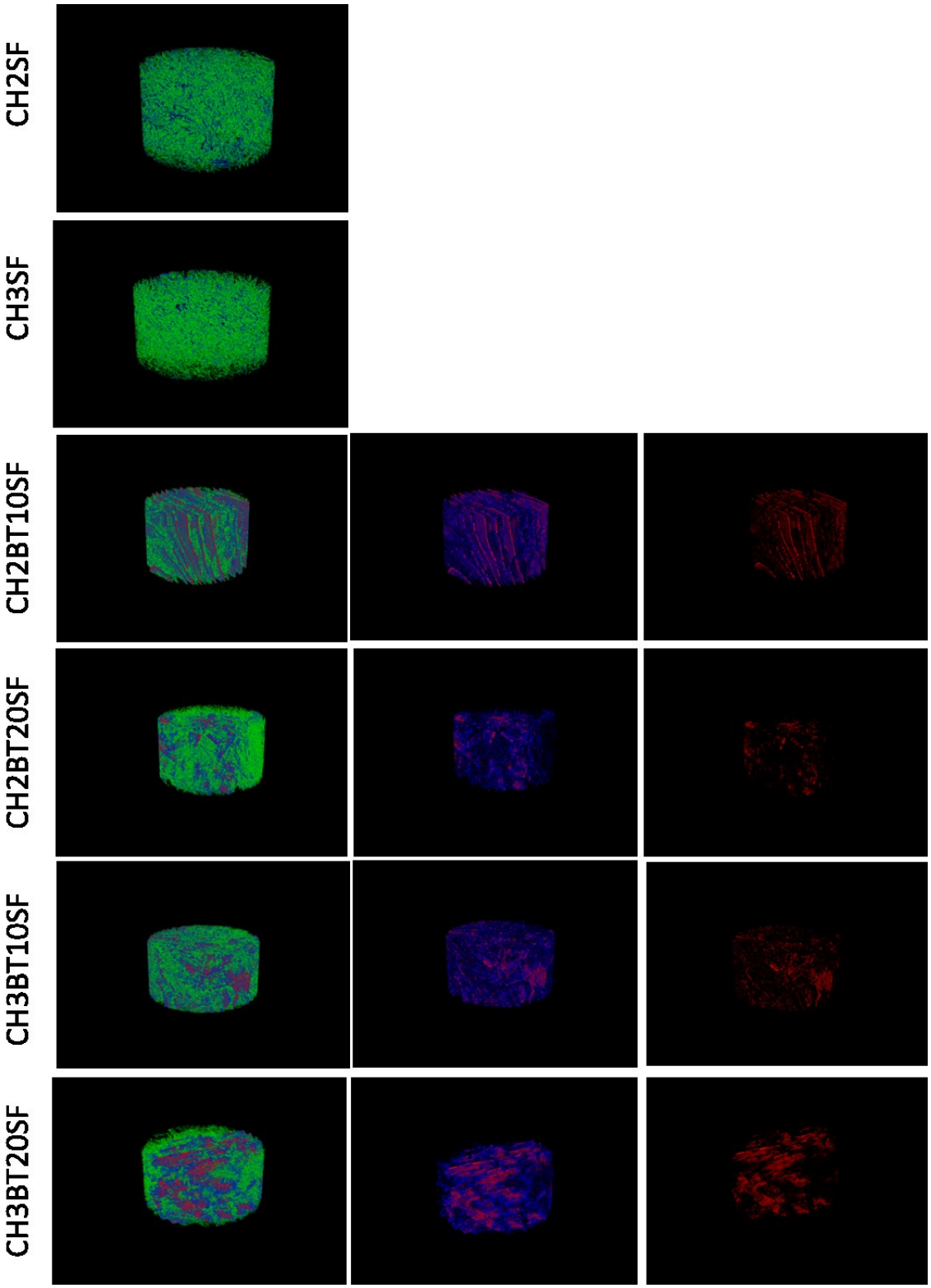

Table 5 - Microstructure data by μ-CT.

Sample	Mean thickness (μm)	Mean pore size (μm)	Porosity (%)	Interconnectivity (%)
CH2	22.77	113.36	82.20	84.10
CH3	22.98	127.59	82.12	55.73
CH2BT10	44.85	100.12	64.97	48.27
CH2BT20	53.60	41.21	40.62	2.31
CH3BT10	48.35	93.98	59.98	25.48
CH3BT20	53.03	39.39	41.44	1.59
CH2SF	7.86	63.43	94.22	99.47
CH3SF	14.94	137.03	94.92	99.71
CH2BT10SF	37.95	173.43	83.21	98.11
CH2BT20SF	39.66	166.37	84.21	98.07
CH3BT10SF	39.54	163.96	85.64	98.63
CH3BT20SF	38.47	213.99	89.23	99.41

In Table 5, it can be observed that the developed scaffolds have porosity around 82% without ceramic load (CH2 and CH3). With the addition of TCP, the porosity decreases to 64% (CH2BT10) and 40% (CH2BT20), respectively. Despite the significant decrease in porosity, there is a gain in the bioactivity and stimulation of bone production (KIM; KNOWLES; KIM, 2005).

The CH3 scaffold has a mean pore size of ~127 μm, and scaffolds with TCP present a pore size in the range of 39-93 μm, respectively. The scaffolds that were covered by 1% silk presented a pore size up to 213 μm (CH3BT20SF). The high interconnectivity (up to 99%) and porosity (up to 94%), with a mean 40 μm layer thickness, showed that the microstructure of the scaffolds were changed after silk coating. Moreover, these features also indicated that these samples may allow the circulation of the nutrients for cell culture.

The osteoblastic cells may adjust with more facility to scaffolds with large pores, leading to direct osteogenesis, without advancing to the formation of cartilage (KARAGEORGIOU; KAPLAN, 2005). The smaller pores (10-25 μm) may assist the diffusion of nutrients along the scaffold (RAJKUMAR et al., 2013). Micropores play a crucial role in nutrient diffusion, cell growth and proliferation, due to a larger surface area. In addition to allowing a substrate to be adsorbed more suitably, e.g. angiogenic and/or osteogenic protein

adsorption and cellular anchorage, a more rapid induction of angiogenesis and bone growth is expected (HING et al., 2005).

The structural changes in different samples were investigated by FTIR (Figure 16 and 17). The main characteristic absorption bands of CH and silk were identified in all samples. The band at 1641 cm^{-1} corresponds to N–H bending vibrations of secondary amide, present in chitosan. The C–O–C bending, C–O bending and C–OH bending are visible at 1173 cm^{-1} (KATTI; KATTI; DASH, 2008). A PO_4^{3-} stretching peak is seen at 1030 cm^{-1} and PO_4^{3-} bending vibrations appears at 604 cm^{-1}.

Figure 16 – Fourier transform infrared spectroscopy (FTIR) spectra of non-coated scaffolds.

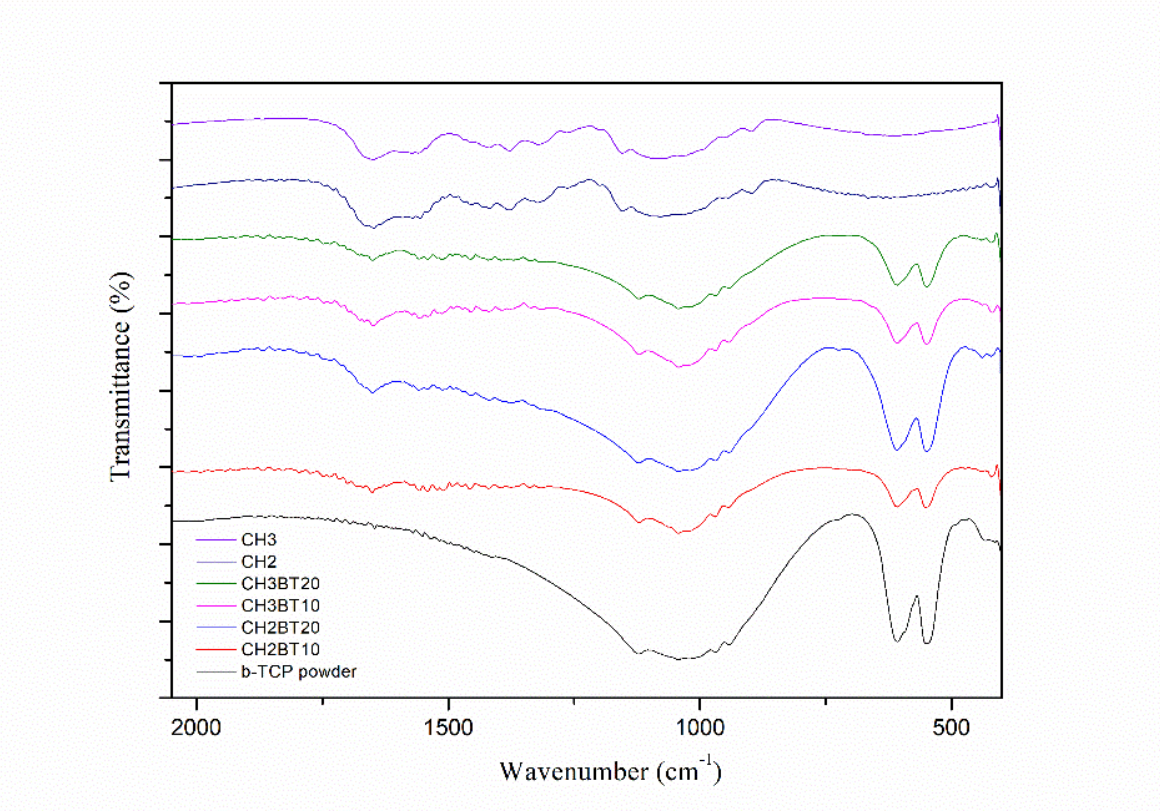

Figure 17 – Fourier transform infrared spectroscopy (FTIR) spectra of silk-coated scaffolds.

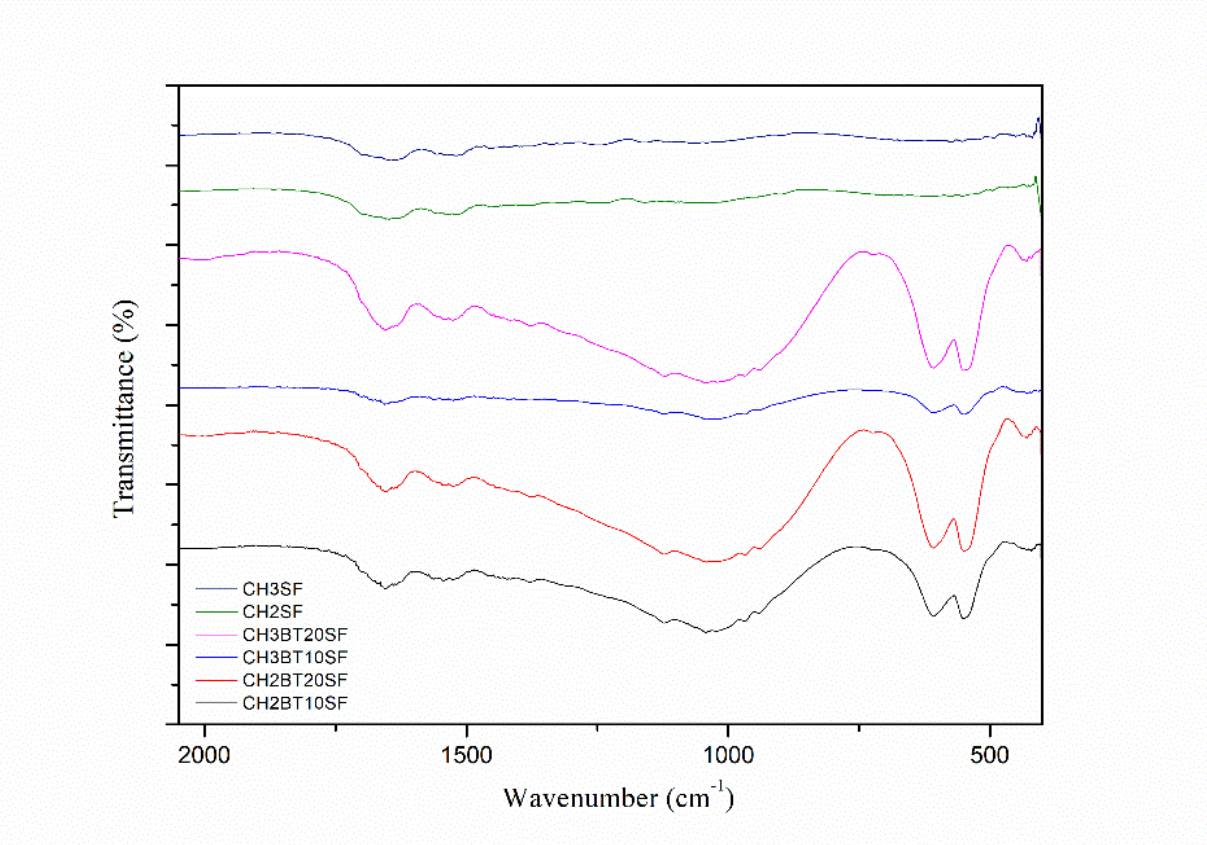

Bioactivity tests were performed through immersion of the samples in SBF for 21 days. SEM micrographs of the scaffolds showed the characteristic formation of apatite (Figure 18, 19 and 20). In Figure 18, the formation of apatite in β-TCP powder in the first day of test can be identified.

Figure 18 - Evaluation of apatite formation on β-TCP powder, after bioactivity test, by SEM.

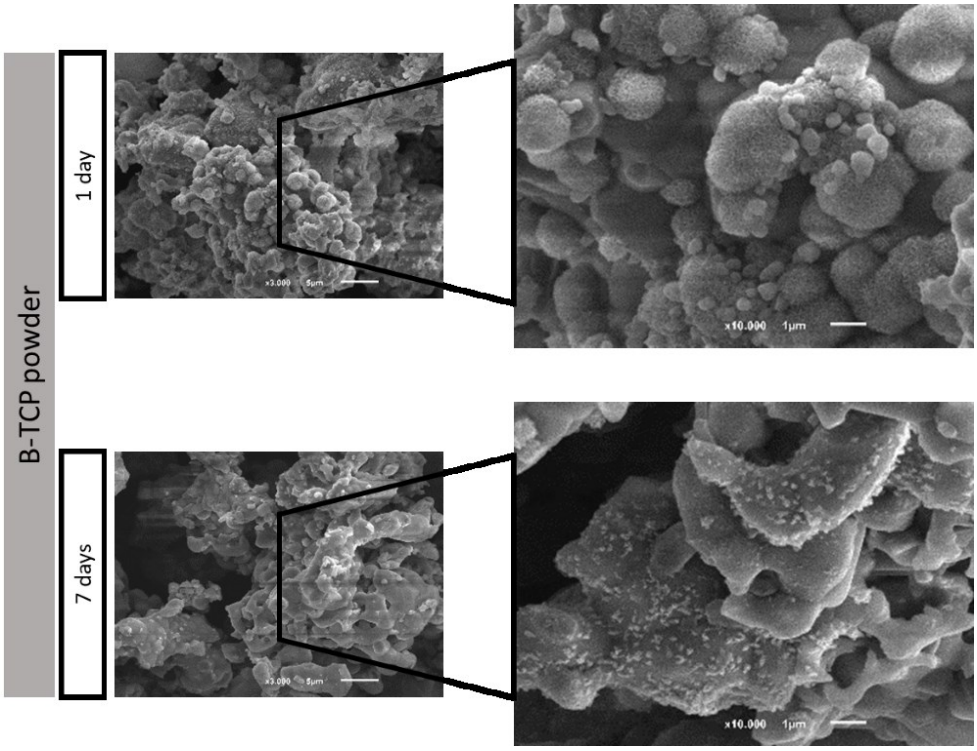

In Figures 19 and 20, the analysis of the SEM images permits to confirm the formation of apatite on all scaffold surfaces after 1 and 7 days of test, respectively.

Figure 19 - Evaluation of apatite formation on non-coated scaffold surfaces, after 1 day of bioactivity test, by SEM 200× (A, C) and 3000× (B, D) magnification.

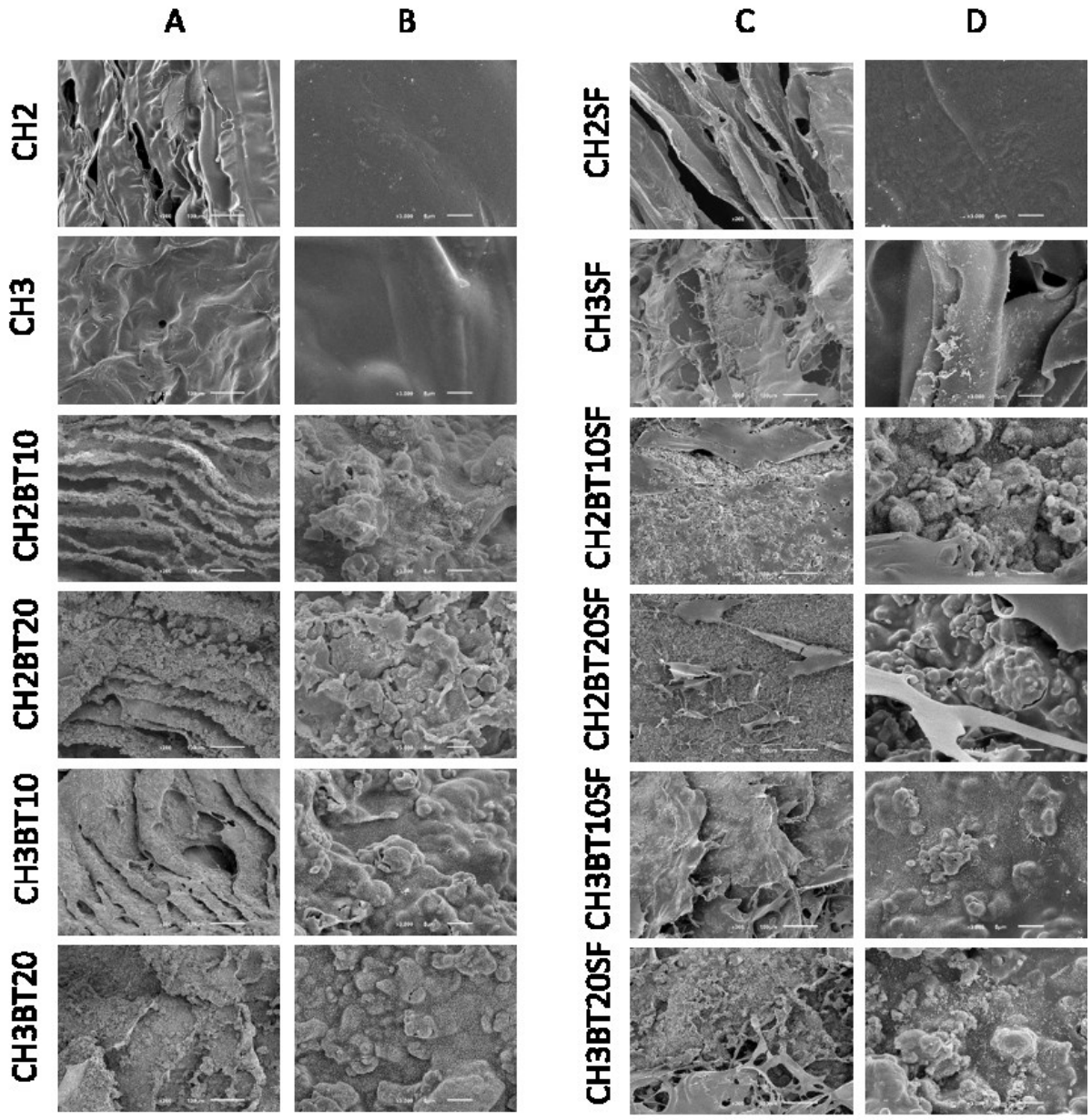

Figure 19 shows the formation of apatite in the samples that present TCP in their composition. On the other hand, silk-coated samples presented apatite formation under coating

Figure 20 - Evaluation of apatite formation on silk-coated scaffold surfaces, after 7 days of bioactivity test, by SEM 200× (A, C) and 3000× (B, D) magnification

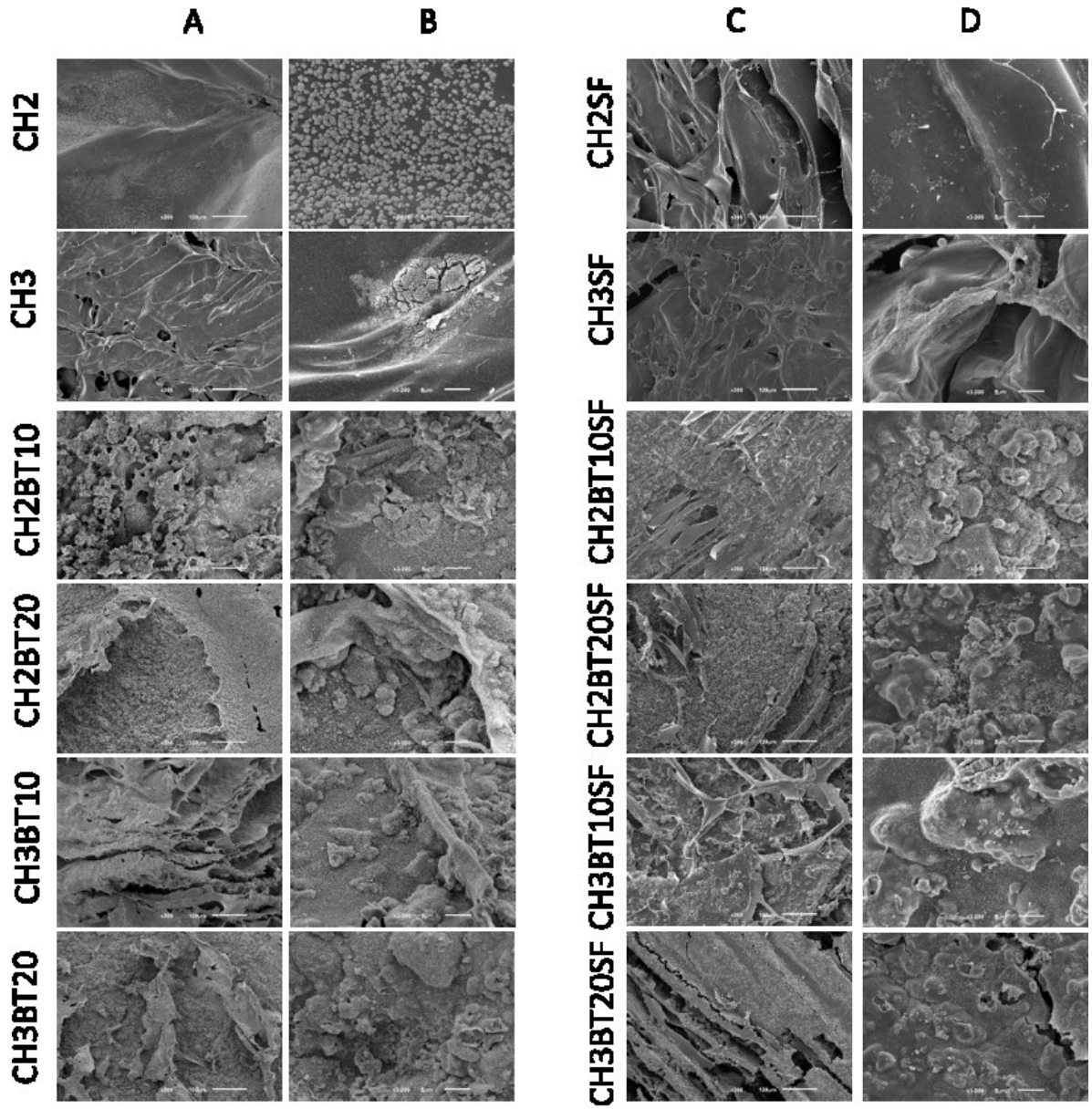

With 7 days with test, all scaffolds samples showed apatite formation, with higher concentration at the surface (Figure 20).

Ca and P concentration data by ICP of the samples after immersion for 21 days are depicted in Figure 21. The amount of Ca over time shows an increase in the amount until the third day. Thereafter, the values tend to maintain a plateau in all silk-coated samples. On the other hand, the concentration of P over time decreases in all cases.

Figure 21 – Data of the ICP analysis. (A, C) Ca concentration (B, D) P concentration the samples are without and with silk coating.

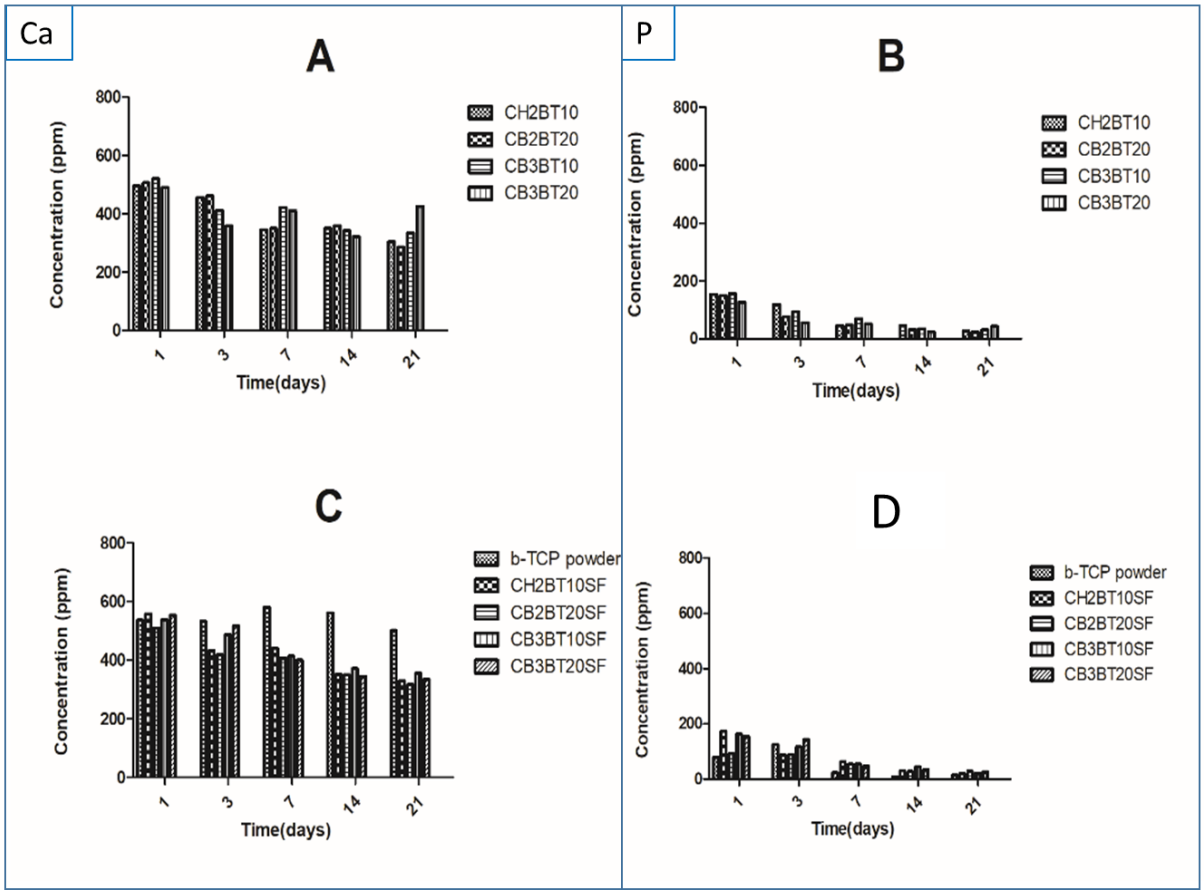

The crystallinity of the scaffolds was analyzed by XRD (Figure 22). An increase in the crystalline phase can be observed in the silk-coated samples (d), (e) and (f). More intense peaks in the CH3BT10 and CH3BT20 were noticed after 7 days of immersion in SBF.

Figure 22 – XRD spectra of scaffolds after CaP deposition. (left) non-coated and (right) silk-coated: (bottom) Scaffolds control; (middle) Data after 7 days bioactivity test; (top) Data after 1 day bioactivity test.

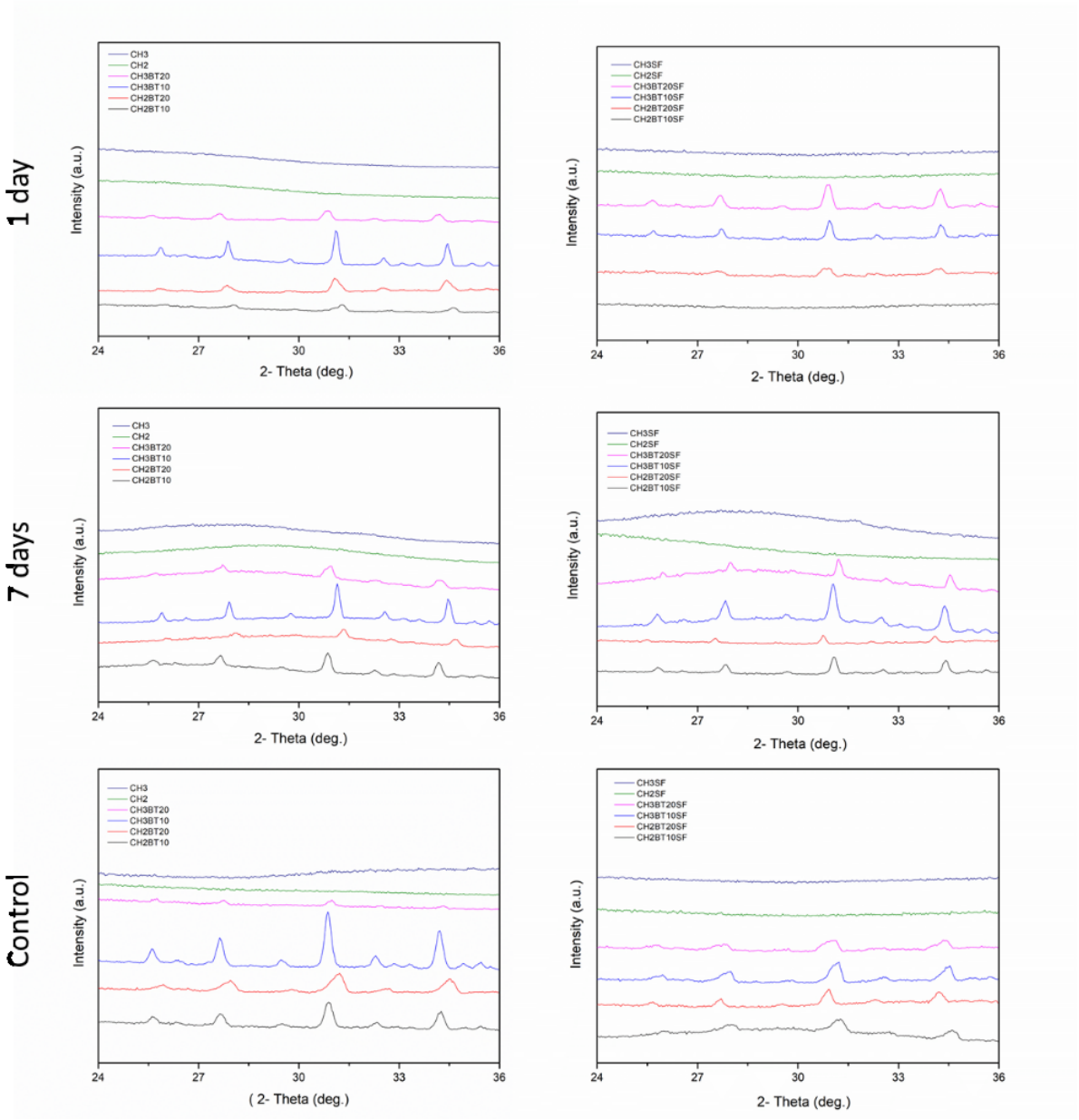

Bioactive materials when implanted in the human body are dissolved over time by body fluids, and they are charged to other regions near the implant. These materials will develop at the surface where they are absorbed a layer of apatite, and thus begin a greater interaction between the substitute and the injured tissue (CAO; HENCH, 1996; KIM, 2011). The

absorption and degradation of the scaffold are important. The new bone should be formed effectively without deformation and lack of nutrients for cellular stimulation.

The enzymatic degradation of the scaffolds was analyzed using lysozyme (Figure 23). This enzyme is present in human blood and degrades preferentially CH. The degradation profile of the samples with and without silk coating presents a variation on loss mass along the time. For both the non-coated and the silk-coated, the profiles of pure chitosan has greater expression in relation to the samples with β-TCP, because the ceramic load tends to delay the depletion of chitosan by the action of the lysozyme.

Figure 23 – Weight loss of the scaffolds. (A, B, E, F) Data degradation for PBS and (C, D, G, H) Data degradation for enzyme.

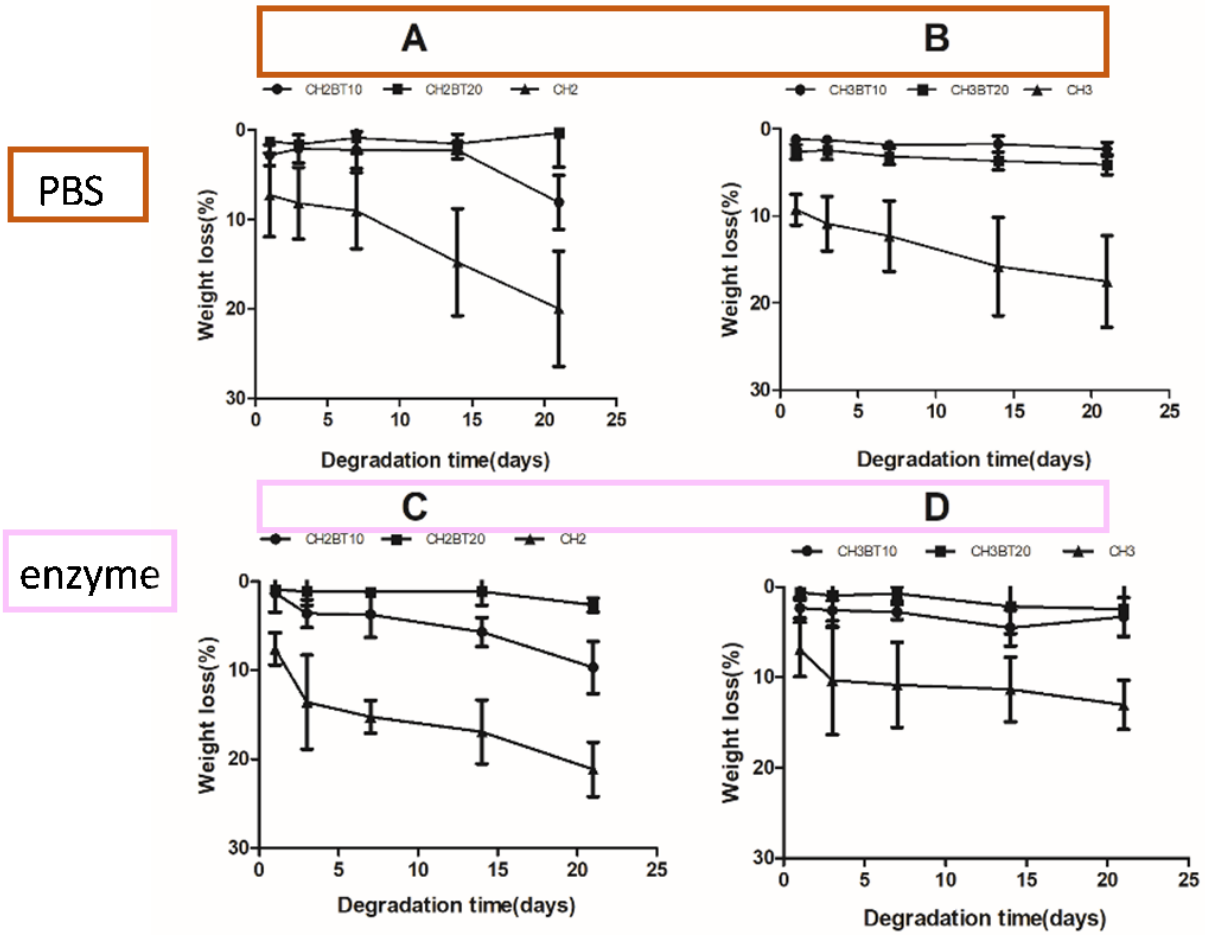

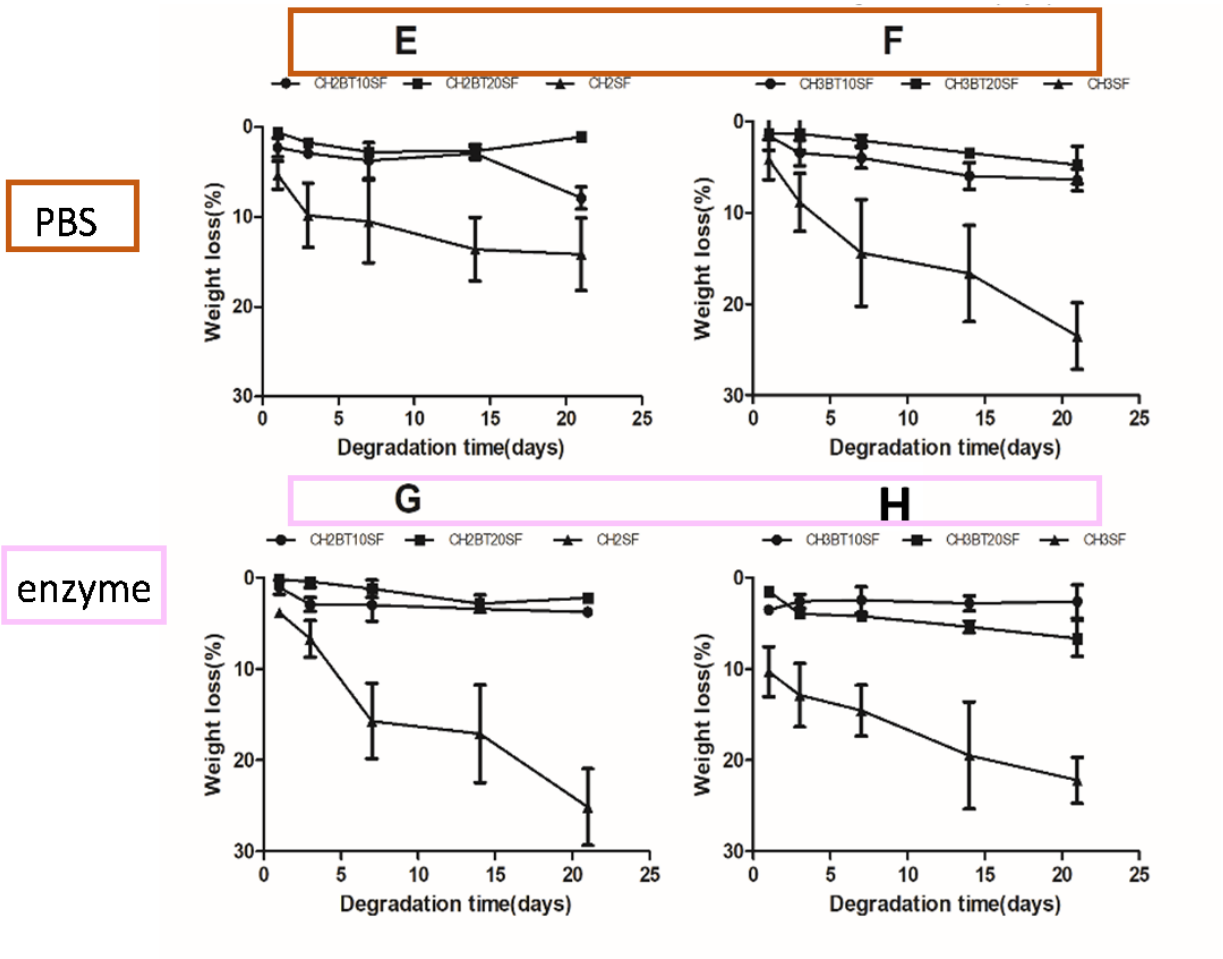

The swelling results of the scaffolds at pH of 5.7; 7.4 and 8.2, showed that the TCP-loaded samples have a similar behavior over time (Figure 24). Scaffold samples of only chitosan (CH2, CH3, CH2SF and CH3SF) assume a specific composition, with greater capacity to swell at pH 8.2 (CH2 and CH3). On the other hand, the coated scaffolds (CH2SF and CH3SF) the profile of greater swelling is at pH 5.7.

Figure 24 – Data of the swelling ratio of the scaffolds: (left) non-coated; (right) silk-coated.

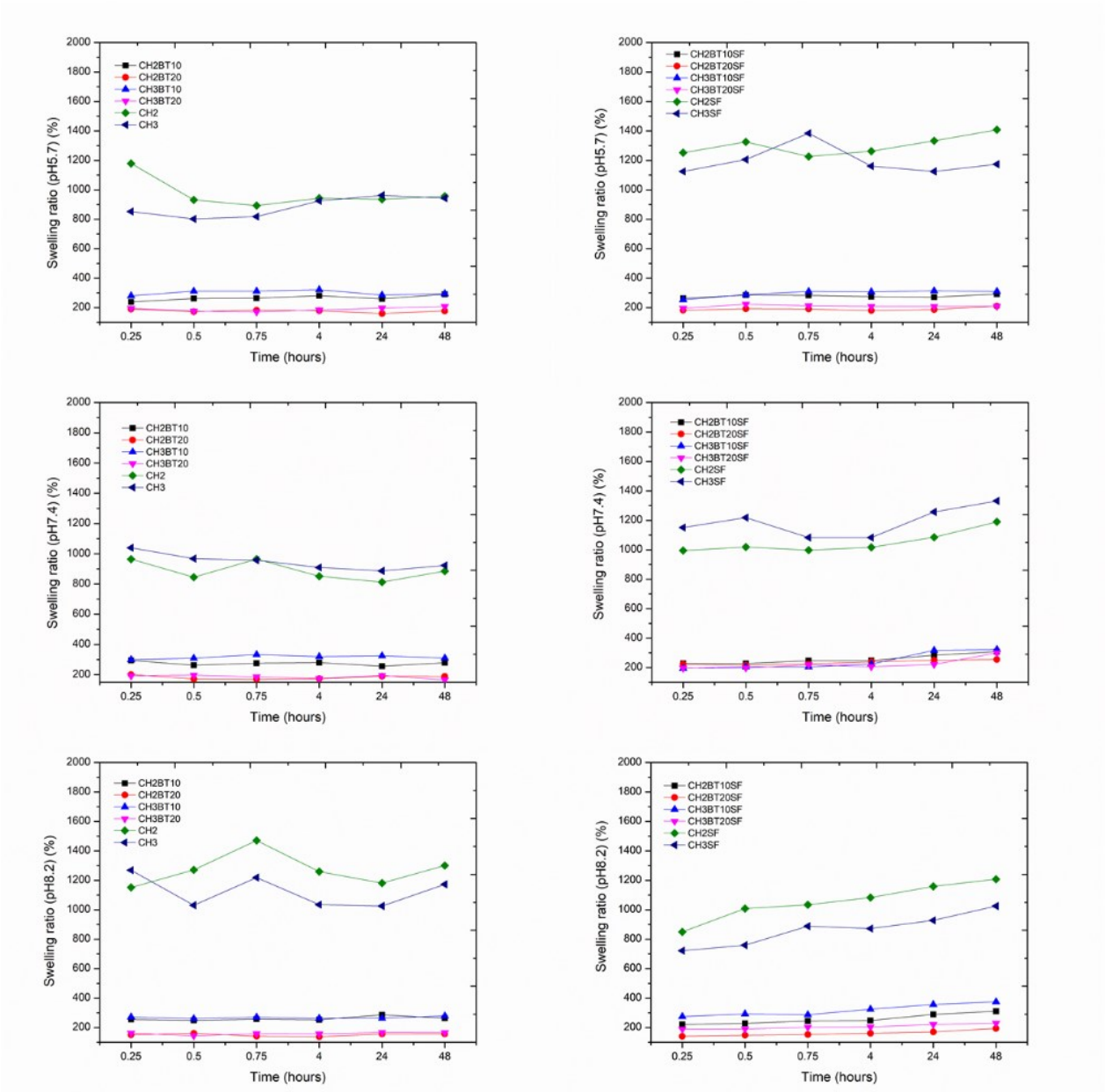

These results are in accordance with other studies in the literature in which the addition of ceramic materials in the scaffold fabrication has resulted in decreased swelling ratio (PRAMANIK et al., 2009). When the scaffold is hydrophilic, it indicates that scaffolds can potentially be applied in tissue engineering, as the scaffold's hydrophilicity will facilitate the absorption of body fluid, which consists mainly of water. This is important for the diffusion of

nutrients and metabolites when this scaffold is implanted in the injured location (SHARMA et al., 2016).

The data obtained for the scaffold microstructures suggests that they can allow a flow of nutrients and body fluids when implanted in the damaged tissue. This will let the incorporation of growth factors to improve tissue regeneration. BMP-2 was used to test the scaffolds as a delivery system of the drug and/or local growth factors. It was impregnated into the structures of CH3BT10SF and CH3SF for 18 h, and then the same structures were added in culture medium, where it was possible to evaluate the release of BMP-2 over 72 h. The data in Figure 25 show a cumulative release until 72 h for all tested scaffolds.

Figure 25 – Cumulative release profile of BMP-2 detected in culture medium as a time function using ELISA assay. (*) 2.5 µm/mL and (#) 5.0 µm/mL of BMP-2 incorporation in scaffolds.

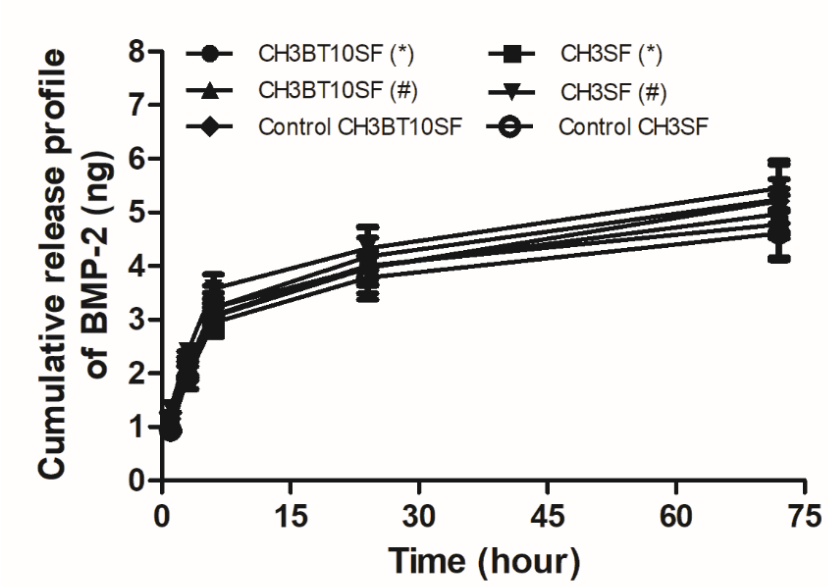

The size of the macropores and the shape of the bioceramic scaffolds are the main structural factors for the bone growth. However, the minimum pore size required for bone regeneration, reported as values between 75 and 100 µm, persists as a challenge (GARIBOLDI; BEST, 2015). Studies showed that osteogenesis could be enhanced with pore sizes larger than 300 µm (BASTAMI et al., 2017; JAFARI et al., 2017). With the data obtained so far, it is suggested that a structure capable of stimulating bone growth has been created, since it presents inorganic and organic components with the ability to bio-absorb, biodegrade, bio-stimulate, and

mechanically support the new tissue that will be created. Besides, the developed scaffolds also serve as a system for the release of factors that stimulated the biological system involved in the production of cells, which are involved in the process of osseous growth.

The cytotoxicity results revealed that the cell morphology does not change after contact with the extracts of produced scaffolds, as showed in Figures 26 B-C.

Figure 26 – Data of the cell cytotoxicity of the materials: (A) cell morphology (40 x); (B) cell growth; (C) cell viability.

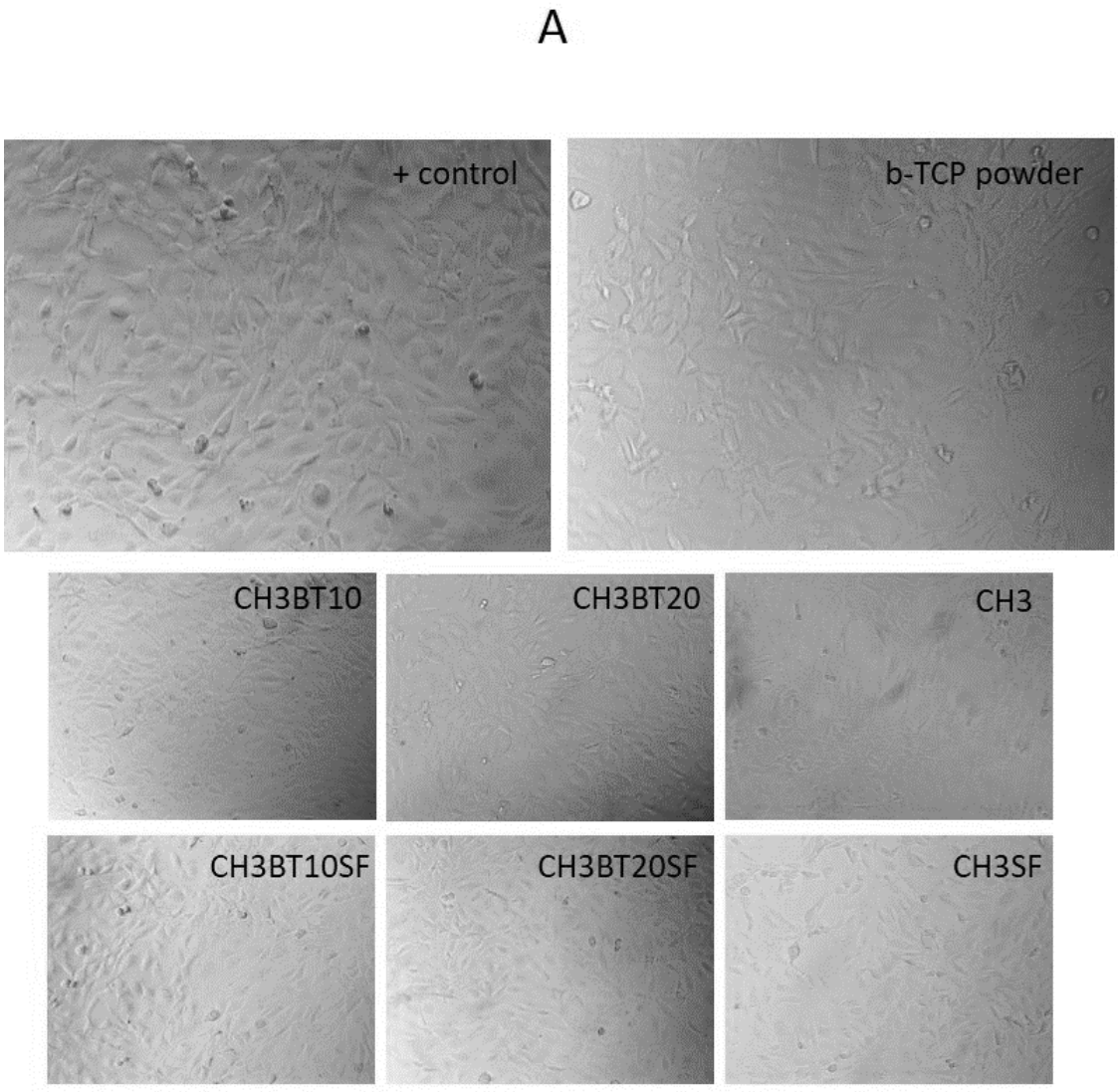

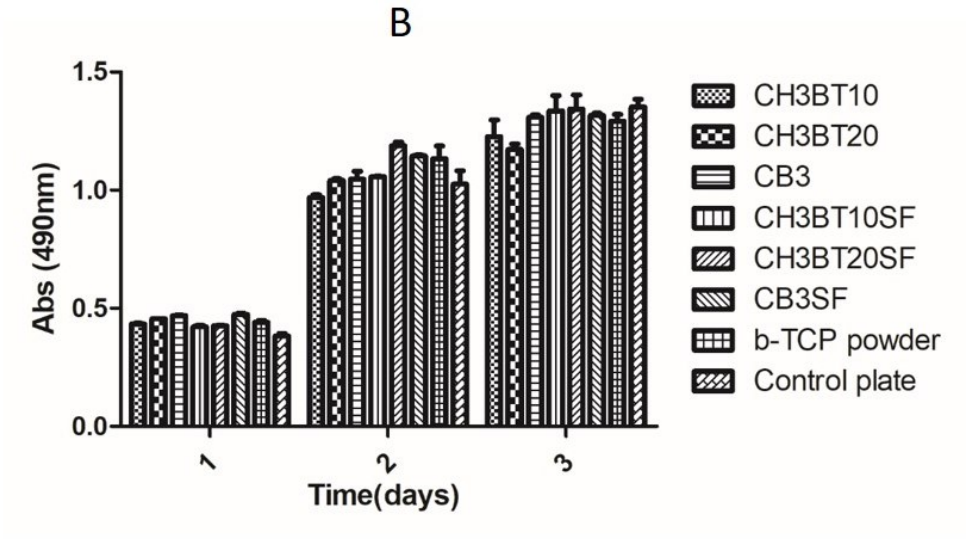

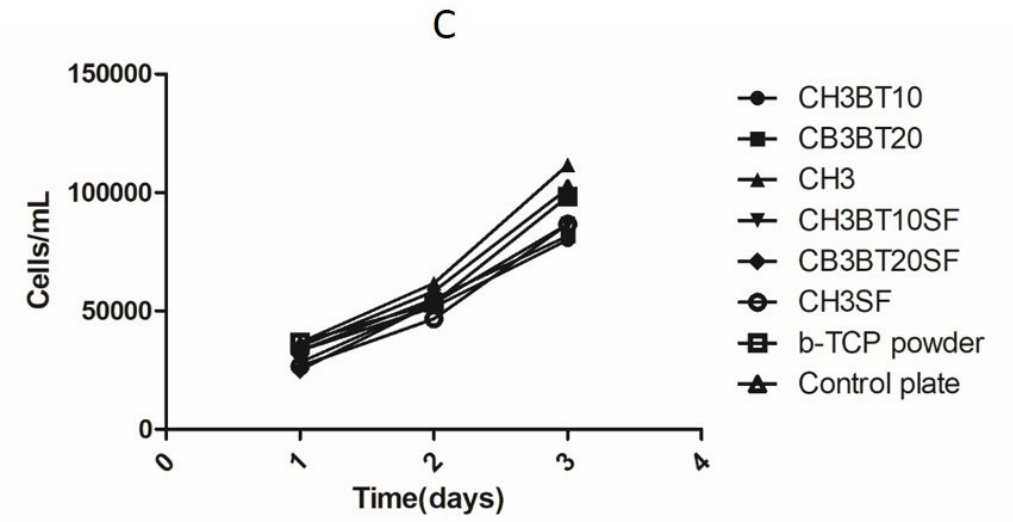

Figure 27-A presents the cell viability data obtained up to 14 days of culture, which demonstrates an increase in viable cells over time, especially in scaffolds with silk fibroin coating. Significant differences were found in the scaffolds between the first and the seventh day of cultivation, as well as between the first and the 14th day. Differences were identified in the third and the 14th day.

The results of cell proliferation by DNA, Figure 27-B, show an increase throughout the cell culture until 14 days. In the silk-coated samples, these values are observed in greater expression mainly in 14 days of culture. Significant differences were found in samples during the period of cell proliferation. Figure 27-C shows values of ALP activity constant up to 7 days of cell culture; in 14 days an increase in the concentration of ALP activity was noticed in all samples.

Figure 27 – Data of biological characterization. (A) Cell viability (* p <0.05). (B) DNA concentration (* ** *** p <0.05). (C) ALP (* ** *** ****p <0.05).

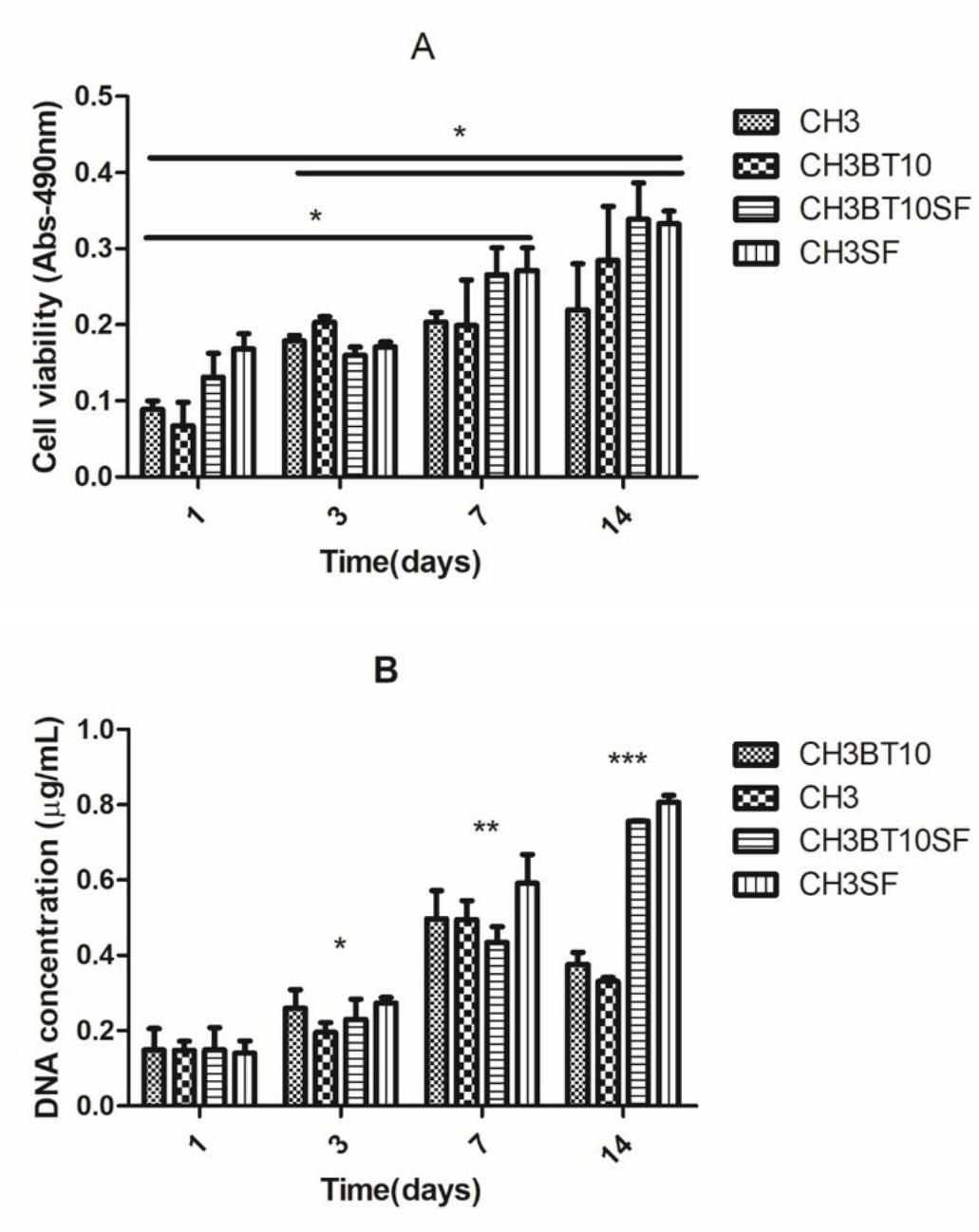

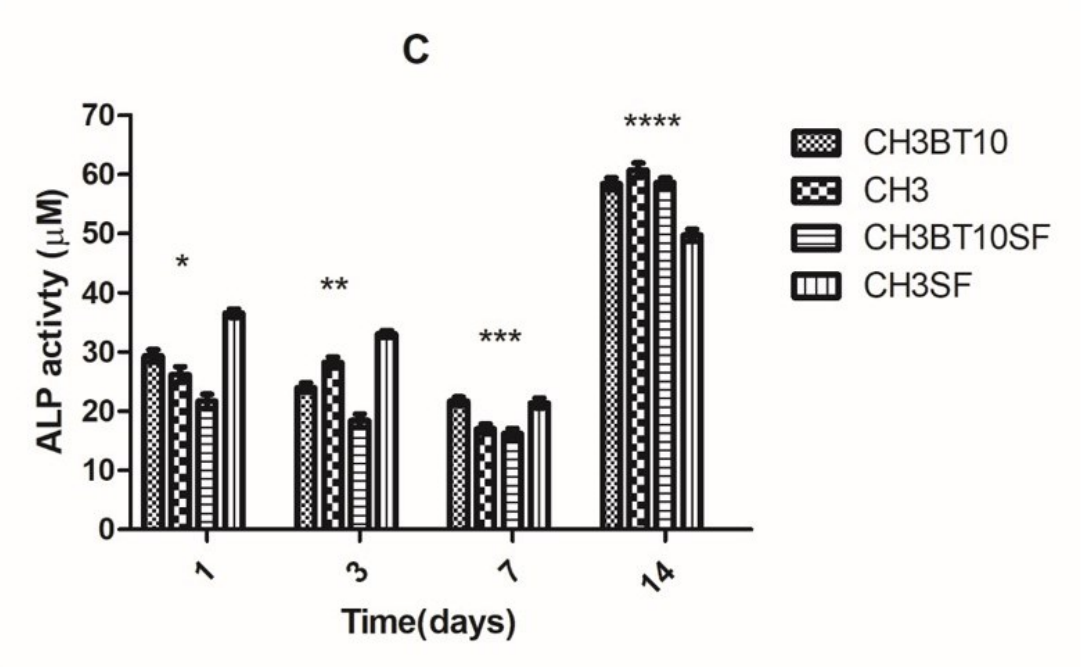

Some studies show that there is proliferation of osteoblasts on rough surfaces of CH and ceramic scaffolds. Besides that, the ceramic helps in the osteoinductivity and osteoconductivity in the implanted tissue (ADAY; GUMUSDERELIOGLU, 2010).

Li and colleagues reported that structures produced with silk coating stimulated cell proliferation and increased osteogenic differentiation in stem cells. This effect was maintained throughout the 21 days culture period for single and multiple silk layers, and a thicker coating was associated with a much more pronounced effect (LI et al., 2017b).

In Figure 28, it can be observed that the cells remain on the surface, as there is no dead cell increase detected.

Figure 28 – Qualitative data of metabolic activity. (A) 3-day (40 x) with living (green) and dead cells (red); (B) cell adhesion in the scaffolds by SEM (1000× and 2000× magnification).

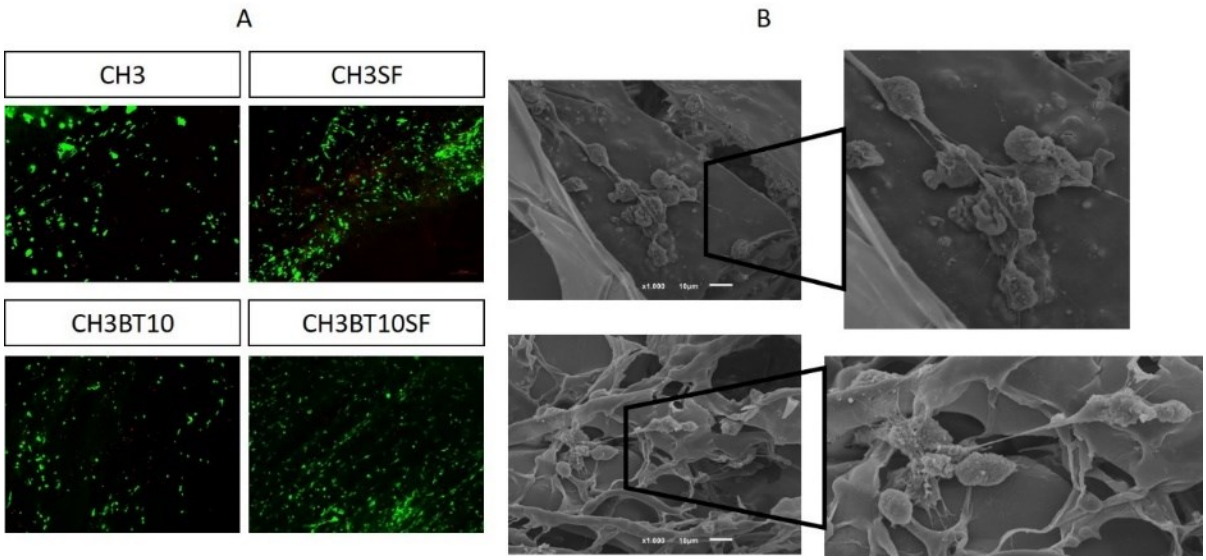

A constant staining was noted for all samples (Figure 29), demonstrating a homogeneous distribution of chitosan in all samples. Nevertheless, it seems that the alizarin red is not an adequate method for calcium quantification, considering that it reacts with CH (control).

Figure 29 – Calcium quantification by alizarin red after: (a) 1 day. (b) 3 days. (c) 7 days. (d) 14 days.

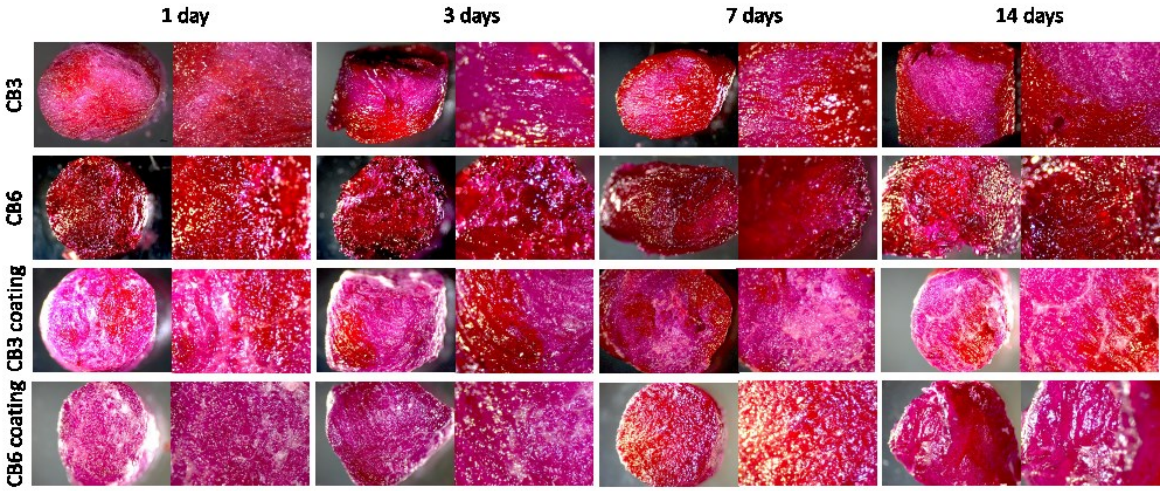

Partial conclusions indicate that scaffolds were successfully manufactured by freeze-drying. The combination of the polymers helped stabilize the structures. The pore size was around 166 μm, 84% porosity and 98% interconnectivity. BMP release suggests that scaffolds have a structure that allows an increase in the released concentration up to 3 hours.

Chapter 5– GENIPIN-CROSSLINKED CHITOSAN/β-TCP/SILK FOR OSTEOCHONDRAL REGENERATION

In this Chapter, a biomimetic bilayer scaffold was developed with a gradient of materials aiming the treatment of osteochondral defects. In the development of bilayer structures it is necessary to obtain stability between the materials involved and to ensure that this structure does not dissolve in contact with the body fluid. Scaffolds were prepared using chitosan/β-tricalcium phosphate for the bone part, and silk fibroin, to mimic the cartilaginous moiety. Moreover, the resulting structures were submitted to crosslinking using genipin. SEM micrographs revealed that the two layers of the scaffolds are well defined, while the results from the μ-CT analysis indicated that the silk portion is infiltrated throughout the scaffolds and that the silk layer presents more significant interconnectivity and porosity values, 59% and 68%, respectively. Ca concentration after bioactivity test with CBSG10 samples reached 900 ppm and the cytotoxicity tests performed by direct contact with MC3T3 and ATCD5 cells revealed good cell viability and proliferation up to 14 days. The results suggest that the structures can be used in osteochondral regeneration.

5.1.INTRODUCTION

The osteochondral tissue presents a hierarchical and organizational structure composed of articular cartilage (hyaline cartilage) and a subchondral bone part. It is subdivided in superficial, intermediate, deep, and calcified zones (JOHNSTONE et al., 2013; POOLE et al., 2001). In addition, there is a specific extracellular matrix organization in this tissue, collagen, chondrocytes and water, distributed at different concentrations throughout the tissue (SEO et al., 2014; SOPHIA FOX; BEDI; RODEO, 2009). The osteochondral injured tissues have limits of self-regeneration and partial repair. Thus, tissue engineering (TE) can promote the development of a tissue-like structure for tissue regeneration to occur. One of the most used TE approaches involves the use of bilayer structures, in which one part recovers the bone tissue, while the other supports the cartilage regeneration (ANSARI; KHORSHIDI; KARKHANEH, 2019; KARAGEORGIOU; KAPLAN, 2005; SEIDI et al., 2011). These scaffolds serve as a guide for cell colonization, as well as a support for the growth of new tissue (LIU et al., 2018a; MALAFAYA; REIS, 2009; OLIVEIRA et al., 2006; SEO et al., 2013; YAN et al., 2015).

Researchers have been intensively investigating the ideal biomaterial for the reconstruction of osteochondral tissue (DI LUCA; VAN BLITTERSWIJK; MORONI, 2015; TAMADDON et al., 2018). This biomaterial should be biocompatible, osteoinductive and osteoconductive, chondroinductive and chondroconductive. It must promote the angiogenesis while being able to provide a structure that is capable of guiding the development of new osteochondral tissue (CASTRO; PATEL; ZHANG, 2015; DENG; CHANG; WU, 2019; HANADA et al., 2001; LIU et al., 2018a; MALAFAYA; REIS, 2009; OLIVEIRA et al., 2006; RIBEIRO et al.,2018, 2019; SEO et al., 2013; YAN et al., 2015). The "soft-to-hard" part of this tissue constitutes a very challenging structural biological complex. Therefore, the development of a structure to reproduce the native tissue requires the use of different materials (SEIDI et al., 2011).

Natural materials such as collagen, silk fibroin (SF) and chitosan (CH) are reported to be used for the development of the bilayer scaffolds for osteochondral tissue regeneration (SEIDI et al., 2011; T.J. et al., 2016). In addition, due to the calcified layer and the subchondral layer of the native osteochondral tissue, ceramic materials including hydroxyapatite, tricalcium phosphate (β-TCP) and bioactive glasses are also added to the scaffolds to aid in the regeneration of the bone that make up the osteochondral tissue. (DA et al., 2013; FAHIMIPOUR et al., 2017; WANG et al., 2014).

However, CH and silk bilayer can dissolve/degrade in aqueous solution (YAO et al., 2004), which may lead to the loss of the scaffold support structure. To reduce this effect, these polymers may be chemically cross-linked with crosslinking agents such as glutaraldehyde or genipin (MUZZARELLI et al., 2015; SILVA et al., 2008b), a chemical compound found in the fruit extract of *Gardenia jasminoides*. The crosslinking agents are used in structures where the stability between the materials is not evident. In this context, they support the stability and delay the degradation of the biomaterial until the formation of the new tissue starts (JÓŹWIAK et al., 2017; SILVA et al., 2008b; ZHANG et al., 2016b).

The present work shows the ability to produce CH/β-TCP/SF bilayered scaffolds, using genipin as a crosslinking agent. We analyzed the structure produced chemically and physically, as well as the cellular behavior in the presence of the structure. Thus, the potential of these composites as supports for the regeneration the osteochondral tissue can be assessed.

5.2. MATERIALS AND METHODS

The materials and methods used were described in Chapter 3.

5.3. RESULTS AND DISCUSSION

The purpose of this study was to design, optimize and characterize an osteochondral scaffold, with integrated layers, via a rational combination of bioactive materials. The design concept involved a scaffold with two integrated layers overlapping at the interface. The two layers were targeted for the regeneration of articular cartilage (silk) and subchondral bone (CH/β-TCP) in the osteochondral unit (Figure 30). The CH concentration was selected based on previous studies, which show that 3 vol.% scaffolds support osteogenic and chondrogenic cell culture (GOBIN; FROUDE; MATHUR, 2005; VISHWANATH; PRAMANIK; BISWAS, 2016).

Figure 30 – Bilateral scaffolds microstructures: (a) optical microscopic (200 µm), (b) 200× and (c) 3000× magnification by SEM.

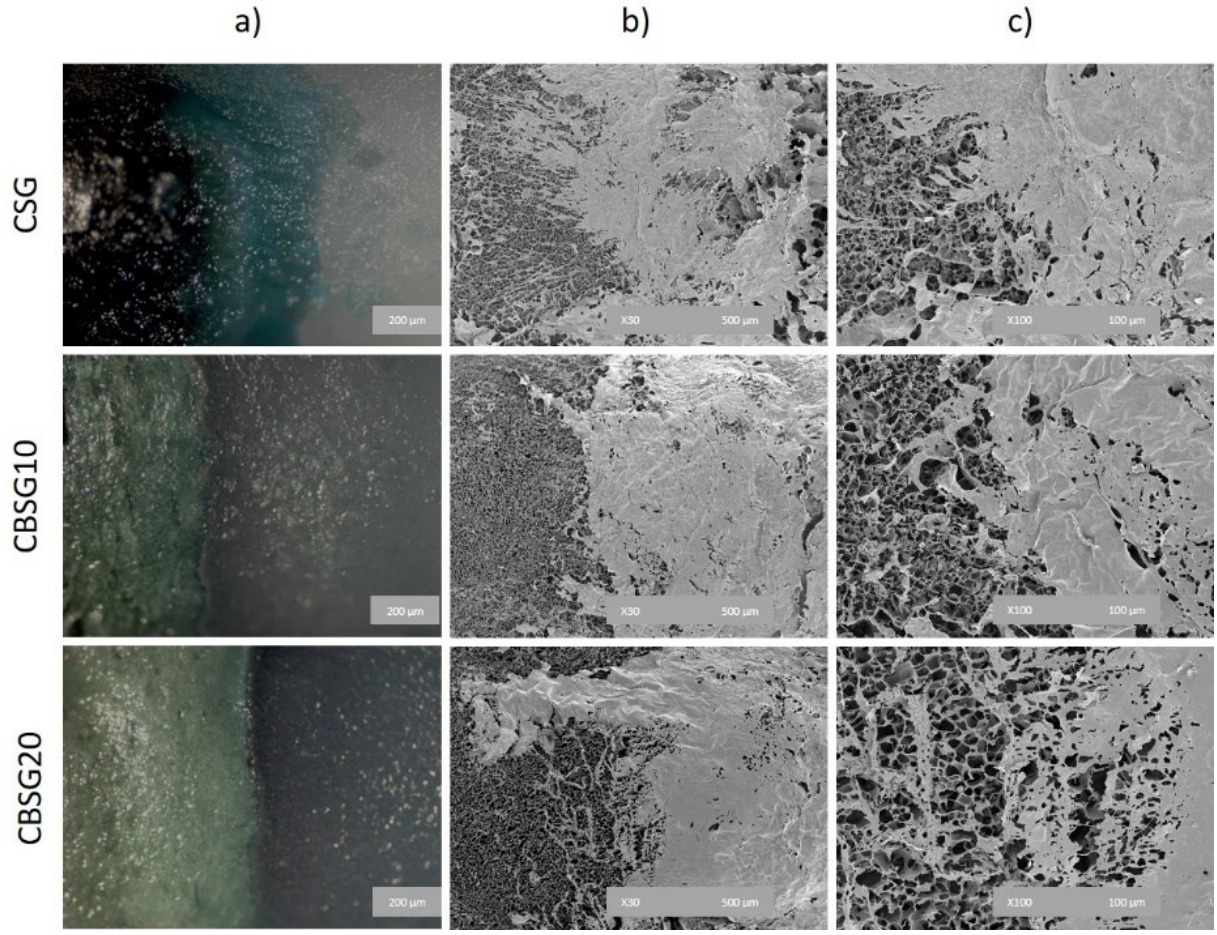

Figure 30 shows the microstructure of the scaffolds CSG, CBSG10, and CBSG20 obtained by optical microscopy (Figure 30a) and SEM (Figures 30b and 30c). By the analysis of the images it is possible to identify two layers: the white part is composed by SF, while the blue/green part represents the CH/β-TCP moiety of the scaffolds. The latter has a more distinct crosslinking by the action genipin. The silk layer constitutes the cartilage fraction and the layer composed by CH/β-TCP forms the bone fraction. Figures 30b and 30c clearly shows the pores formed in the CH/β-TCP layer, while the pores in the SF layer are not so evident.

Genipin, used as a crosslinking agent, presents good stability, biocompatibility, no cytotoxicity and well-defined composition (MUZZARELLI et al., 2015). It reacts with amine groups and with proteins (ZHANG; YANG; GUO, 2011). The mechanism of the reaction can be explained by the nucleophilic attack of the CHI C-2 to the C-3 group of genipin, forming radical groups that create a conjugated heterocyclic bonding (GAO et al., 2014) (CHEN et al., 2005). The produced scaffolds presented a crosslinking degree of up to 24%, which was

determined using trypan blue assay. In this test, trypan blue quantifies the free amines and the value of amine concentration can be subtracted to determine the degree of crosslinking of the material (SHEN; YANG; RYSER, 1984).

A quantitative analysis of the 3D morphometric parameters that characterize the produced scaffolds was performed by μ-CT analysis. The 3D images of the scaffolds are showed in Figure 31.

Figure 31 – 3D perspective of scaffolds (a). A - CH/β-TCP/silk. B - CH/silk. C - silk. D - CH. E - β-TCP. The blue color represents CH; red, β-TCP; and green, silk.

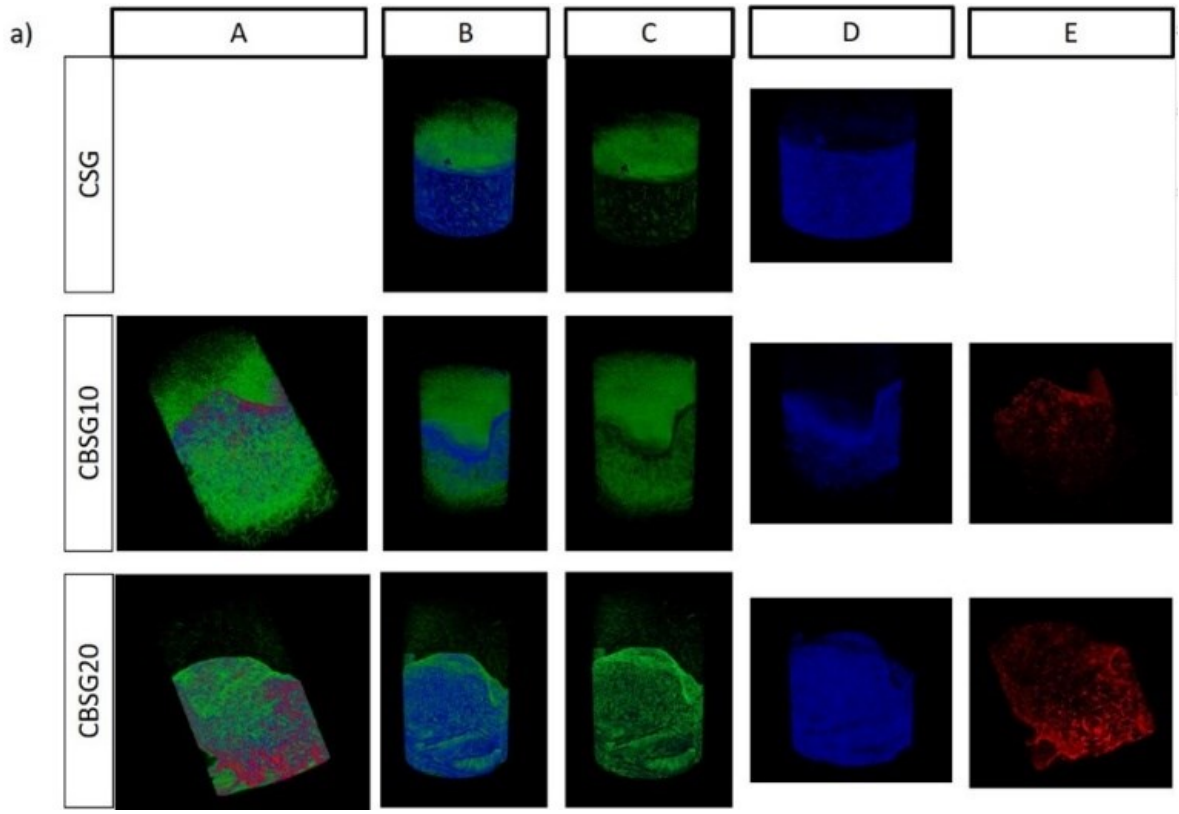

Each material used in the manufacture of scaffolds can be identified by different colors. The part equivalent to CH is represented in blue (Figure 31D); β-TCP (Figure 31E); , in red; and silk (Figure 31C), in green. Silk distribution involves the entire structure as shown in Figure 31, whereas the part where there is a mixture of CH/β-TCP shows the homogeneity of the components throughout the fraction (Figure 31A). As bilayer is identified and demonstrates the well-designed interface of the structure. The results by μ-CT allow estimating the pore size distribution, porosity and interconnectivity (Table 6).

Table 6- Microstructure data by μ-CT of the analysis with bilayer scaffolds.

	Samples	Mean thickness (μm)	Mean pore size (μm)	Porosity (%)	Interconnectivity (%)
Top	CSG	35.91	73.71	62.91	25.95
	CBSG10	55.16	84.12	59.88	54.24
	CBSG20	44.18	148.95	67.35	58.59
Interface	CSG	44.58	65.22	62.40	30.27
	CBSG10	80.27	47.10	31.55	3.05
	CBSG20	57.94	30.91	31.20	6.96
Bottom	CSG	42.12	77.37	69.83	30.27
	CBSG10	100.17	35.73	18.15	3.56
	CBSG20	103.86	25.85	8.71	0.59

The scaffolds show distinct structural characteristics in the bilayer region. However, the sample CSG presents a microstructure with similar values between the two layers. In samples CBSG10 and CBSG20, the values of interconnectivity, porosity and pore size decreased due to the silk infiltration along the CH/β-TCP layer. The infiltration of silk in the scaffolds is noticeable in Figures 31A and 31C.

Differences in porosity and interconnectivity from the top to the bottom of the scaffolds are also presented in Table 6. In the layer composed only by silk (top), the values remain in the range of 60-68% porosity and 26-59% interconnectivity. At the interface, there is a decrease of these values, as the ceramic component is present, suggesting its influence on the scaffolds microstructure. The bottom layer is composed basically by CH and β-TCP; the values of porosity and interconnectivity decrease reaching values of 9%, suggesting that the β-TCP influences the porosity.

In the chemical characterization of the scaffolds, it was possible to identify specific bands of each compound along the spectrum obtained by FTIR (Figure 32). Characteristic absorption bands of CH/β-TCP/SF were identified. A peak around 3260 cm^{-1} represents the N-H stretching vibration of the CH, which became lower when increasing the β-TCP ratio. The peak at 1650 cm^{-1} is associated with intermolecular TCP-sheet bands, presented in the S-rich

moiety, while the peak at 1500 cm^{-1} is related with C-O and at 1000 cm^{-1} with the PO_4^{-2} groups. (MARTINS et al., 2018).

Figure 32 - Fourier transform infrared (FTIR) spectra of scaffolds CSG, CBSG10 and CBSG20.

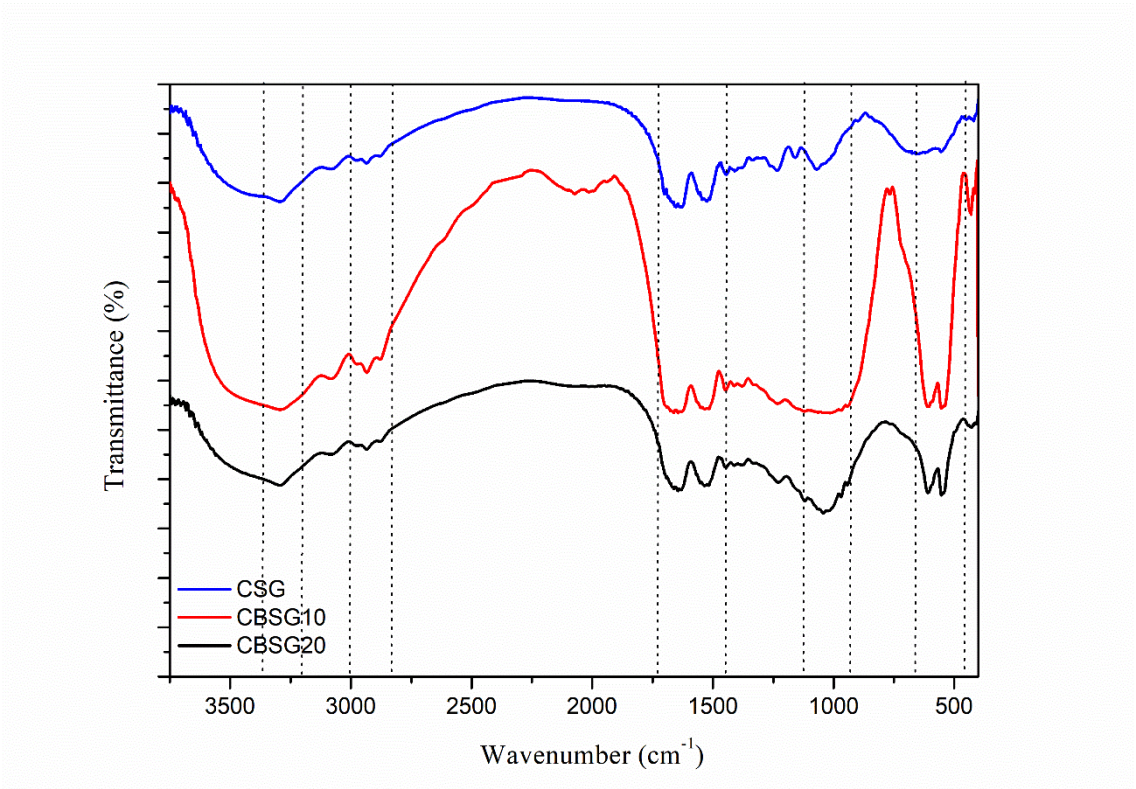

In Figure 33A (a/b/c), it can be observed the morphology and the formation of apatite crystals in the surface of the scaffolds, after immersion in a SBF solution, which mimics body fluids, for 1, 3 and 7 days. The CSG, CBSG10 and CBSG20 samples showed a progressive formation of apatite during the tested period, in areas where it has the highest concentration of β-TCP.

Figure 33 – Evaluation of apatite formation on scaffold surfaces by SEM. Surface after 1 (a), 3 (b) and 7 (c) days of bioactivity test: ICP analysis (A); Concentration of Ca (B); Concentration of P (C).

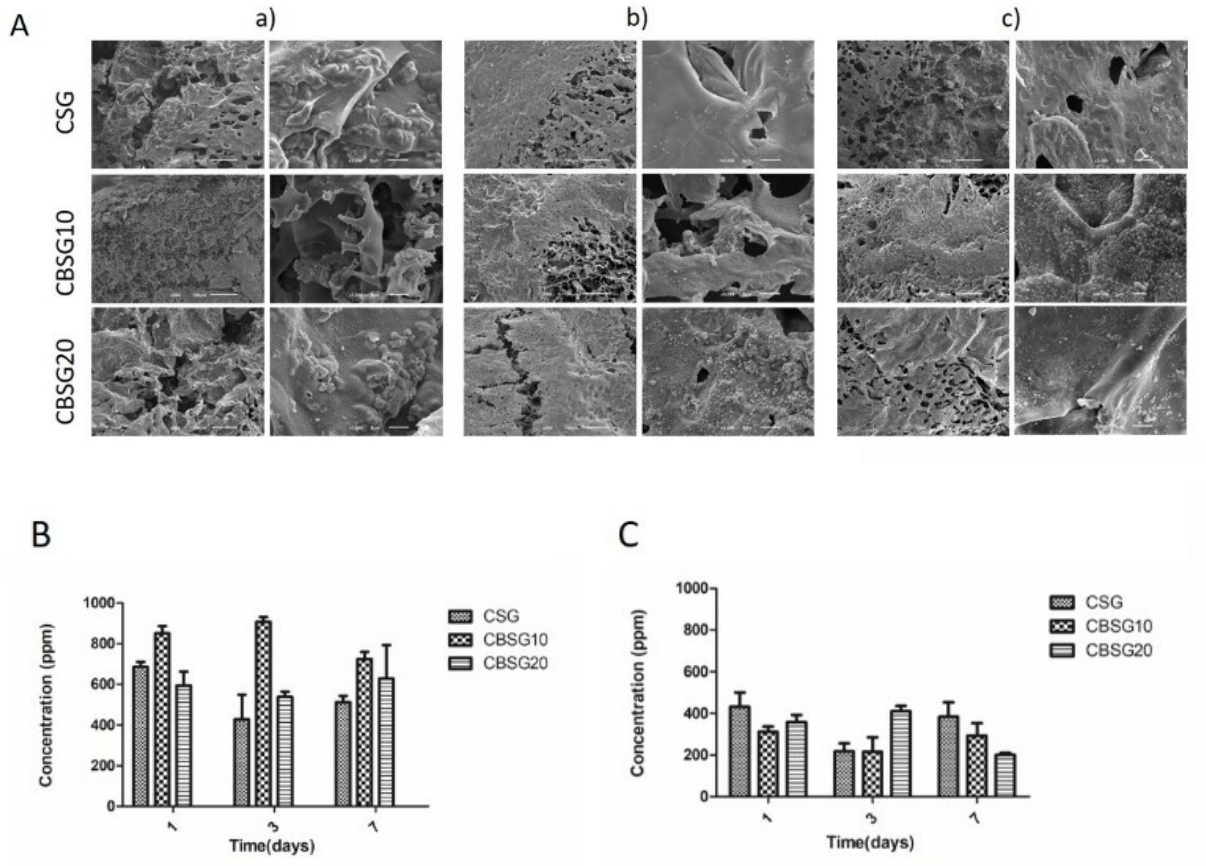

Figures 33B and 33C shows that the concentration of Ca was higher for all samples during the bioactivity test, when comparing with the P concentration. Moreover, the concentration of P was higher in CBSG20 and CSG, what is an indication of structure activity in SBF solution.

The results observed in Figure 33 show the bioactive response of the tested scaffolds, which is related with the ability to induce bioceramic mineralization under physiological conditions, also associated with β-TCP bioactivity (CANILLAS et al., 2017; LEE; PAI; CHANG, 2013).

The data for the degradation assay is presented in Figure 34. By the analysis of the graphs it is possible to conclude that the structures presented 15% degradation.

Figure 34 – Weight loss of the scaffolds (A). Data of the swelling ratio at pH 7.4 (B) and pH 5.7 (C).

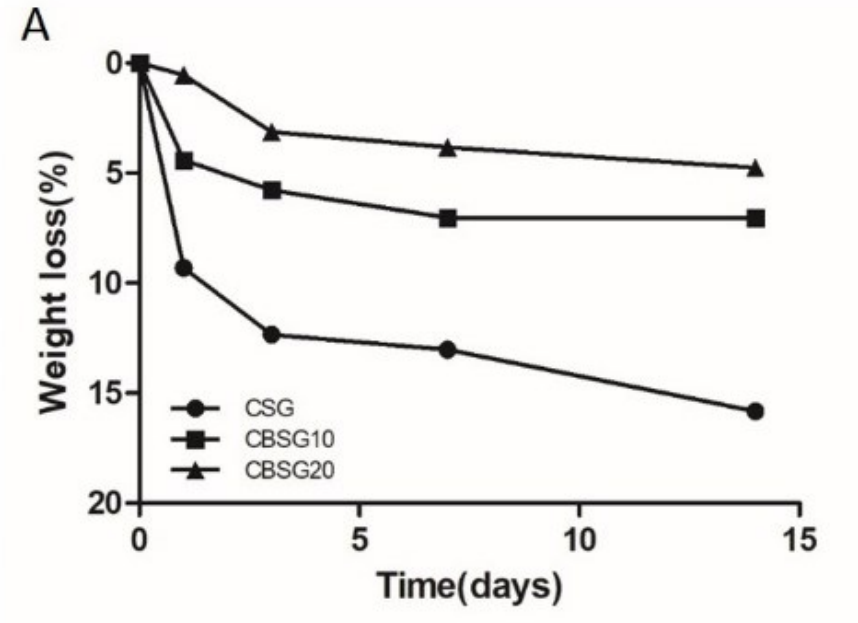

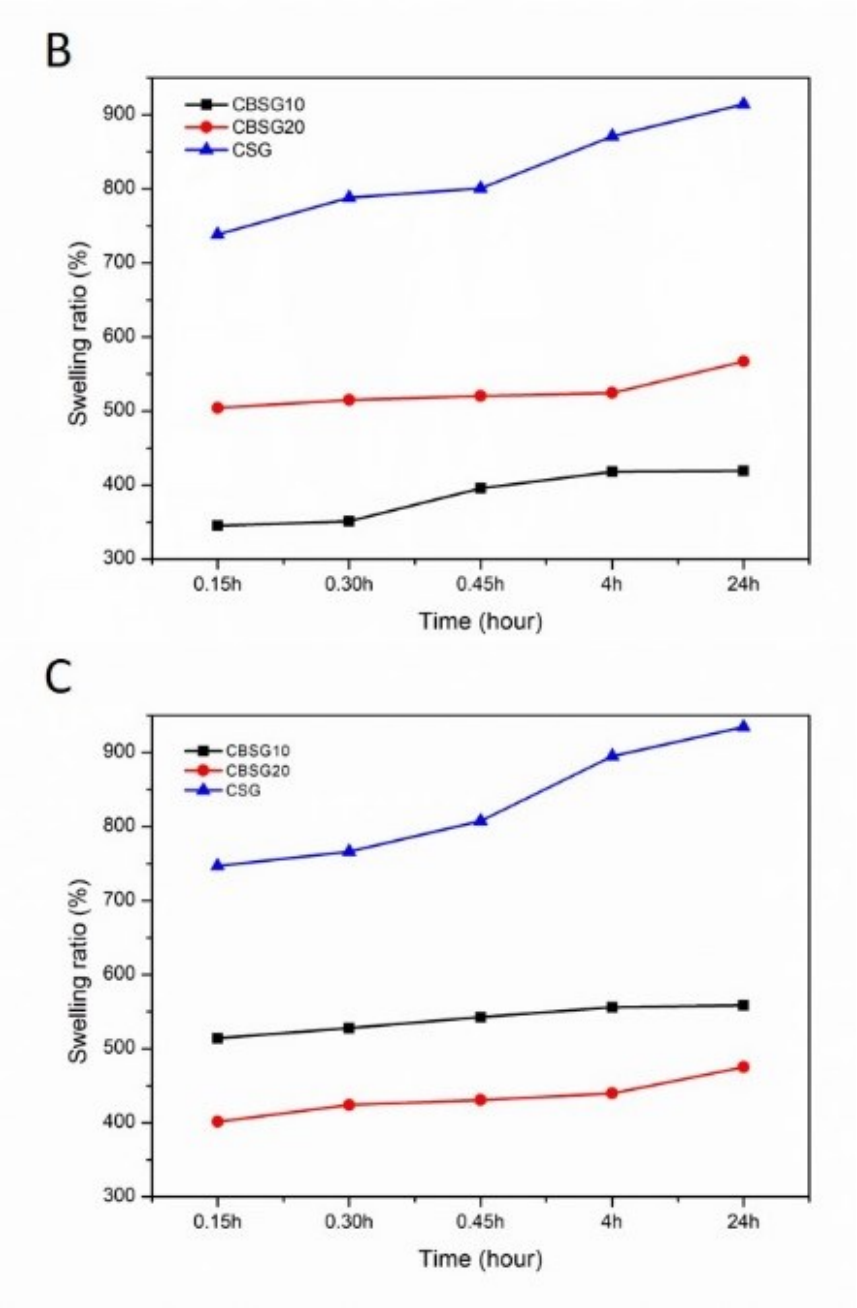

The water retention ability of the scaffolds was tested at different pH solutions (5.7 and 7.4). The data presented in Figure 34A for PBS and 34B for the solution at pH 5.7 show an increase after 4 h of analysis in the case of CBSG20. The CBSG20 and CBSG10 scaffolds retained less water when compared to CSG. The scaffolds CBSG20 and CBSG10, which have 20 and 10% β-TCP, respectively, exhibit higher water retention at pH 7.4 than at pH 5.7. Taking this into account, it is possible to conclude that a lower ceramic load leads to a higher retention.

It is known that the degradation of CH occurs by hydrolysis, by action of lysozyme, which is present in the human body. The interaction of the polymer network with water molecules occurs by fractionation of the chains, forming smaller chains of β-1-4 units. This reaction releases aminoacids, which can be incorporated into the metabolic pathways or excreted by the body (KEAN; THANOU, 2010; LIU; ZHOU; SUN, 2012; REN et al., 2005). Other products derived from CH degradation include saccharides, which become part of the normal metabolic process. In the present work, the reduction of the degradation rate on the scaffolds CBSG10 an CBSG20 may be attributed to the TCP concentration in the material, since the acidic products of CH may be neutralized by the alkali groups of the ceramics (QASIM et al., 2017).

Several works report that the use of ceramic charge for the production of polymeric scaffolds promotes osteogenesis, and a greater interaction with the polymer, which is shown both in *in vitro* and *in vivo* tests (KUTTAPPAN; MATHEW; NAIR, 2016; RIBEIRO et al., 2019; YAN et al., 2013, 2015).

The cytotoxicity results showed unchanged cell morphology (Figure 35A) after contact with the extracts of the materials, as well as an increase in growth (Figure 35C) and cell viability (Figure 35B).

Figure 35 - Data of the cell cytotoxicity of the materials: Cell morphology (A); Cell viability (B); cell growth (C).

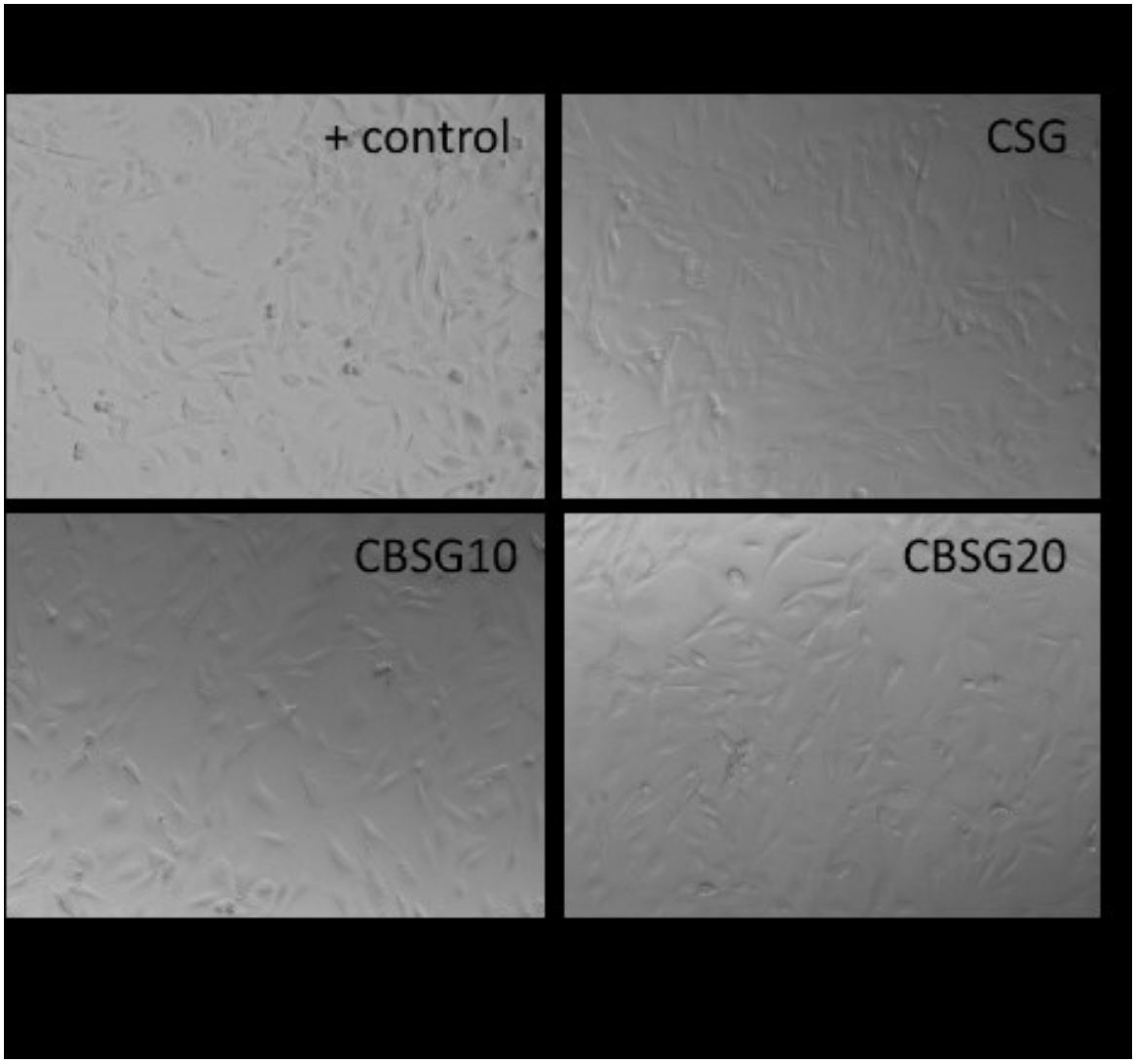
+ control
CSG
CBSG10
CBSG20

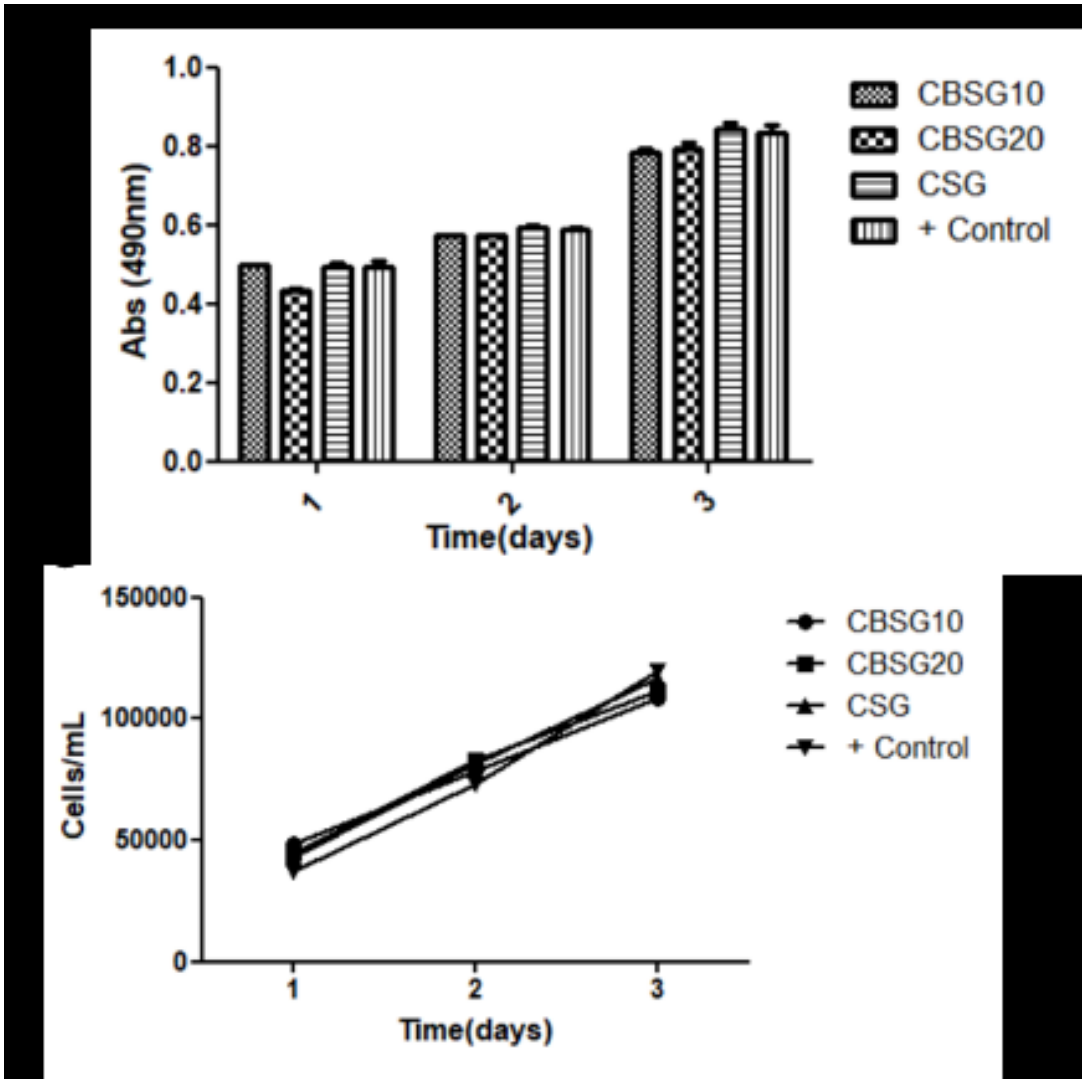

The results of physical and chemical characterization suggest that the developed scaffolds allow a good flow of nutrients, vital for cell culture in the two layers, according to the needs of each part of the tissue involved. The materials used are biodegradable (Figure 34), bioactive and promote mechanical support, while stimulating new tissue formation without cytotoxicity (Figure 35) when in contact with the native tissue (ARAHIRA; MARUTA; MATSUYA, 2017; BASTAMI et al., 2017; CROSS et al., 2016; GOTHARD et al., 2014; WEISGERBER et al., 2016).

Cell attachment, proliferation and migration in the bilayer scaffold were determined using two-cell lines: MC3T3 was seeded in the bone layer, and ATCD5 was seeded in the cartilage one. Both cell lines were used aiming to mimic native tissue. The cell viability results showed significant differences ($p > 0.05$) after 1, 3, and 7 days, when compared to 14 days of culture. In the results of cell proliferation there were significant differences between 1 and 3 days, when comparing with the values after 7 and 14 days of culture (Figure 36).

Figure 36 – Data of biological characterization: (a) Cell viability; (b) DNA concentration; (c) ALP. * Indicates significant differences between the samples along of the time points P(<0.05).

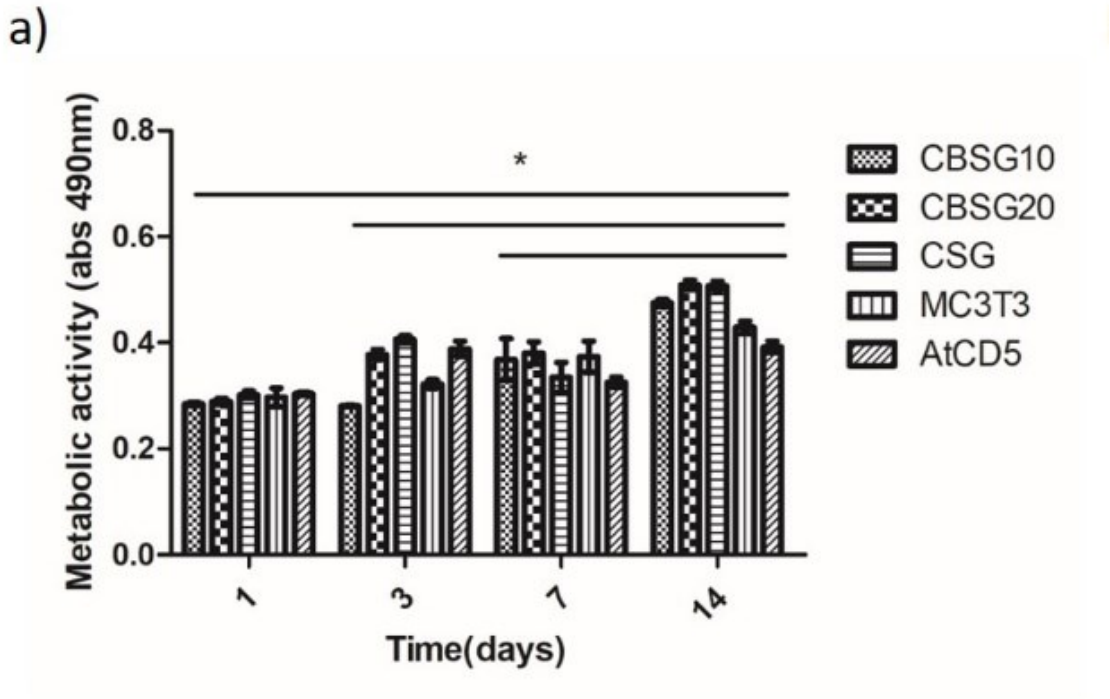

b)

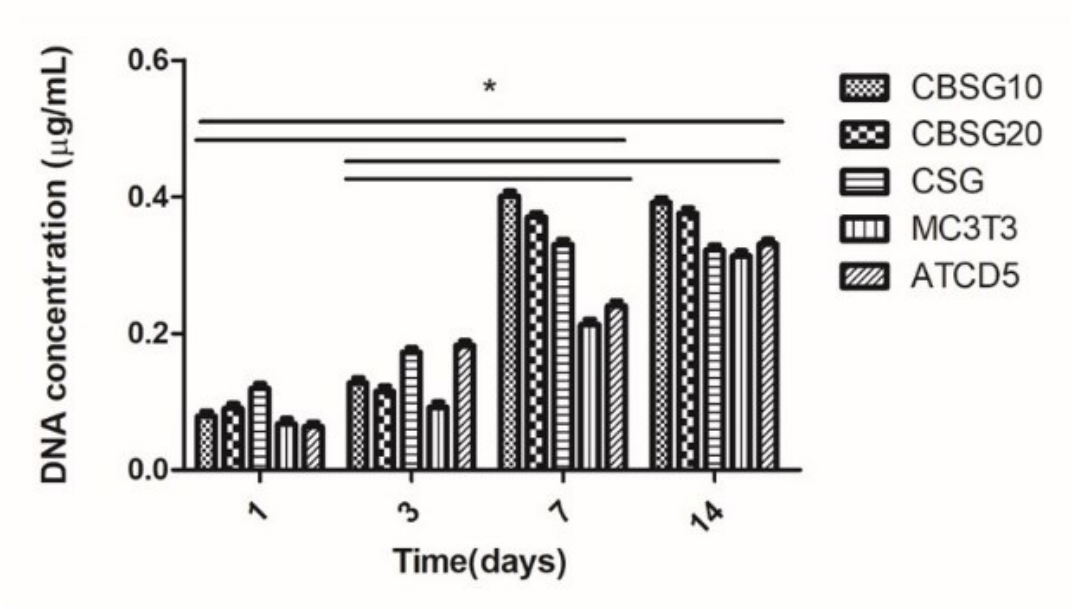

c)

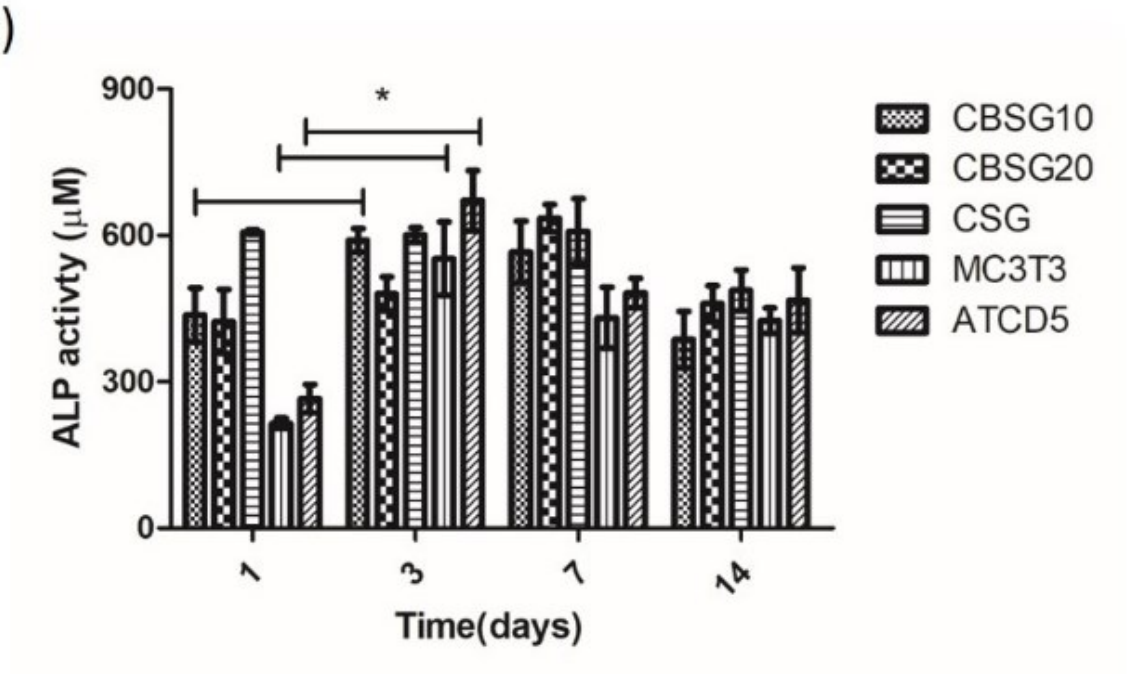

In the ALP data, it can be observed that there are significant differences between 1 and 3 days of culture on the scaffolds CBSG10 and in the controls of MC3T3 and ATCD5. (Figure 36c), regarding the cell viability data, up to two weeks, with cell proliferation, and ALP expression from the first day of culture (Figure 36).

Cell proliferation and viability in each scaffold layer was determined using fluorescence microscopy, (Figure 37A). The qualitative live/dead data show a large number of

living cells (green) on the surface and almost no dead cells (red). Cells adhered to the scaffolds and between adhered cells (Figure 37B).

Figure 37 – Qualitative live/dead data (A) and morphology cell by SEM (B).

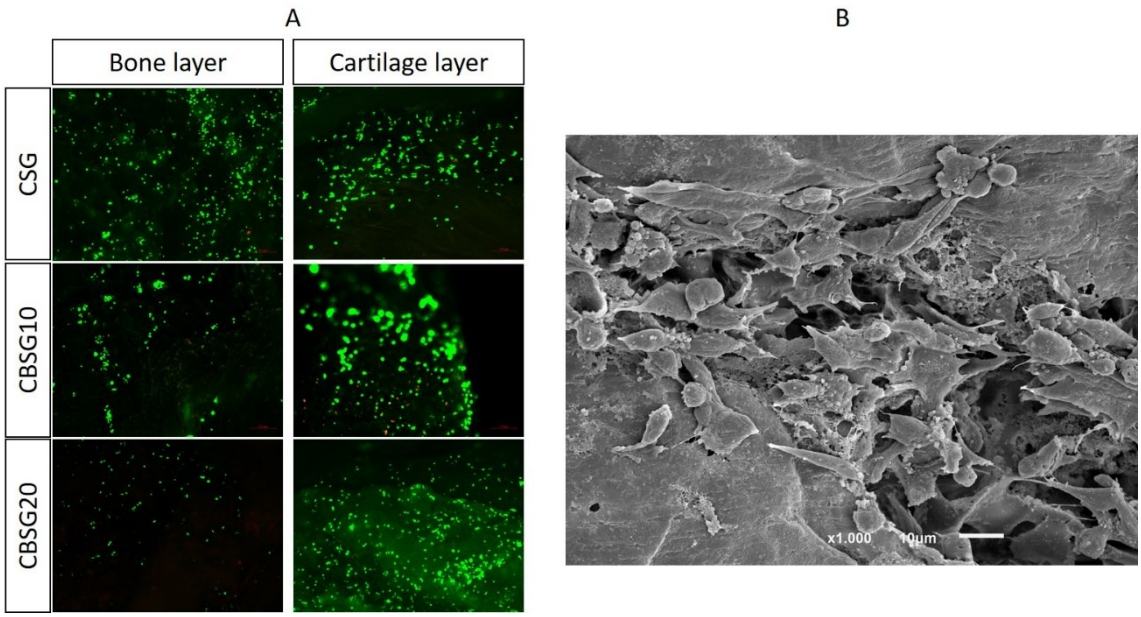

The increase of adherent cells in the scaffolds is own to the presence of calcium phosphate that leads to proliferation of osteoblasts (SOWMYA et al., 2011). The addition of microparticles increases the roughness and the surface area, which promotes the proliferation of osteoblasts, as well as their adhesion (SOWMYA et al., 2011).

Partial conclusions indicate that the scaffolds were stabilized by the action of the crosslinking agent. The data of the scaffolds were around 60% porosity and 54% interconnectivity (top); 31% porosity and 3% interconnectivity (interface) and 18% porosity and 3% interconnectivity (bottom). Stable, preserved the microstructure characteristics, and did not alter the cytotoxicity of the material. Scaffolds are compatible for cellular colonization, due to the suitable porosity and pore interconnectivity difference along the structure.

Chapter 6 – CONCLUSIONS AND FUTURE WORK

6.1.CONCLUSIONS

We can conclude that the scaffolds developed for bone and ostechondral regeneration were successfully synthesized. Both presented stability in structure, microstructure with differentiated porosity allowing a flow of cells and body fluid. Thus, they are supposed to be colonized and produce a new functional tissue. Through biological characterization, the scaffolds showed cell viability and proliferation when in contact with cells specific for each tissue. Further testing to confirm their potential for tissue regeneration is suggested, though.

Regarding silk-coated chitosan/β-TCP composites, we can conclude that silk-coated CH/β-TCP composites were successfully manufactured by freeze-drying. In this case, the combination of polymers helped to stabilize the scaffolds. The addition of β-TCP to the scaffold matrix conferred an osteoinductive source, which improved the adhesion and proliferation of osteoblasts. This was proved by the in vitro tests, that suggest the formation of the new bone once further implanted. The good hydrophilicity of the scaffold indicates that it is easily absorved by the body and promotes a good diffusion of nutrients. Coating scaffolds presented more suitable microstructure, with pore sizes around 166 μm, in addition to 84% porosity and 98% interconnectivity. In this case, silk had a positive influence on the structure, creating a smoother environment, propitious for cell development. Among the scaffolds, we indicate that CB3BT10 has promising features for future tests. BMP release suggests that scaffolds have a structure that allows an increase in the released concentration up to 3 hours. Afterwards, there is a tendency to seek BMP release stability. These results indicate their potential for tissue regeneration.

Regarding the genipin-crosslinked chitosan/β-TCP/silk for osteochondral regeneration, we can conclude than the bilayer structures were constructed with optimized stability by the action of the crosslinking agent. Genipin allowed the scaffold to be stable, preserved the microstructure characteristics, and did not alter the cytotoxicity of the material. The microstructure data are compatible for cellular colonization, due to the suitable porosity and pore interconnectivity difference along the structure, suggesting the creation of a structure similar to osteochondral tissue. The cells presented viability and proliferation up to 14 days, and it was possible to verify the adhesion under the material. Thus, CBSG10 has the potential to be used as an option for osteochondral tissue regeneration.

6.2. FUTURE WORKS

BMP release study should be performed in cell culture, as well as *in vivo* tests to validate *in situ* the regeneration of bone and osteochondral tissue using the scaffolds developed in this work.

Biological tests should be carried out on the structures using stem cells.

REFERENCES

ADAY, S.; GUMUSDERELIOGLU, M. Bone-Like apatite-coated chitosan scaffolds: Characterization and osteoblastic activity. **Polymer Composites**, v. 31, n. 8, p. 1418–1426, 2010.

AGARWAL, R.; GARCÍA, A. J. Biomaterial strategies for engineering implants for enhanced osseointegration and bone repair. **Advanced Drug Delivery Reviews**, v. 94, p. 53–62, 2015.

AMINI, A. R.; LAURENCIN, C. T.; NUKAVARAPU, S. P. Bone Tissue Engineering: Recent Advances and Challenges. **Critical Reviews™ in Biomedical Engineering**, v. 40, n. 5, p. 363–408, 2012.

ANSARI, S.; KHORSHIDI, S.; KARKHANEH, A. Engineering of gradient osteochondral tissue: From nature to lab. **Acta Biomaterialia**, v. 87, n. January, p. 41–54, 2019.

ARAHIRA, T.; MARUTA, M.; MATSUYA, S. Characterization and in vitro evaluation of biphasic α-tricalcium phosphate/β-tricalcium phosphate cement. **Materials Science and Engineering C**, v. 74, p. 478–484, 2017.

ARPORNMAEKLONG, P.; PRESSLER, M. J. Effects of ß-TCP scaffolds on neurogenic and osteogenic differentiation of human embryonic stem cells. **Annals of Anatomy**, v. 215, p. 52–62, 2018.

ARVIDSON, K. et al. Bone regeneration and stem cells. **Journal of Cellular and Molecular Medicine**, v. 15, n. 4, p. 718–746, 2011.

ATESOK, K. et al. Multilayer scaffolds in orthopaedic tissue engineering. **Knee Surgery, Sports Traumatology, Arthroscopy**, v. 24, n. 7, p. 2365–2373, 2016.

AZEVEDO, A. S. et al. Use of chitosan and β-tricalcium phosphate, alone and in combination, for bone healing in rabbits. **Journal of Materials Science: Materials in Medicine**, v. 25, n. 2, p. 481–486, 2014.

BAE, I.-H. et al. Evaluation of a Thiolated Chitosan Scaffold for Local Delivery of BMP-2 for Osteogenic Differentiation and Ectopic Bone Formation. **BioMed Research International**, v. 2013, p. 1–10, 2013.

BASTAMI, F. et al. Fabrication of a three-dimensional beta-tricalcium-phosphate/gelatin containing chitosan-based nanoparticles for sustained release of bone morphogenetic protein-2: Implication for bone tissue engineering. **Materials science & engineering. C, Materials for biological applications**, v. 72, p. 481–491, 2017.

BECK, E. C.; DETAMORE, M. S. Nanomaterials for hard-soft tissue interfaces. In:

Nanomaterials in Tissue Engineering: Fabrication and Applications. p. 363–386.

BIAN, W. et al. Morphological characteristics of cartilage-bone transitional structures in the human knee joint and CAD design of an osteochondral scaffold. **BioMedical Engineering Online**, v. 15, n. 1, p. 1–14, 2016.

BIANCO, P. et al. Bone marrow stromal stem cells: nature, biology, and potential applications. **Stem cells**, v. 19, n. 3, p. 180–192, 2001.

BLAIR, H. C.; SUN, L.; KOHANSKI, R. A. **Balanced regulation of proliferation, growth, differentiation, and degradation in skeletal cells**Annals of the New York Academy of Sciences. **Anais**...2007

BOSE, S.; TARAFDER, S.; BANDYOPADHYAY, A. Effect of Chemistry on Osteogenesis and Angiogenesis Towards Bone Tissue Engineering Using 3D Printed Scaffolds. **Annals of Biomedical Engineering**, v. 45, n. 1, p. 261–272, 2017.

BOUET, G. et al. In vitro three-dimensional bone tissue models: from cells to controlled and dynamic environment. **Tissue engineering. Part B, Reviews**, v. 21, n. 1, p. 133–56, 2015.

BURCHARDT, H. The Biology of Bone Graft Repair. **Clinical Orthopaedics and Related Research**, v. 174, p. 28–42, 2006.

CANILLAS, M. et al. Calcium phosphates for biomedical applications. **Boletin de la Sociedad Espanola de Ceramica y Vidrio**, v. 56, n. 3, p. 91–112, 2017.

CAO, W.; HENCH, L. L. Bioactive materials. **Ceramics International**, v. 22, n. 6, p. 493–507, 1996.

CARUTA, B. Ceramics and composite materials: New research. p. 56–64, 2006.

CASTRO, N. J.; PATEL, R.; ZHANG, L. G. Design of a Novel 3D Printed Bioactive Nanocomposite Scaffold for Improved Osteochondral Regeneration. **Cellular and Molecular Bioengineering**, v. 8, n. 3, p. 416–432, 2015.

CHAN, B. P.; LEONG, K. W. Scaffolding in tissue engineering: General approaches and tissue-specific considerations. **European Spine Journal**, v. 17, n. SUPPL. 4, 2008.

CHEN, H. et al. Reaction of chitosan with genipin and its fluorogenic attributes for potential microcapsule membrane characterization. **Journal of Biomedical Materials Research - Part A**, v. 32, n. 2, 2005.

CHEN, J. et al. Simultaneous regeneration of articular cartilage and subchondral bone in vivo using MSCs induced by a spatially controlled gene delivery system in bilayered

integrated scaffolds. **Biomaterials**, v. 32, n. 21, p. 4793–805, 2011.

CHEN, Y. H. et al. Guided bone regeneration activity of different calcium phosphate/chitosan hybrid membranes. **International Journal of Biological Macromolecules**, v. 126, p. 159–169, 2019.

CHIONO, V. et al. Genipin-crosslinked chitosan/gelatin blends for biomedical applications. **Journal of Materials Science: Materials in Medicine**, v. 19, n. 2, p. 889–98, 2008.

COSTA-PINTO, A. R.; REIS, R. L.; NEVES, N. M. Scaffolds Based Bone Tissue Engineering: The Role of Chitosan. **Tissue Engineering Part B: Reviews**, v. 17, n. 5, p. 331–347, 2011.

CROSS, L. M. et al. Nanoengineered biomaterials for repair and regeneration of orthopedic tissue interfaces. **Acta Biomaterialia**, v. 42, p. 2–17, 2016.

DA, H. et al. The Impact of Compact Layer in Biphasic Scaffold on Osteochondral Tissue Engineering. **PLoS ONE**, v. 8, n. 1, p. e54838, 2013.

DADSETAN, M. et al. Effect of calcium phosphate coating and rhBMP-2 on bone regeneration in rabbit calvaria using poly(propylene fumarate) scaffolds. **Acta Biomaterialia**, v. 18, p. 9–20, 2015.

DE OBALDIA, E. E. et al. Analysis of the mechanical response of biomimetic materials with highly oriented microstructures through 3D printing, mechanical testing and modeling. **Journal of the Mechanical Behavior of Biomedical Materials**, v. 48, p. 70–85, 2015.

DENG, C.; CHANG, J.; WU, C. Bioactive scaffolds for osteochondral regeneration. **Journal of Orthopaedic Translation**, v. 17, p. 15–25, 2019.

DESCHASEAUX, F.; SENSÉBÉ, L.; HEYMANN, D. Mechanisms of bone repair and regeneration. **Trends in Molecular Medicine**, v. 15, n. 9, p. 417–429, 2009.

DI LUCA, A.; VAN BLITTERSWIJK, C.; MORONI, L. The osteochondral interface as a gradient tissue: From development to the fabrication of gradient scaffolds for regenerative medicine. **Birth Defects Research Part C - Embryo Today: Reviews**, v. 105, n. 1, p. 34–52, 2015.

DI MARTINO, A.; SITTINGER, M.; RISBUD, M. V. Chitosan: A versatile biopolymer for orthopaedic tissue-engineering. **Biomaterials**, v. 26, n. 30, p. 5983–5990, 2005.

DU, Y. et al. Selective laser sintering scaffold with hierarchical architecture and gradient composition for osteochondral repair in rabbits. **Biomaterials**, v. 137, p. 37–48, 2017.

DUPIN, S. et al. Microstructural origin of physical and mechanical properties of

polyamide 12 processed by laser sintering. **European Polymer Journal**, v. 48, n. 9, p. 1611–1621, 2012.

FABBRI, M.; CELOTTI, G. C.; RAVAGLIOLI, A. Granulates based on calcium phosphate with controlled morphology and porosity for medical applications: physico-chemical parameters and production technique. **Biomaterials**, v. 15, n. 6, p. 474–7, 1994.

FAHIMIPOUR, F. et al. Collagenous matrix supported by a 3D-printed scaffold for osteogenic differentiation of dental pulp cells. **Dental Materials**, p. 209–220, 2017.

FAROKHI, M. et al. Silk fibroin/hydroxyapatite composites for bone tissue engineering. **Biotechnology Advances**, v. 36, n. 1, p. 68–91, 2018.

FARRELL, E. et al. A collagen-glycosaminoglycan scaffold supports adult rat mesenchymal stem cell differentiation along osteogenic and chondrogenic routes. **Tissue engineering**, v. 12, n. 3, p. 459–468, 2006.

FENG, S.; HE, F.; YE, J. Hierarchically porous structure, mechanical strength and cell biological behaviors of calcium phosphate composite scaffolds prepared by combination of extrusion and porogen burnout technique and enhanced by gelatin. **Materials Science and Engineering C**, v. 82, n. August 2017, p. 217–224, 2018.

FERNANDEZ-YAGUE, M. A. et al. Biomimetic approaches in bone tissue engineering: Integrating biological and physicomechanical strategies. **Advanced Drug Delivery Reviews**, v. 84, p. 1–29, 2015.

FLORENCIO-SILVA, R. et al. Biology of Bone Tissue: Structure, Function, and Factors That Influence Bone Cells. **BioMed Research International**, p. 421746, 2015.

FURUSAWA, T. et al. Enhancement of mechanical strength and in vivo cytocompatibility of porous β-tricalcium phosphate ceramics by gelatin coating. **International Journal of Implant Dentistry**, v. 2, n. 1, p. 4, 2017.

GAO, L. et al. Effects of genipin cross-linking of chitosan hydrogels on cellular adhesion and viability. **Colloids and Surfaces B: Biointerfaces**, v. 117, p. 398–405, 2014.

GARIBOLDI, M. I.; BEST, S. M. Effect of Ceramic Scaffold Architectural Parameters on Biological Response. **Frontiers in Bioengineering and Biotechnology**, v. 3, p. 151, 2015.

GERSTENFELD, L. C. et al. Fracture healing as a post-natal developmental process: Molecular, spatial, and temporal aspects of its regulation. **Journal of Cellular Biochemistry**, v. 88, n. 5, p. 873–884, 2003.

GOBIN, A. S.; FROUDE, V. E.; MATHUR, A. B. Structural and mechanical

characteristics of silk fibroin and chitosan blend scaffolds for tissue regeneration. **Journal of Biomedical Materials Research - Part A**, v. 74, n. 3, p. 465–73, 2005.

GOLDRING, M. B. Chondrogenesis, chondrocyte differentiation, and articular cartilage metabolism in health and osteoarthritis. **Therapeutic Advances in Musculoskeletal Disease**, v. 4, n. 4, p. 269–285, 2012.

GOTHARD, D. et al. Tissue engineered bone using select growth factors: A comprehensive review of animal studies and clinical translation studies in man. **European cells & materials**, v. 28, p. 166- 207; discussion 207–8, 2014.

GRIFFITH, L. G. Emerging design principles in biomaterials and scaffolds for tissue engineering. **Annals of the New York Academy of Sciences**, v. 961, p. 83–95, 2002.

GRUSKIN, E. et al. Demineralized bone matrix in bone repair: History and use. **Advanced Drug Delivery Reviews**, v. 64, n. 12, p. 1063–77, 2012.

HANADA, K. et al. BMP-2 induction and TGF-1 modulation of rat periosteal cell chondrogenesis. **Journal of Cellular Biochemistry**, v. 81, n. 2, p. 284–294, 2001.

HARRIS, R. et al. Chitosan nanoparticles and microspheres for the encapsulation of natural antioxidants extracted from Ilex paraguariensis. **Carbohydrate Polymers**, v. 84, n. 2, p. 803–806, 2011.

HAUGH, M. G.; MURPHY, C. M.; O'BRIEN, F. J. Novel Freeze-Drying Methods to Produce a Range of Collagen–Glycosaminoglycan Scaffolds with Tailored Mean Pore Sizes. **Tissue Engineering Part C: Met hods**, v. 16, n. 5, p. 887–894, 2009.

HENKEL, J. et al. Bone Regeneration Based on Tissue Engineering Conceptions — A 21st Century Perspective. **Bone Research**, v. 1, n. 3, p. 216–248, 2013.

HING, K. A. et al. Microporosity enhances bioactivity of synthetic bone graft substitutes. **Journal of Materials Science: Materials in Medicine**, v. 16, n. 5, p. 467–75, 2005.

HO-SHUI-LING, A. et al. Bone regeneration strategies: Engineered scaffolds, bioactive molecules and stem cells current stage and future perspectives. **Biomaterials**, v. 180, p. 143–162, 2018.

HUH, J. T. et al. Preparation and characterization of gelatin/α-TCP/SF biocomposite scaffold for bone tissue regeneration. **International Journal of Biological Macromolecules**, v. 110, p. 488–496, 2018.

HUTMACHER, D. W. Scaffolds in tissue engineering bone and cartilage. **Biomaterials**, v. 21, n. 24, p. 2529–2543, 2000.

INZANA, J. A. et al. 3D printing of composite calcium phosphate and collagen scaffolds for bone regeneration. **Biomaterials**, v. 35, n. 13, p. 4026–4034, 2014.

ISHACK, S. et al. Bone regeneration in critical bone defects using three-dimensionally printed β-tricalcium phosphate/hydroxyapatite scaffolds is enhanced by coating scaffolds with either dipyridamole or BMP-2. **Journal of Biomedical Materials Research - Part B Applied Biomaterials**, p. 1–10, 2015.

IVIGLIA, G. et al. Novel bioceramic-reinforced hydrogel for alveolar bone regeneration. **Acta Biomaterialia**, v. 44, n. 2016, p. 97–109, 2016.

JAFARI, M. et al. Polymeric scaffolds in tissue engineering: a literature review. **Journal of Biomedical Materials Research - Part B Applied Biomaterials**, v. 105, n. 2, p. 431–459, 2017.

JAHAN, K.; TABRIZIAN, M. Composite biopolymers for bone regeneration enhancement in bony defects. **Biomater. Sci.**, v. 4, p. 25–39, 2015.

JI, W. et al. Local delivery of small and large biomolecules in craniomaxillofacial bone. **Advanced Drug Delivery Reviews**, v. 64, n. 12, p. 1152–1164, 2012.

JOHNSTONE, B. et al. Tissue engineering for articular cartilage repair--the state of the art. **European cells & materials**, v. 25, p. 248–267, May 2013.

JÓŹWIAK, T. et al. Effect of ionic and covalent crosslinking agents on properties of chitosan beads and sorption effectiveness of Reactive Black 5 dye. **Reactive and Functional Polymers**, v. 114, p. 58–74, 2017.

JUDAS, F. et al. Estrutura E Dinâmica Do Tecido Ósseo. **Cerâmica**, p. 51, 2012.

KANG, H.-W. et al. **Rapid Prototyping of Biomaterials**. [s.l.] Woodhead Publishing Limited, 2014.

KARAGEORGIOU, V.; KAPLAN, D. **Porosity of 3D biomaterial scaffolds and osteogenesisBiomaterials**, 2005.

KATTI, K. S.; KATTI, D. R.; DASH, R. Synthesis and characterization of a novel chitosan/montmorillonite/ hydroxyapatite nanocomposite for bone tissue engineering. **Biomedical Materials**, v. 3, n. 3, p. 034–056, 2008.

KEAN, T.; THANOU, M. Biodegradation, biodistribution and toxicity of chitosan. **Advanced drug delivery reviews**, v. 62, n. 3, p. 11, 2010.

KEENEY, M.; PANDIT, A. The Osteochondral Junction and Its Repair via Bi-Phasic Tissue Engineering Scaffolds. **Tissue Engineering Part B: Reviews**, v. 15, p. 55–73, 2009.

KEOGH, M. B.; O'BRIEN, F. J.; DALY, J. S. A novel collagen scaffold supports human osteogenesis - Applications for bone tissue engineering. **Cell and Tissue Research**, v.

340, n. 1, p. 169–177, 2010.

KHOJASTEH, A. et al. Development of PLGA-coated β-TCP scaffolds containing VEGF for bone tissue engineering. **Materials Science and Engineering C**, v. 69, p. 780–788, 2016.

KHOJASTEH, A. et al. Bone engineering in dog mandible: Coculturing mesenchymal stem cells with endothelial progenitor cells in a composite scaffold containing vascular endothelial growth factor. **Journal of Biomedical Materials Research - Part B Applied Biomaterials**, v. 105, n. 7, p. 1767–1777, 2017.

KIM, H.-M. Bioactive Ceramics: Challenges and Perspectives. **Journal of the Ceramic Society of Japan**, v. 109, p. 49–57, 2011.

KIM, H. J. et al. Bone tissue engineering with premineralized silk scaffolds. **Bone**, v. 42, n. 6, p. 1226–1234, 2008.

KIM, H. W.; KNOWLES, J. C.; KIM, H. E. Hydroxyapatite and gelatin composite foams processed via novel freeze-drying and crosslinking for use as temporary hard tissue scaffolds. **Journal of Biomedical Materials Research - Part A**, v. 72, n. 2, p. 136–45, 2005.

KIM, U. J. et al. Three-dimensional aqueous-derived biomaterial scaffolds from silk fibroin. **Biomaterials**, v. 26, n. 15, p. 2775–2785, 2005.

KOKUBO, T. et al. Solutions able to reproduce in vivo surface-structure changes in bioactive glass-ceramic A-W3. **Journal of Biomedical Materials Research**, v. 24, n. 6, p. 721–734, 1990.

KUCHARSKA, M. et al. Fabrication of in-situ foamed chitosan/β-TCP scaffolds for bone tissue engineering application. **Materials Letters**, v. 85, p. 124–127, 2012.

KUTTAPPAN, S.; MATHEW, D.; NAIR, M. B. Biomimetic composite scaffolds containing bioceramics and collagen/gelatin for bone tissue engineering - A mini review. **International Journal of Biological Macromolecules**, v. 93, p. 1390–1401, 2016.

LAFLAMME, C.; ROUABHIA, M. Effect of BMP-2 and BMP-7 homodimers and a mixture of BMP-2/BMP-7 homodimers on osteoblast adhesion and growth following culture on a collagen scaffold. **Biomedical Materials**, v. 3, n. 1, p. 015008, 2008.

LANGER, R.; VACANTI, J. P. Tissue engineering. **Science (New York, N.Y.)**, v. 260, p. 920–926, 1993.

LEE, D. H. et al. Enhanced osteogenesis of β-tricalcium phosphate reinforced silk fibroin scaffold for bone tissue biofabrication. **International Journal of Biological Macromolecules**, v. 95, p. 14–23, 2017.

LEE, D. S. H.; PAI, Y.; CHANG, S. Effect of Thermal Treatment of the

Hydroxyapatite Powders on the Micropore and Microstructure of Porous Biphasic Calcium Phosphate Composite Granules. **Journal of Biomaterials and Nanobiotechnology**, v. 4, n. 2, p. 114–118, 2013.

LEE, E. J.; KIM, H. E. Accelerated bony defect healing by chitosan/silica hybrid membrane with localized bone morphogenetic protein-2 delivery. **Materials Science and Engineering C**, v. 59, p. 339–345, 2016.

LEGEROS, R. Z. Properties of osteoconductive biomaterials: calcium phosphates. **Clinical orthopaedics and related research**, n. 395, p. 81–98, 2002.

LEGEROS, R. Z. Calcium phosphate-based osteoinductive materials. **Chemical Reviews**, v. 108, n. 11, p. 4742–4753, 2008.

LEVINGSTONE, T. J. et al. A biomimetic multi-layered collagen-based scaffold for osteochondral repair. **Acta Biomaterialia**, v. 10, n. 5, p. 1996–2004, 2014.

LI, J. et al. Production of Composite Scaffold Containing Silk Fibroin, Chitosan, and Gelatin for 3D Cell Culture and Bone Tissue Regeneration. **Medical Science Monitor**, v. 23, p. 5311–5320, 2017a.

LI, J. J. et al. Silk coating on a bioactive ceramic scaffold for bone regeneration: effective enhancement of mechanical and in vitro osteogenic properties towards load-bearing applications. **Journal of Tissue Engineering and Regenerative Medicine**, v. 11, n. 6, p. 1741–1753, 2017b.

LIU, J. et al. Chitosan-based nanofibrous membrane unit with gradient compositional and structural features for mimicking calcified layer in osteochondral matrix. **International Journal of Molecular Sciences**, v. 19, n. 8, 2018a.

LIU, J. et al. Chitosan-Based Nanofibrous Membrane Unit with Gradient Compositional and Structural Features for Mimicking Calcified Layer in Osteochondral Matrix. **International Journal of Molecular Sciences**, v. 79, p. 2330, 2018b.

LIU, Y.; ZHOU, C.; SUN, Y. A biomimetic strategy for controllable degradation of chitosan scaffolds. **Journal of Materials Research**, v. 27, n. 14, p. 1859–1868, 2012.

LOCA, D. et al. **Porous hydroxyapatite for drug delivery**. [s.l.] Elsevier Ltd., 2015.

LOPA, S.; MADRY, H. Bioinspired Scaffolds for Osteochondral Regeneration. **Tissue Engineering Part A**, v. 20, p. 2052–76, 2014.

LOW, A. et al. Gypsum-based biomaterials: Evaluation of physical and mechanical properties, cellular effects and its potential as a pulp liner. **Dental Materials Journal**, v. 34, n.

4, p. 522–528, 2015.

M.E., G. et al. Cytocompatibility and response of osteoblastic-like cells to starch-based polymers: Effect of several additives and processing conditions. **Biomaterials**, v. 22, n. 13, p. 1911–1917, 2001.

MADRY, H.; VAN DIJK, C. N.; MUELLER-GERBL, M. The basic science of the subchondral bone. **Knee Surgery, Sports Traumatology, Arthroscopy**, v. 18, n. 4, p. 419–33, 2010.

MAJI, K. et al. Preparation and characterization of gelatin-chitosan-nanoβ-TCP based scaffold for orthopaedic application. **Materials Science and Engineering C**, v. 86, n. February, p. 83–94, 2018.

MALAFAYA, P. B.; REIS, R. L. Bilayered chitosan-based scaffolds for osteochondral tissue engineering: Influence of hydroxyapatite on in vitro cytotoxicity and dynamic bioactivity studies in a specific double-chamber bioreactor. **Acta Biomaterialia**, v. 5, n. 2, p. 644–60, 2009.

MAO, D. et al. Porous stable poly(lactic acid)/ethyl cellulose/hydroxyapatite composite scaffolds prepared by a combined method for bone regeneration. **Carbohydrate Polymers**, v. 180, n. October 2017, p. 104–111, 2018.

MARTINS, A. M. et al. Electrically Conductive Chitosan/Carbon Sca ff olds for Cardiac Tissue Engineering. **Biomacromolecules**, v. 15, p. 635–643, 2014.

MARTINS, T. et al. In vitro degradation of chitosan composite foams for biomedical applications and effect of bioactive glass as a crosslinker. **Biomedical Glasses**, v. 4, n. 1, 2018.

MATASSI, F. et al. New biomaterials for bone regeneration. **Clinical Cases in Mineral and Bone Metabolism**, v. 8, n. 1, p. 21–24, 2011.

MAUNEY, J. R. et al. Engineering adipose-like tissue in vitro and in vivo utilizing human bone marrow and adipose-derived mesenchymal stem cells with silk fibroin 3D scaffolds. **Biomaterials**, v. 28, n. 35, p. 5280–90, 2007.

MINA, A. et al. Determination of physical properties for β-TCP + chitosan biomaterial obtained on metallic 316L substrates. **Materials Chemistry and Physics**, v. 160, p. 296–307, 2015.

MONTJOVENT, M.-O. et al. VEGF incorporated into calcium phosphate ceramics promotes vascularisation and bone formation in vivo. **European Cells and Materials**, v. 19, p. 30–40, 2010.

MORI, H.; TSUKADA, M. New silk protein: Modification of silk protein by gene engineering for production of biomaterials. **Reviews in Molecular Biotechnology**, v. 74, p.

95–103, 2000.

MUZZARELLI, R. A. A. et al. Genipin-crosslinked chitosan gels and scaffolds for tissue engineering and regeneration of cartilage and bone. **Marine Drugs**, v. 13, n. 12, p. 7314–7338, 2015.

NOOEAID, P. et al. Osteochondral tissue engineering: Scaffolds, stem cells and applications. **Journal of Cellular and Molecular Medicine**, v. 16, n. 10, p. 2247–70, 2012.

NUKAVARAPU, S. P.; DORCEMUS, D. L. Osteochondral tissue engineering: Current strategies and challenges. **Biotechnology Advances**, v. 31, n. 5, p. 706–21, 2013.

O'BRIEN, F. J. Biomaterials & scaffolds for tissue engineering. **Materials Today**, v. 14, n. 3, p. 88–95, 2011.

OLIVEIRA, J. M. et al. Novel hydroxyapatite/chitosan bilayered scaffold for osteochondral tissue-engineering applications: Scaffold design and its performance when seeded with goat bone marrow stromal cells. **Biomaterials**, v. 27, n. 36, p. 6123–6137, 2006.

OVERMAN, J. R. et al. Growth factor gene expression profiles of bone morphogenetic protein-2-treated human adipose stem cells seeded on calcium phosphate scaffolds in vitro. **Biochimie**, v. 95, n. 12, p. 2304–2313, 2013a.

OVERMAN, J. R. et al. Growth factor gene expression profiles of bone morphogenetic protein-2-treated human adipose stem cells seeded on calcium phosphate scaffolds in vitro. **Biochimie**, v. 95, n. 12, p. 2304–2313, Dec. 2013b.

OZKAN, S. et al. Multifunctional protein-encapsulated polycaprolactone scaffolds: Fabrication and in vitro assessment for tissue engineering. **Biomaterials**, v. 30, n. 26, p. 4336–4347, 2009.

PALLELA, R. et al. Biophysicochemical evaluation of chitosan-hydroxyapatite-marine sponge collagen composite for bone tissue engineering. **Journal of Biomedical Materials Research - Part A**, v. 100 A, n. 2, p. 486–495, 2012.

PATI, F. et al. Ornamenting 3D printed scaffolds with cell-laid extracellular matrix for bone tissue regeneration. **Biomaterials**, v. 37, p. 230–241, 2015.

PEREIRA, D. R. et al. Injectable gellan-gum/hydroxyapatite-based bilayered hydrogel composites for osteochondral tissue regeneration. **Applied Materials Today**, 2018.

PIAIA, L.; PAES, C. Q.; PORTO, L. M. Viability of human dermal fibroblasts cultured on bacterial cellulose and Aloe vera composites. **BMC Proceedings**, v. 8, n. Suppl 4, p. P61, 2014.

PINA, S. et al. Biofunctional Ionic-Doped Calcium Phosphates: Silk Fibroin Composites for Bone Tissue Engineering Scaffolding. **Cells Tissues Organs**, v. 204, n. 3–4, p. 150–163, 2017.

PINA, S.; OLIVEIRA, J. M.; REIS, R. L. Natural-based nanocomposites for bone tissue engineering and regenerative medicine: A review. **Advanced Materials**, v. 27, n. 7, p. 1143–1169, 2015.

POOLE, A. R. et al. Composition and structure of articular cartilage: a template for tissue repair. **Clinical orthopaedics and related research**, n. 391 Suppl, p. S26-33, Oct. 2001.

PRAMANIK, N. et al. Chemical Synthesis, Characterization, and Biocompatibility Study of Hydroxyapatite/Chitosan Phosphate Nanocomposite for Bone Tissue Engineering Applications. **International Journal of Biomaterials**, p. 8, 2009.

QASIM, S. B. et al. In-vitro and in-vivo degradation studies of freeze gelated porous chitosan composite scaffolds for tissue engineering applications. **Polymer Degradation and Stability**, v. 136, p. 31–38, 2017.

QIU, J. et al. In vitro investigation on the biodegradability and biocompatibility of genipin cross-linked porcine acellular dermal matrix with intrinsic fluorescence. **ACS Applied Materials and Interfaces**, v. 5, p. 344–50, 2013.

RAJKUMAR, M. et al. Nanohydroxyapatite-chitosan-gelatin polyelectrolyte complex with enhanced mechanical and bioactivity. **Materials Science and Engineering C**, v. 33, n. 6, p. 3237–3244, 2013.

RAZAVI, M. et al. In vivo assessments of bioabsorbable AZ91 magnesium implants coated with nanostructured fluoridated hydroxyapatite by MAO/EPD technique for biomedical applications. **Materials Science and Engineering C**, v. 48, p. 21–27, 2015.

REN, D. et al. The enzymatic degradation and swelling properties of chitosan matrices with different degrees of N-acetylation. **Carbohydrate Research**, v. 340, n. 15, p. 2403–10, 2005.

RIBEIRO, V. P. et al. Silk-based anisotropical 3D biotextiles for bone regeneration. **Biomaterials**, v. 123, p. 92–106, 2017.

RIBEIRO, V. P. et al. Enzymatically Cross-Linked Silk Fibroin-Based Hierarchical Scaffolds for Osteochondral Regeneration. **ACS Applied Materials and Interfaces**, v. 11, n. 4, p. 3781–3799, 2019.

RODRIGUES, A. I. et al. Combinatorial Effect of Silicon and Calcium Release from Starch-Based Scaffolds on Osteogenic Differentiation of Human Adipose Stem Cells. **ACS Biomaterials Science and Engineering**, v. 1, n. 9, 2015.

ROOHANI-ESFAHANI, S. I. et al. Unique microstructural design of ceramic scaffolds for bone regeneration under load. **Acta Biomaterialia**, v. 9, n. 6, p. 7014–7024, 2013.

ROSETI, L. et al. Scaffolds for Bone Tissue Engineering: State of the art and new perspectives. **Materials Science and Engineering C**, v. 78, p. 1246–1262, 2017.

SAI NIEVETHITHA, S. et al. Nanoceramics on osteoblast proliferation and differentiation in bone tissue engineering. **International Journal of Biological Macromolecules**, v. 98, p. 67–74, 2017.

SCHWARTZ, C. Review of 15 years of use of synthetic bone substitutes in orthopaedic surgery and traumatology. In: **e-mémoires de l'Académie Nationale de Chirurgie,**. p. 56–68.

SEIDI, A. et al. Gradient biomaterials for soft-to-hard interface tissue engineering. **Acta Biomaterialia**, v. 7, n. 4, p. 1441–1451, 2011.

SEO, J. P. et al. Effects of bilayer gelatin/β-tricalcium phosphate sponges loaded with mesenchymal stem cells, chondrocytes, bone morphogenetic protein-2, and platelet rich plasma on osteochondral defects of the talus in horses. **Research in Veterinary Science**, v. 95, n. 3, p. 1210–1216, 2013.

SEO, S.-J. et al. Strategies for osteochondral repair: Focus on scaffolds. **Journal of tissue engineering**, v. 5, p. 50, 8 Jul. 2014.

SHARMA, C. et al. Fabrication and characterization of novel nano-biocomposite scaffold of chitosan-gelatin-alginate-hydroxyapatite for bone tissue engineering. **Materials Science and Engineering C**, v. 64, p. 416–427, 2016.

SHAVANDI, A. et al. A novel squid pen chitosan/hydroxyapatite/β-tricalcium phosphate composite for bone tissue engineering. **Materials Science and Engineering C**, v. 55, p. 373–383, 2015.

SHEN, W. C.; YANG, D.; RYSER, H. J. P. Colorimetric determination of microgram quantities of polylysine by trypan blue precipitation. **Analytical Biochemistry**, 1984.

SIGNINI, R.; SÉRGIO, P. Características e Propriedades de Quitosanas Purificadas nas Formas Neutra , Acetato e Cloridrato. v. 11, p. 58–64, 2001.

SILVA, J. M. et al. Multilayered Hollow Tubes as Blood Vessel Substitutes. **ACS Biomaterials Science and Engineering**, v. 2, n. 12, p. 2304–2314, 2016.

SILVA, S. S. et al. Novel Genipin-Cross-Linked Chitosan / Silk Fibroin Sponges for Cartilage Engineering Strategies Novel Genipin-Cross-Linked Chitosan / Silk Fibroin Sponges

for Cartilage Engineering Strategies. **Time**, p. 2764–2774, 2008a.

SILVA, S. S. et al. Genipin-modified silk-fibroin nanometric nets. **Macromolecular Bioscience**, v. 8, n. 8, p. 766–74, 2008b.

SIMS, N. A.; VRAHNAS, C. Regulation of cortical and trabecular bone mass by communication between osteoblasts, osteocytes and osteoclasts. **Archives of Biochemistry and Biophysics**, v. 561, p. 22–28, 2014.

SIONKOWSKA, A. Current research on the blends of natural and synthetic polymers as new biomaterials: Review. **Progress in Polymer Science (Oxford)**, v. 36, n. 9, p. 1254–1276, 2011.

SIQUEIRA, L. et al. Influence of the addition of β-TCP on the morphology, thermal properties and cell viability of poly (lactic acid) fibers obtained by electrospinning. **Materials science & engineering. C, Materials for biological applications**, v. 52, p. 135–43, 2015.

SIVASHANKARI, P. R.; PRABAHARAN, M. Prospects of chitosan-based scaffolds for growth factor release in tissue engineering. **International Journal of Biological Macromolecules**, v. 93, p. 1382–1389, 2016.

SOHIER, J. et al. Porous beta tricalcium phosphate scaffolds used as a BMP-2 delivery system for bone tissue engineering. **Journal of Biomedical Materials Research - Part A**, v. 92, n. 3, p. 1105–14, 2010.

SOPHIA FOX, A. J.; BEDI, A.; RODEO, S. A. The basic science of articular cartilage: structure, composition, and function. **Sports health**, v. 1, n. 6, p. 461–468, Nov. 2009.

SOWMYA, S. et al. Biocompatible β-chitin hydrogel/nanobioactive glass ceramic nanocomposite scaffolds for periodontal bone regeneration. **Trends in Biomaterials and Artificial Organs**, v. 25, p. 1–11, 2011.

T.J., L. et al. Repair of osteochondritis dissecans lesions using a novel osteochondral defect repair scaffold in a sporthorse filly. **Journal of Orthopaedic Research**, v. 5, p. 56–62, 2016.

TAMADDON, M. et al. Osteochondral tissue repair in osteoarthritic joints: clinical challenges and opportunities in tissue engineering. **Bio-Design and Manufacturing**, v. 1, n. 2, p. 101–114, 2018.

TANAKA, K. et al. Determination of the site of disulfide linkage between heavy and light chains of silk fibroin produced by Bombyx mori. **Biochimica et Biophysica Acta - Protein Structure and Molecular Enzymology**, n. 1, p. 92–103, 1999.

TEIMOURI, A. et al. Nano-composite of silk fibroin-chitosan/Nano ZrO2for tissue engineering applications: Fabrication and morphology. **International Journal of Biological**

Macromolecules, v. 76, p. 292–302, 2015.

THAVORNYUTIKARN, B. et al. Bone tissue engineering scaffolding: computer-aided scaffolding techniques. **Progress in Biomaterials**, v. 3, n. 2–4, p. 61–102, 2014.

THEIN-HAN, W. W.; MISRA, R. D. K. Biomimetic chitosan–nanohydroxyapatite composite scaffolds for bone tissue engineering. **Acta Biomaterialia**, v. 5, n. 4, p. 1182–1197, 2009.

TORRES, J. et al. Bone Substitutes. **Implant Dentistry**, p. 91–108, 2011.

VISHWANATH, V.; PRAMANIK, K.; BISWAS, A. Optimization and evaluation of silk fibroin-chitosan freeze-dried porous scaffolds for cartilage tissue engineering application. **Journal of Biomaterials Science, Polymer Edition**, v. 27, n. 7, p. 657–74, 2016.

WAGNER-ECKER, M. et al. The collagen component of biological bone graft substitutes promotes ectopic bone formation by human mesenchymal stem cells. **Acta Biomaterialia**, v. 9, n. 7, p. 7298–7307, 2013.

WANG, S.; JAIN, H. High surface area nanomacroporous bioactive glass scaffold for hard tissue engineering. **Journal of the American Ceramic Society**, v. 93, n. 10, p. 100, 2010.

WANG, X. et al. Nanolayer biomaterial coatings of silk fibroin for controlled release. **Journal of Controlled Release**, v. 121, n. 3, p. 190–9, 2007.

WANG, Y. et al. Fabrication and in vitro evaluation of an articular cartilage extracellular matrix-hydroxyapatite bilayered scaffold with low permeability for interface tissue engineering. **BioMedical Engineering Online**, v. 13, p. 80, 2014.

WAYNE, J. S. et al. In Vivo Response of Polylactic Acid–Alginate Scaffolds and Bone Marrow-Derived Cells for Cartilage Tissue Engineering. **Tissue Engineering**, n. 6, p. 953–63, 2005.

WEISGERBER, D. W. et al. Evaluation of multi-scale mineralized collagen – polycaprolactone composites for bone tissue engineering. **Journal of the Mechanical Behavior of Biomedical Materials**, v. 61, p. 318–327, 2016.

WU, J. et al. Rheological, mechanical and degradable properties of injectable chitosan/silk fibroin/hydroxyapatite/glycerophosphate hydrogels. **Journal of the Mechanical Behavior of Biomedical Materials**, v. 64, p. 161–172, 2016.

WU, J. et al. Thermally triggered injectable chitosan/silk fibroin/bioactive glass nanoparticle hydrogels for in-situ bone formation in rat calvarial bone defects. **Acta Biomaterialia**, v. 91, p. 60–71, 2019.

XIAO, H. et al. Osteochondral repair using scaffolds with gradient pore sizes constructed with silk fibroin, chitosan, and nano-hydroxyapatite. **International Journal of Nanomedicine**, v. 14, p. 2011–2027, 2019.

YAN, L. et al. Bioactive macro / micro porous silk fibroin / nano-sized calcium phosphate scaffolds with potential for bone-tissue-engineering applications. **Nanomedicine**, v. 8, n. 3, p. 359–378, 2013.

YAN, L. P. et al. Bilayered silk/silk-nanoCaP scaffolds for osteochondral tissue engineering: In vitro and in vivo assessment of biological performance. **Acta Biomaterialia**, v. 12, n. 1, p. 227–241, 2015.

YANG, H. S. et al. Apatite-coated collagen scaffold for bone morphogenetic protein-2 delivery. **Tissue engineering. Part A**, v. 17, p. 2153–2164, 2011.

YANG, P. J.; TEMENOFF, J. S. Engineering Orthopedic Tissue Interfaces. **Tissue Engineering Part B: Reviews**, 2009.

YAO, C.-H. et al. Preparation of networks of gelatin and genipin as degradable biomaterials. **Materials Chemistry and Physics**, v. 83, n. 2, p. 204–208, 2004.

YAO, C.-H. et al. Wound-healing effect of electrospun gelatin nanofibres containing Centella asiatica extract in a rat model. **Journal of tissue engineering and regenerative medicine**, Feb. 2015.

YE, P. et al. Application of silk fibroin/chitosan/nano-hydroxyapatite composite scaffold in the repair of rabbit radial bone defect. **Experimental and Therapeutic Medicine**, v. 14, n. 6, p. 5547–5553, 2017.

YIN, Y. et al. Preparation and characterization of macroporous chitosan-gelatin/beta-tricalcium phosphate composite scaffolds for bone tissue engineering. **Journal of biomedical materials research. Part A**, v. 67, n. 3, p. 844–855, 2003.

ZANIN, H. et al. Assisted deposition of nano-hydroxyapatite onto exfoliated carbon nanotube oxide scaffolds. **Nanoscale**, v. 7, p. 10218–10232, 2015.

ZHANG, Q.; YAN, S.; LI, M. Silk fibroin based porous materials. **Materials**, v. 2, p. 2276–2295, 2009.

ZHANG, W. et al. The promotion of osteochondral repair by combined intra-articular injection of parathyroid hormone-related protein and implantation of a bi-layer collagen-silk scaffold. **Biomaterials**, v. 34, n. 25, p. 6046–57, 2013.

ZHANG, W. et al. Cell-Derived Extracellular Matrix: Basic Characteristics and Current Applications in Orthopedic Tissue Engineering. **Tissue Engineering Part B: Reviews**, v. 22, n. 3, p. 193–207, 2016a.

ZHANG, Y. et al. Mesoporous bioactive glass nanolayer-functionalized 3D-printed scaffolds for accelerating osteogenesis and angiogenesis. **Nanoscale**, v. 7, p. 19207–19221, 2015.

ZHANG, Y. et al. Preparation, characterization, and evaluation of genipin crosslinked chitosan/gelatin three-dimensional scaffolds for liver tissue engineering applications. **Journal of Biomedical Materials Research - Part A**, v. 104, n. 8, p. 1863–70, 2016b.

ZHANG, Y.; YANG, Y.; GUO, T. Genipin-crosslinked hydrophobical chitosan microspheres and their interactions with bovine serum albumin. **Carbohydrate Polymers**, v. 83, n. 4, p. 2016–2021, 2011.